

INFN SoUP 2022

The 2nd INFN School on Underground Physics: Theory & Experiments



New Photodetectors

Ettore Segreto

Universidade Estadual de Campinas - **UNICAMP** (Brazil)

SoUP 2022 – Laboratori Nazionale del Gran Sasso – 24th June 2022



Outline

- Introduction
- Vacuum Photosensor
 - ✓ *PMTs, MaPMTs, LAPPD, ...*
- Solid State detectors
 - ✓ *APD, SiPM*
- Hybrid Photosensors
- Estimating the Light Yield of a detector

Light detection in particle physics

- **Light detection** played a *central role in particle physics in the last century*
- Light production is ***one of the mechanisms through which the energy deposited by a charged particle is transformed spontaneously into a detectable signal*** (as ionization, phonons, acoustic, heat,...)
- Light signal can be produced through **different processes**: *scintillation, Cherenkov radiation, transition radiation, ...*
- Light signals carry a **lot of information about the incoming particle**: *time of arrival, type, direction, energy loss (related to dE/dx and LET)*
- Enough reasons to justify **the enormous effort that experimental particle physicists have done to detect them** with high efficiency to extract as much as information as possible

Triangle of fire



Triangle of light



Triangle of light



Triangle of light

Determined by the characteristics of the incoming particle:

- **Deposited energy** (or better LET – linear energy transfer): the number of emitted photons is usually proportional to the energy deposited in the medium (unless quenching process are in act)
- **Particle type**: in many scintillators the emission of light happens through the *transition of an excited molecule from the first excited state to ground state*. Depending on the total spin of the excited state (triplet or singlet) *the de-excitation can be fast or slow*. **The abundance of fast and slow components in the light signals depends on the particle type**
- **Direction**: Especially in **Cherenkov detectors** ==> The shape of the Cherenkov rings give the direction of the particle

Triangle of light



Triangle of light

This is the **transport/propagation of the produced photons to the active photo-sensors** and comprises:

- ***Attenuation of the signal*** due to absorption of the radiator or of impurities present on the radiator
- ***Rayleigh elastic scattering***
- ***Wavelength shifting of the photons*** to match the sensitivity curve of the photosensors
- *Can be done diluting optically active compound in liquid or solid scintillators or depositing shifting compounds on the photo-sensors and/or on the inner surface of the detector*

LIGHT PRODUCTION

Triangle of light

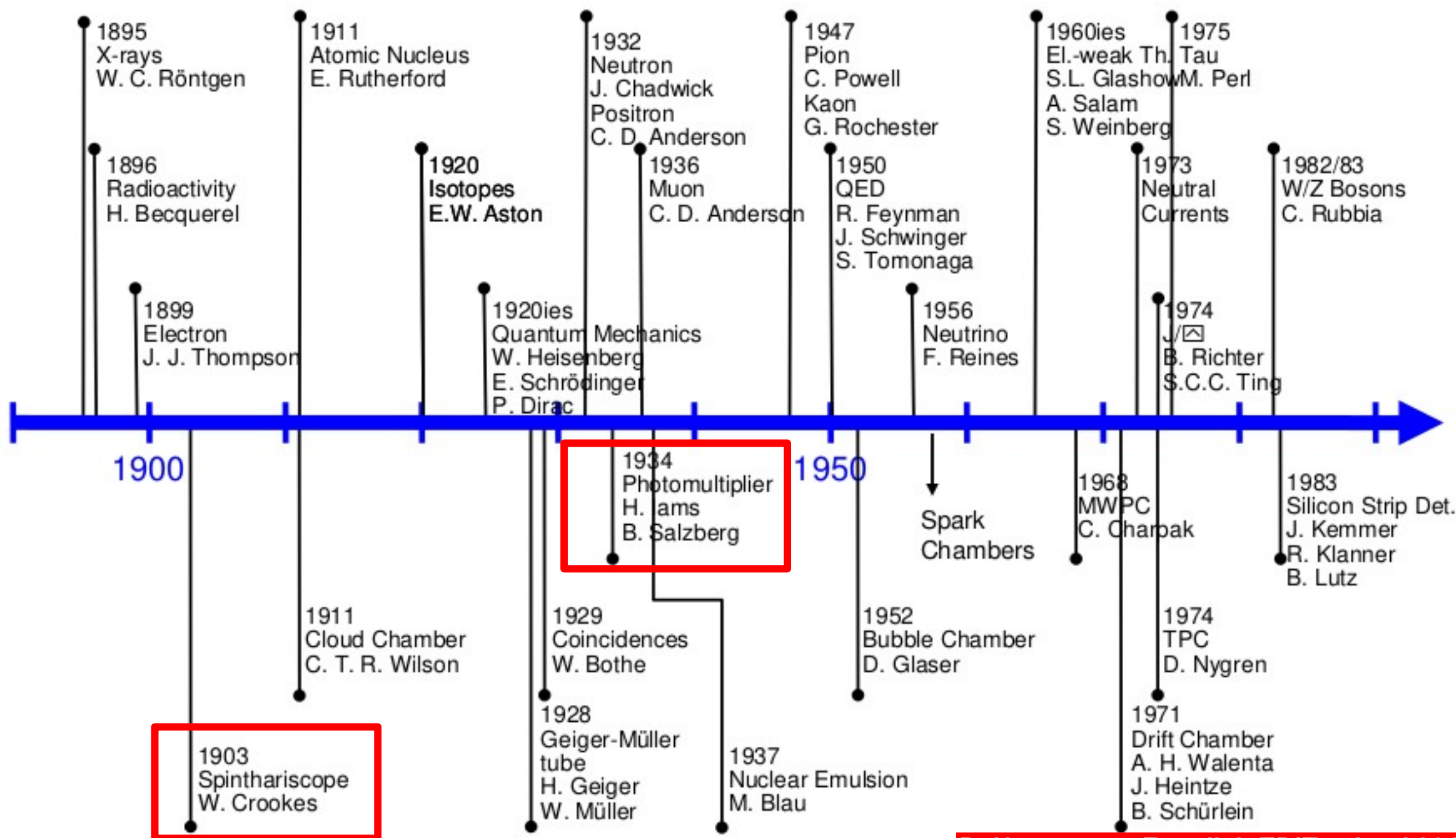


Triangle of light

The conversion of photons into an electrical signal that we measure:

- It ***does not exist the perfect photodetector but the most suited for our application***
- The most suited photon detector is chosen on the basis of the *information we want to extract from the light signal, from the characteristics of the light signal (wavelength, shape, intensity,..) itself, geometrical constraints for the photo-sensor, cost,*

LIGHT PRODUCTION



Spinthariscopes

- Invented by *William Crookes* in 1903!
- Allows to observe the scintillation light emitted from a thin foil of zinc sulfide with a lens in a dark little box
- Crookes named his device from Ancient Greek: *σπινθήρ (spinthēr)* "spark"
- Photon detector is human eye...



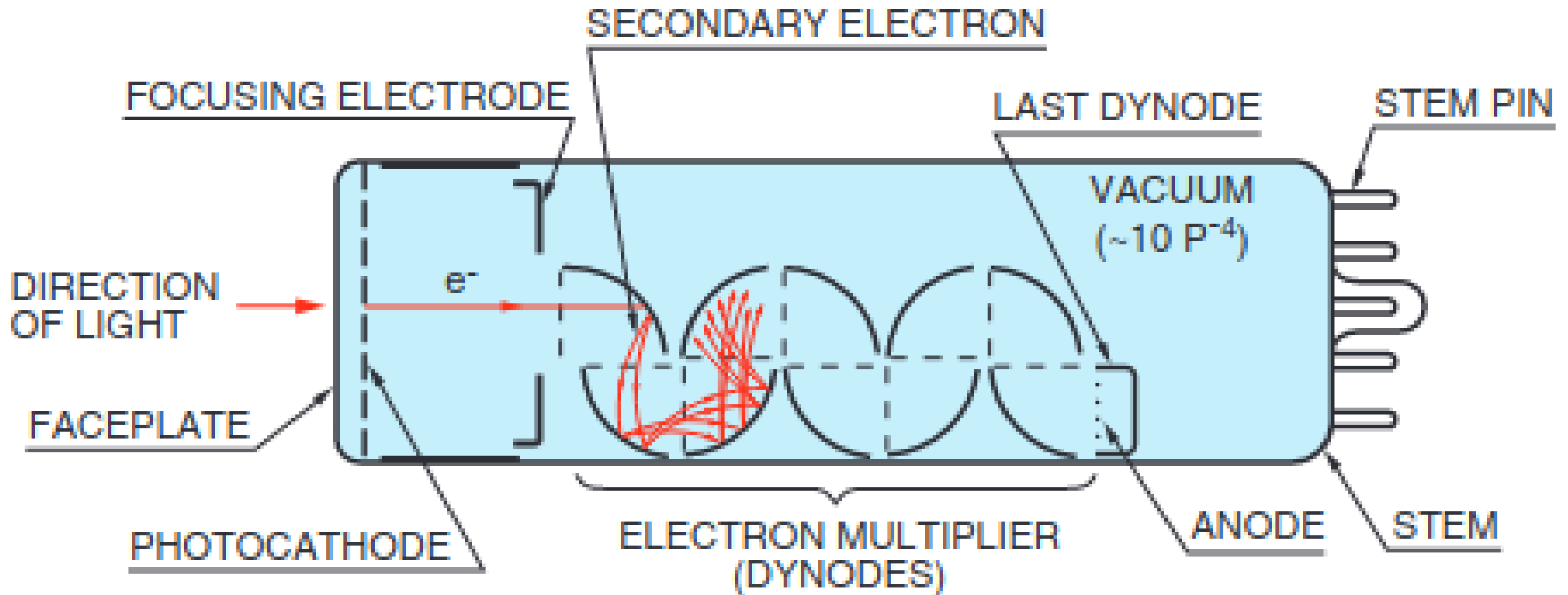
Copyright © 2003 Theodore W. Gray

Photomultiplier tube

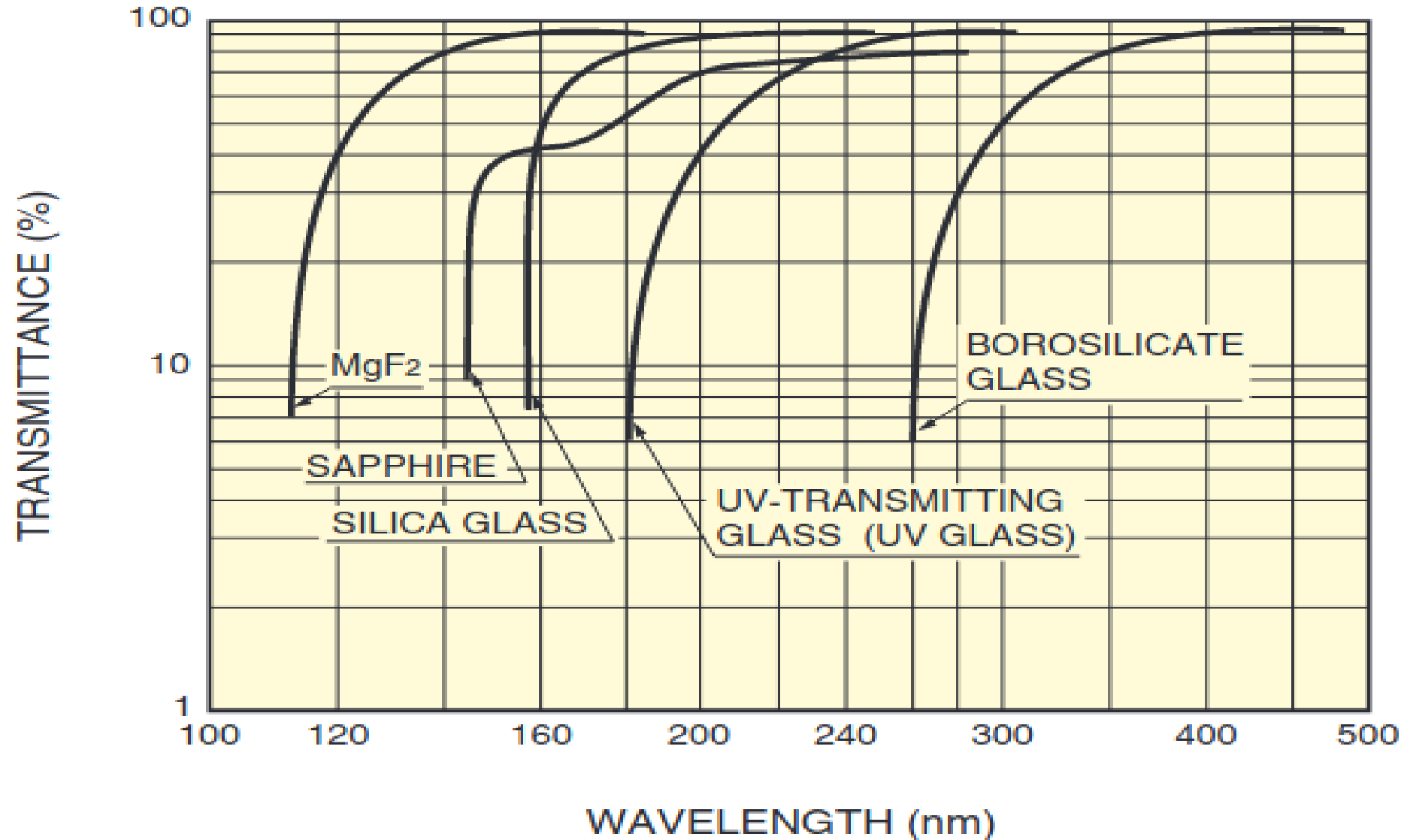
- The *first demonstration of a photomultiplier* (PMT) dates back to 1934. The floor for the invention of PMTs had been set up by the discovery (H. Hertz, 1887) and theoretical explanation (A. Einstein, 1905) of the **photoelectric effect** and by the discovery of the **secondary electron emission** (Villard, 1902)
- PMTs were a **sort of spin-off** of the technology developed to build the **first practical television cameras** (iconoscope, orthicon...)
- H. Iams and B. Salzberg realized *the first prototype of PMT integrating a photocathode and a single stage of multiplication*. The tube had a gain of **8 and operated at frequencies above 10 kHz!**



PMT scheme



PMT basic principles: window

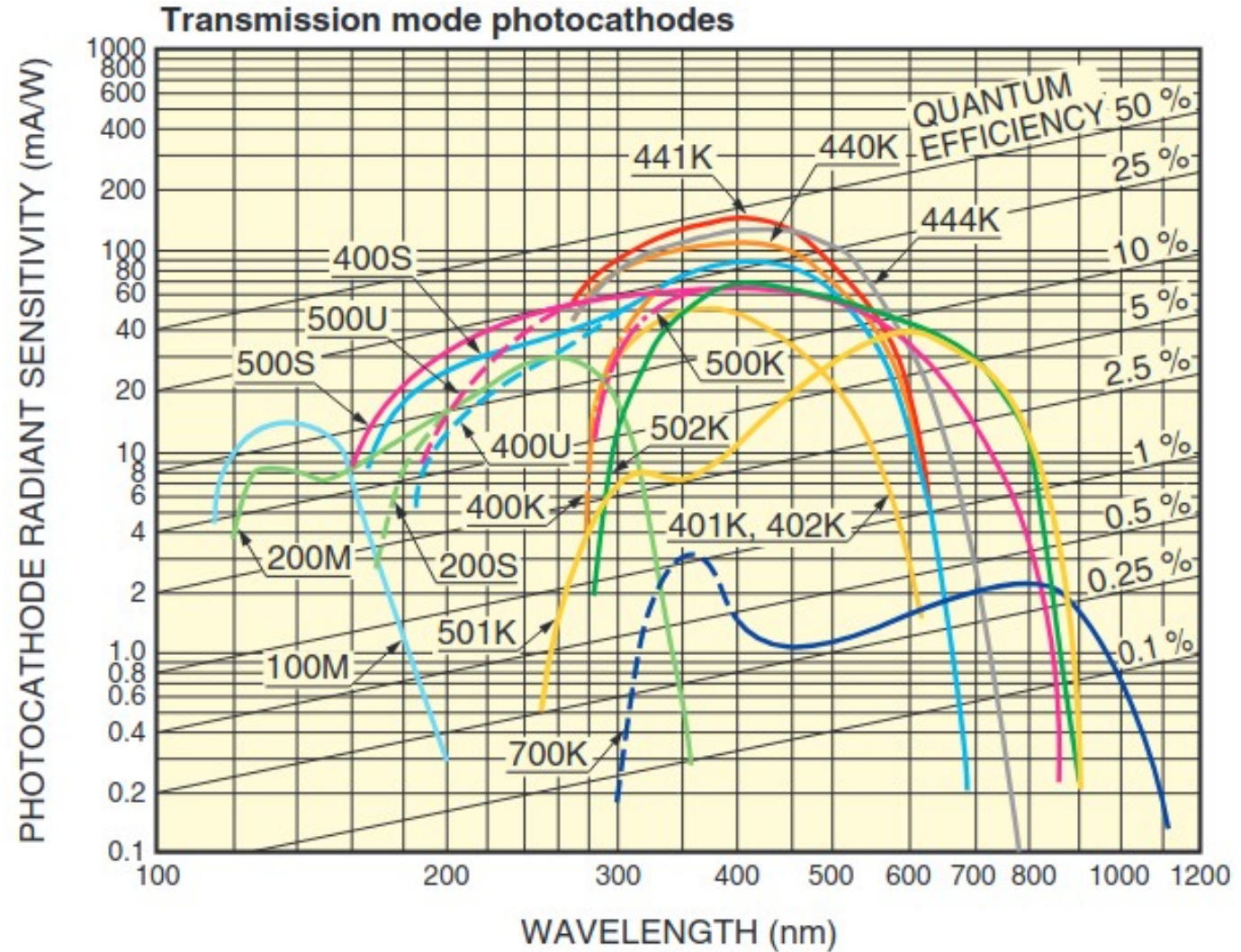
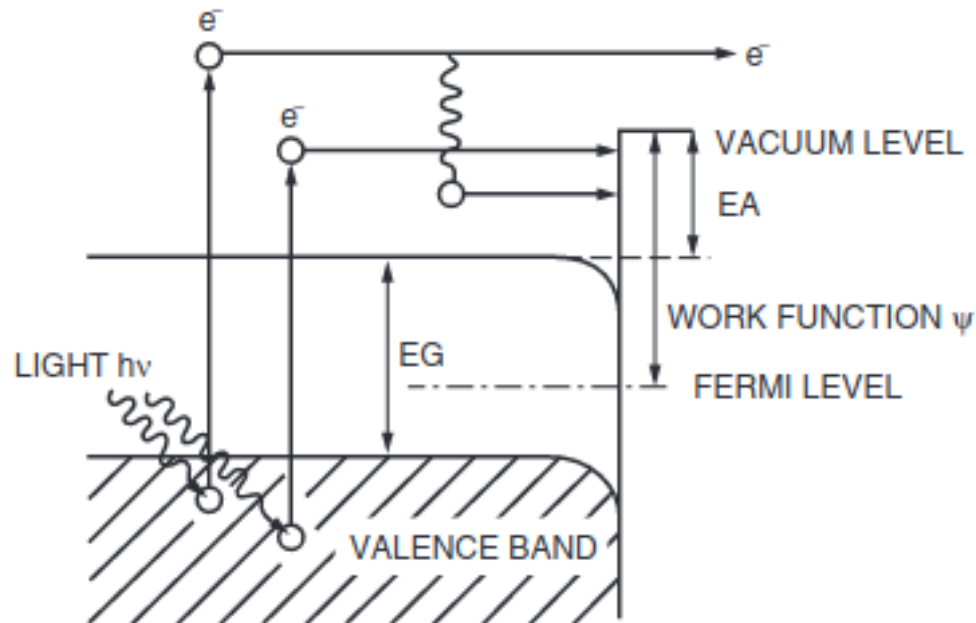


PMT basic principles: photocathode

Photoelectric emission and cathode
Quantum efficiency

$$QE(\lambda) = (1 - R) P_v \frac{1}{1 + \lambda_a / \lambda_e} P_{escape}$$

ALKALI PHOTOCATHODE

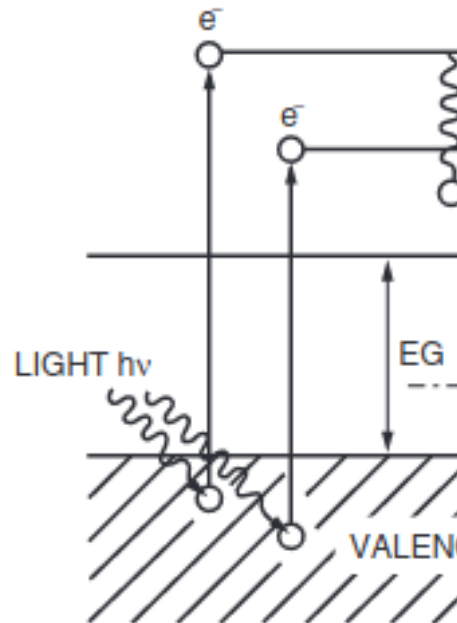


PMT ba

Photoelectric emission
Quantum efficiency

$$QE(\lambda) = (1 - R) F$$

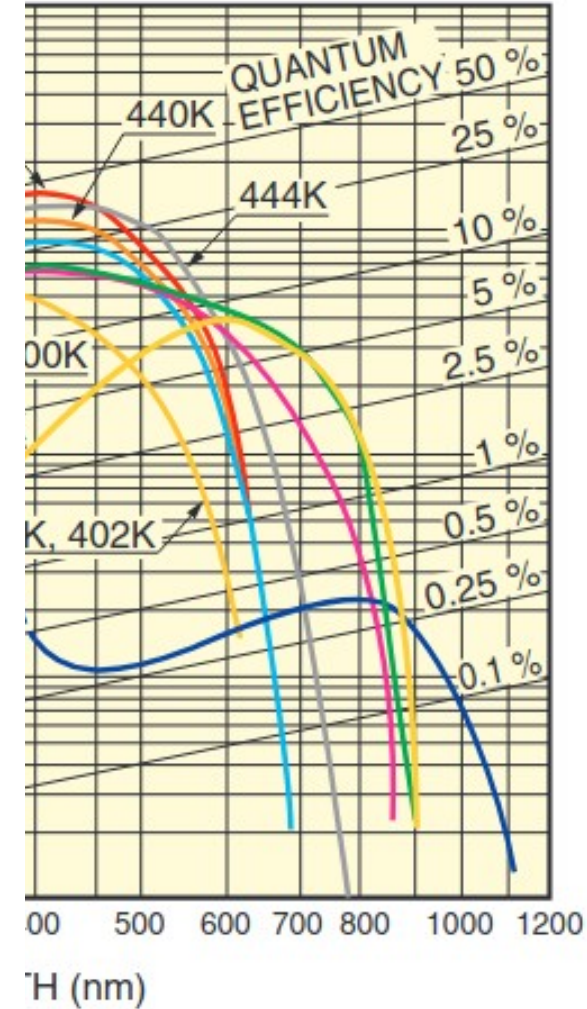
ALKALI PHOTOCATHODE



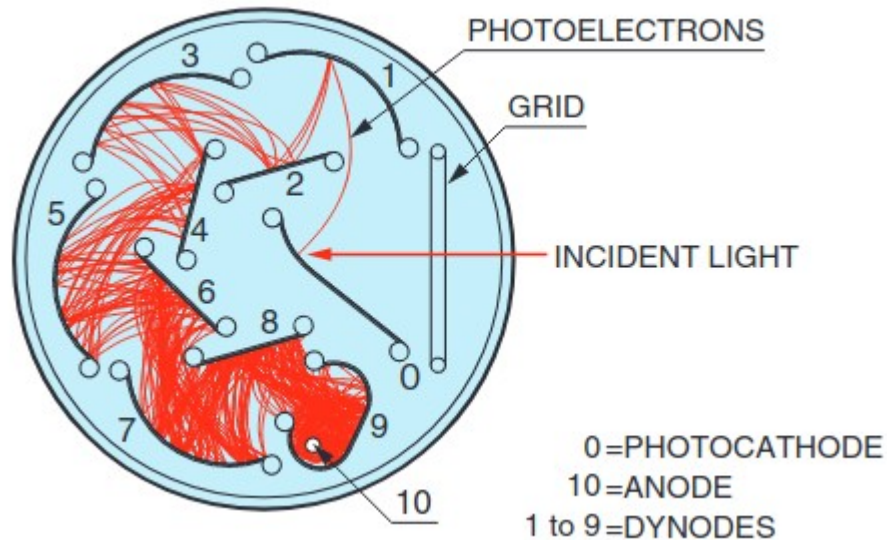
Transmission mode photocathodes

Curve code	Photocathode material	Window material	Luminous sensitivity (Typ.) ($\mu\text{A}/\text{lm}$)	Spectral range (nm)	Spectral response			
					Peak wavelength		Quantum efficiency (%)	Quantum efficiency (nm)
					Radiant sensitivity (mA/W)	(nm)		
100M	Cs-I	MgF ₂	—	115 to 200	14	140	13	130
200S	Cs-Te	Silica	—	160 to 320	29	240	16	210
200M	Cs-Te	MgF ₂	—	115 to 320	29	240	17	200
201S	Cs-Te	Silica	—	160 to 320	31	240	17	210
400K	Bialkali	Borosilicate	95	300 to 650	88	420	27	390
400U	Bialkali	UV	95	185 to 650	88	420	27	390
400S	Bialkali	Silica	95	160 to 650	88	420	27	390
401K	High temp. bialkali	Borosilicate	40	300 to 650	51	375	17	375
402K	Low noise bialkali	Borosilicate	40	300 to 650	54	375	18	375
500K	Multialkali	Borosilicate	150	300 to 850	64	420	20	375
500U	Multialkali	UV	150	185 to 850	64	420	25	280
500S	Multialkali	Silica	150	160 to 850	64	420	25	280
501K	Extended red multialkali	Borosilicate	200	300 to 900	40	600	8	580
502K	Multialkali	Borosilicate (prism)	230	300 to 900	69	420	20	390
600K	GaAsP(Cs)	Borosilicate	700	280 to 720	180	550 to 650	40	480 to 530
601K	Extended red GaAsP(Cs)	Borosilicate	750	280 to 820	160	550 to 650	36	480 to 530
602K	GaAs(Cs)	Borosilicate	700	370 to 920	85	750 to 850	12	600 to 750
700K	Ag-O-Cs	Borosilicate	20	400 to 1200	2.2	800	0.36	740
900S	InP/InGaAsP(Cs)	Silica	—	950 to 1200	18	1100	2	1000 to 1100
901S	InP/InGaAs(Cs)	Silica	—	950 to 1700	24	1500	2	1000 to 1550
440K	Super bialkali	Borosilicate	105	300 to 650	110	400	35	350
441K	Ultra bialkali	Borosilicate	135	300 to 650	130	400	43	350
442K	Super bialkali	Borosilicate	105	230 to 700	110	400	35	350
443K	Ultra bialkali	Borosilicate	135	230 to 700	130	400	43	350
444K	Extended green bialkali	Borosilicate	160	300 to 700	127	420	40	380

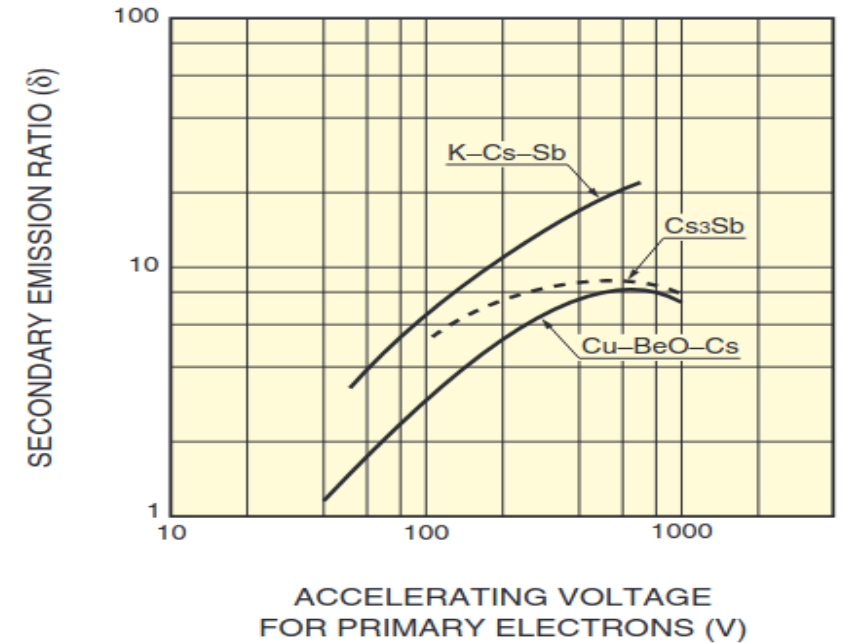
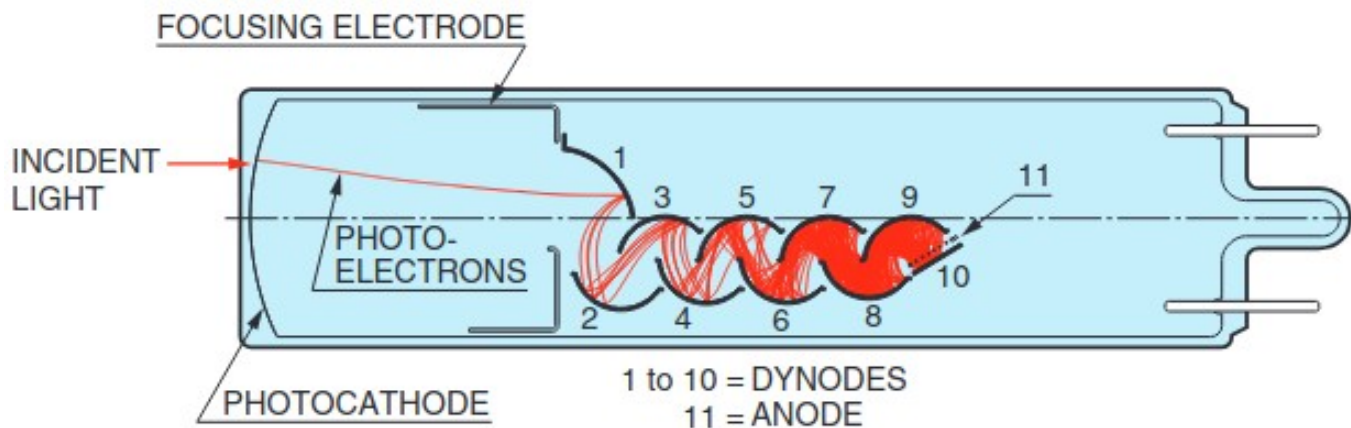
Photocathode



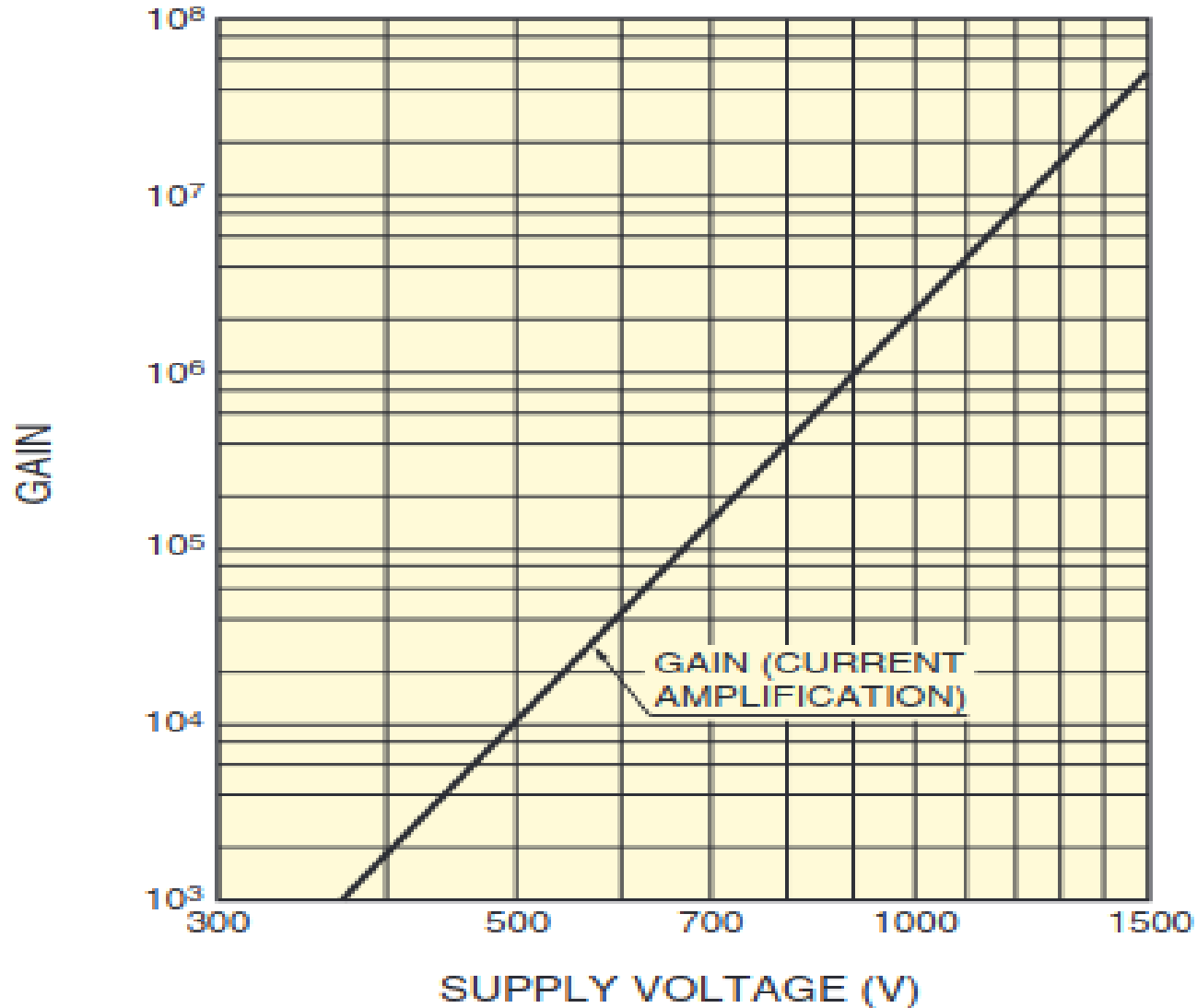
PMT basic principles: dynodes



- Photoelectrons from the cathode are focused on the **first multiplication stage (dynode)**
- If multiplication factor of one dynode is $\delta \Rightarrow$ overall gain is δ^n , where n is the number of dynodes
- $\delta \sim aE^k$

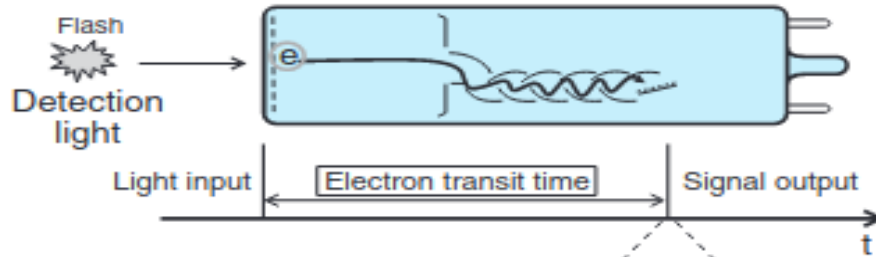


PMT basic principles: gain

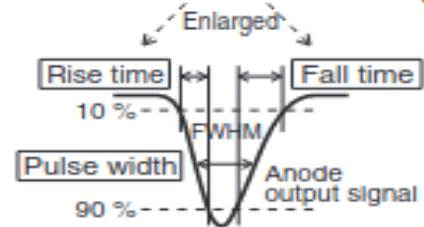


- $G = \delta^n = (aE^k)^n$

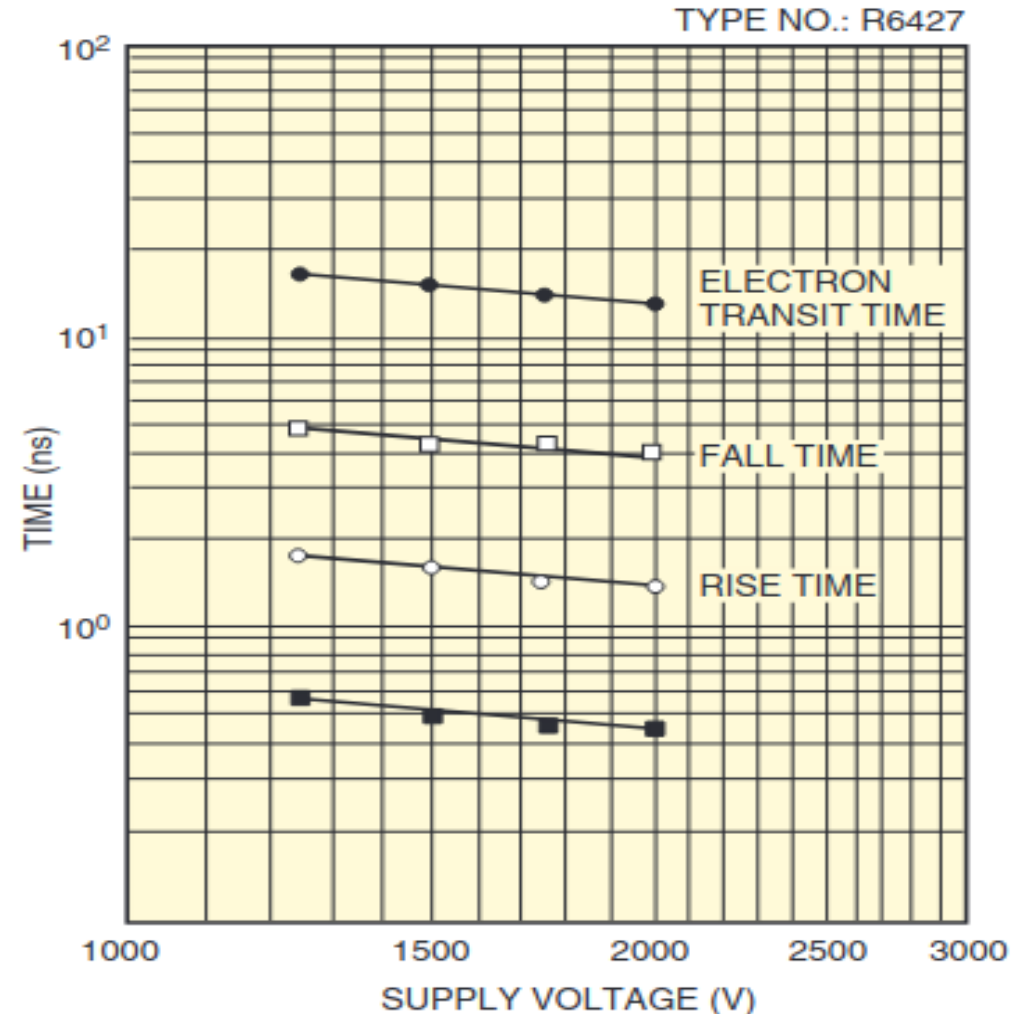
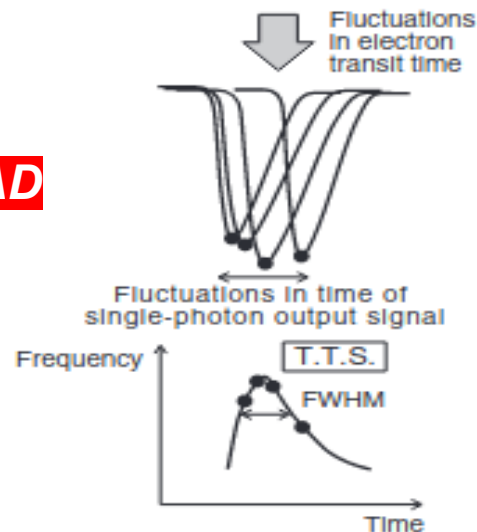
PMT basic principles: timing



PULSE SHAPE



TRANSIT TIME SPREAD



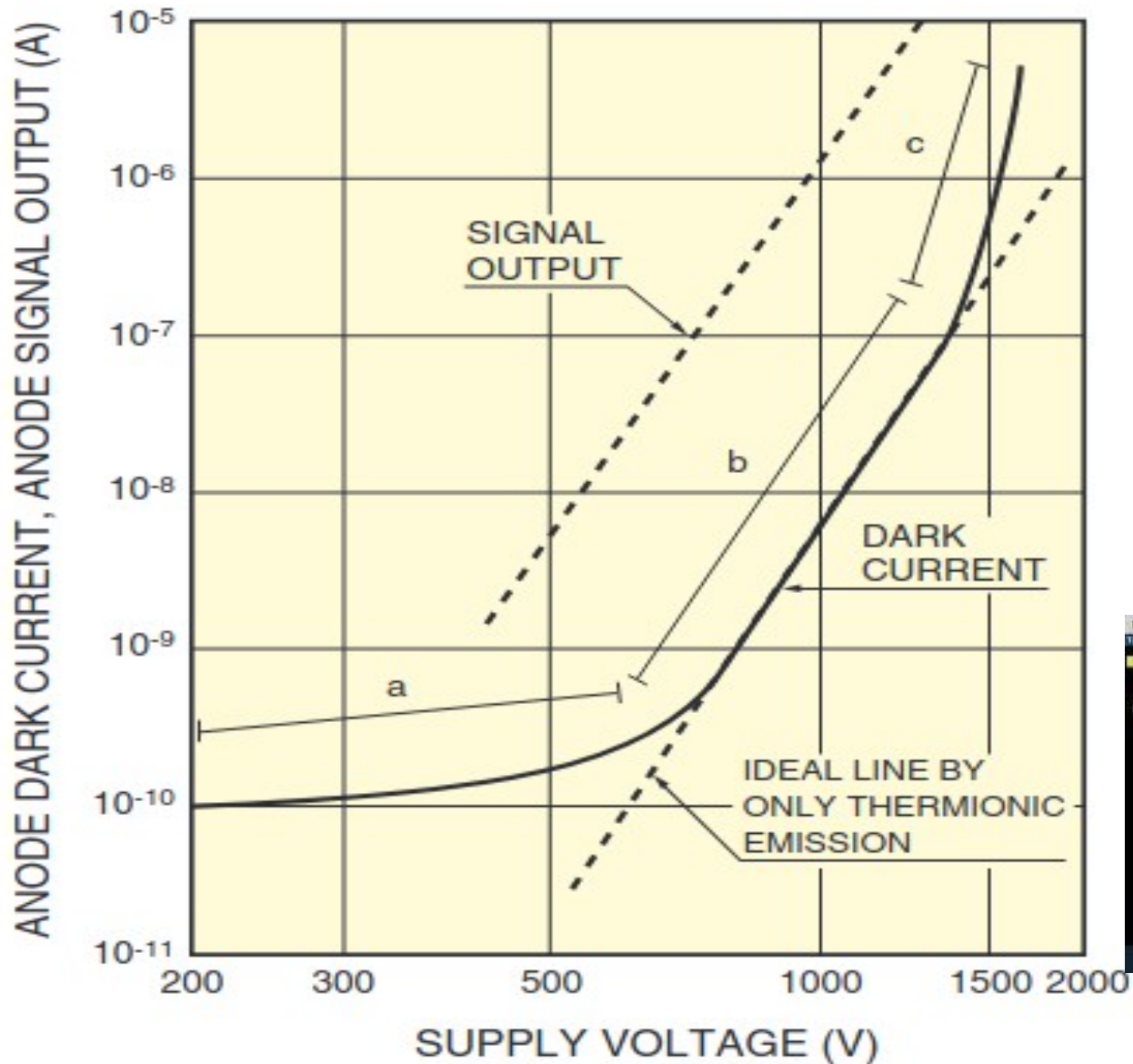
PMT basic principles: timing

Unit: ns

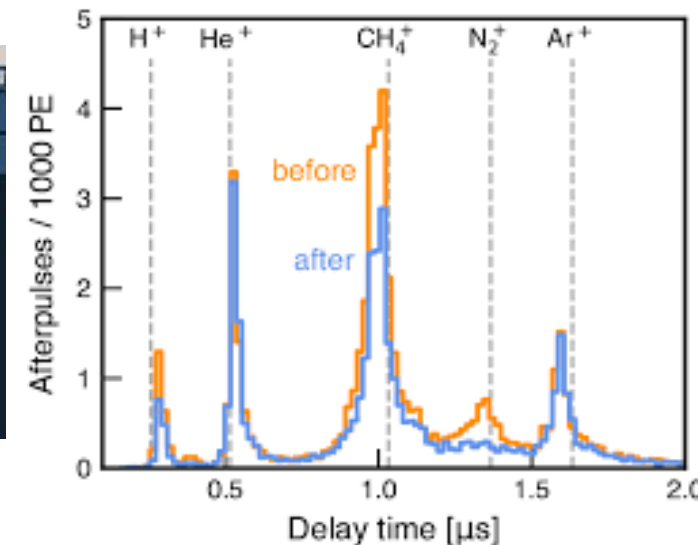
Dynode type	Rise time	Fall time	Pulse width (FWHM)	Electron transit time	T.T.S.
Linear-focused	0.7 to 3	1 to 10	1.3 to 5	16 to 50	0.37 to 1.1
Circular-cage	3.4	10	7	31	3.6
Box-and-grid	to 7	25	13 to 20	57 to 70	Less than 10
Venetian blind	to 7	25	25	60	Less than 10
Mesh	2.5 to 2.7	4 to 6	5	15	Less than 0.45
Metal channel	0.65 to 1.5	1 to 3	1.5 to 3	4.7 to 8.8	0.4

T.T.S.: Transit Time Spread

PMT dark current and afterpulses



- **Region a** dominated by *leakage current*
- **Region b** dominated by *thermoionic emisison from the cathode*
- **Region c** dominated by *field emission and scintillation of the materials*
- **Region b** in general offers the best S/N
- **Afterpulsing is a correlated noise**, which manifests itself as **delayed pulses**
- Produced by the ionization of the residual gas



Photomultipliers: pros and cons

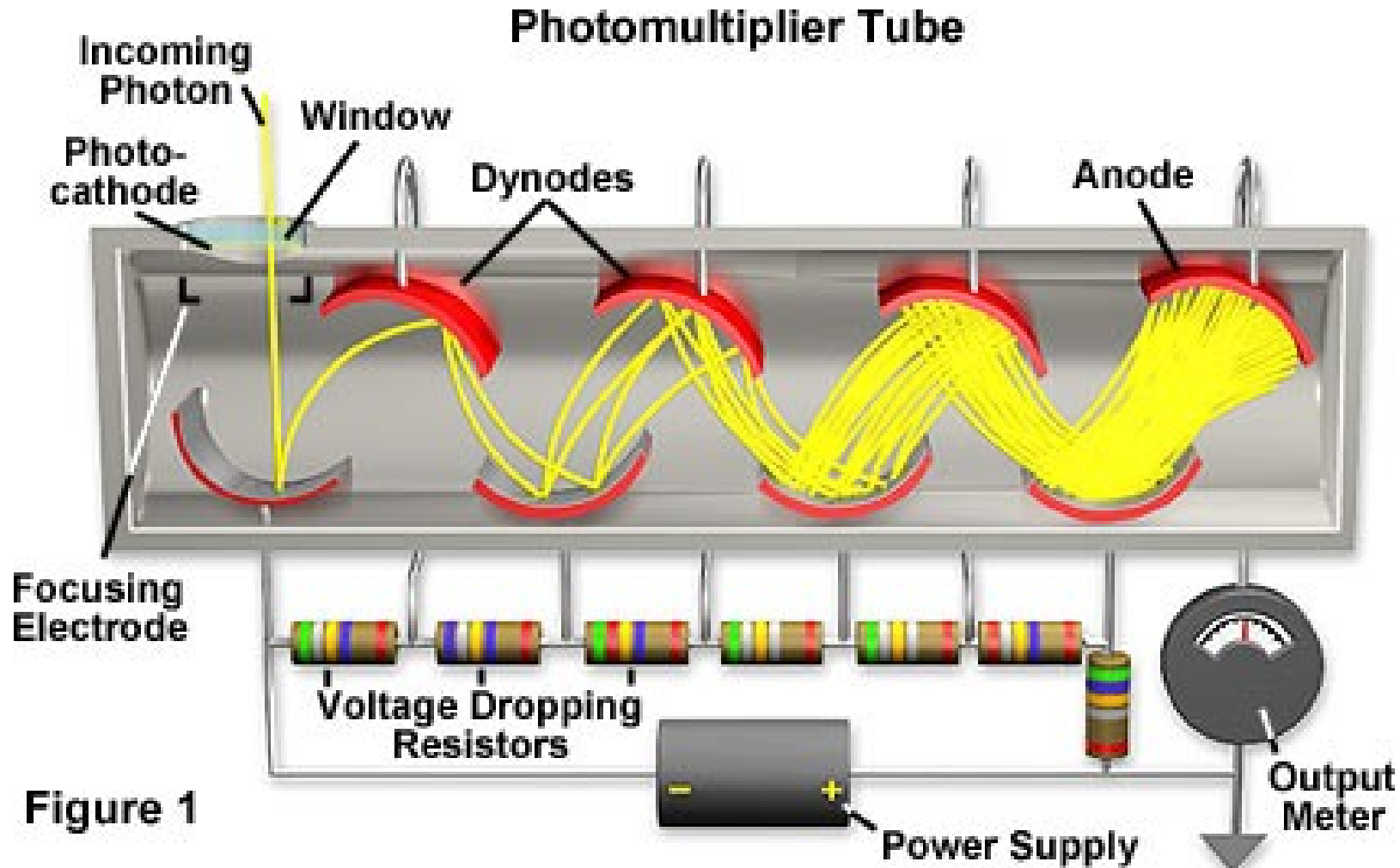


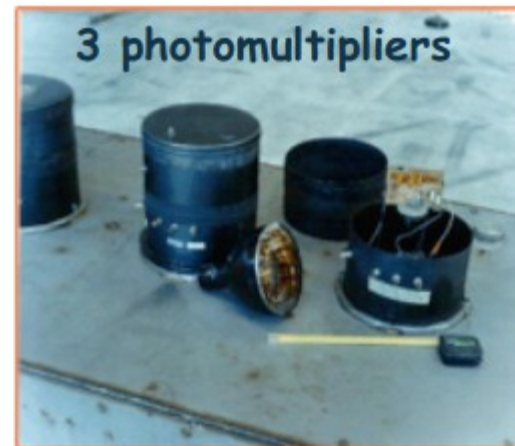
Figure 1

- *Well known and mastered technology*
- *Good detection efficiency (10 – 30%)*
- *Needs high voltage (1000 – 3000 Volt)*
- *Typically large devices which occupies a big volume*
- *Not so easy to make them radiopure*

PMTs in Astroparticle: LVD



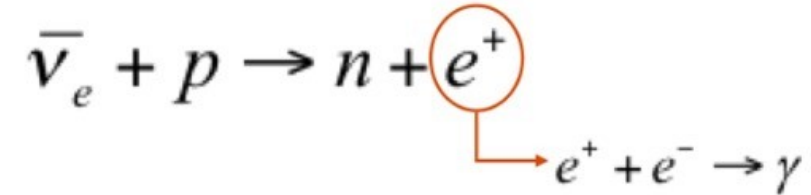
- *Observatory for Supernova neutrino Burst operating since 1992*
- **840 scintillator counters** of 1,5 m³ in three independent towers
- Each counter viewed by **three 15 cm PMTS** => **FEU49b or FEU125**
- Detects (anti) neutrino through **inverse beta decay** => two correlated signals: a prompt one from *emission and annihilation of the positron* and a *delayed neutron absorption*



PMTs in Astroparticle: LVD

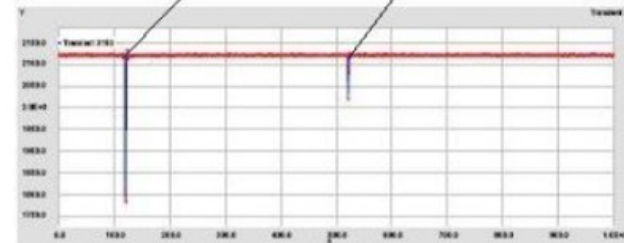
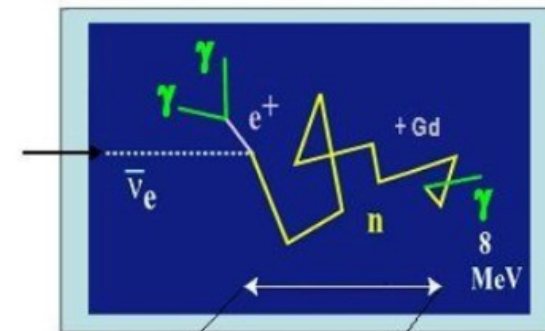


the Inverse Beta Decay:

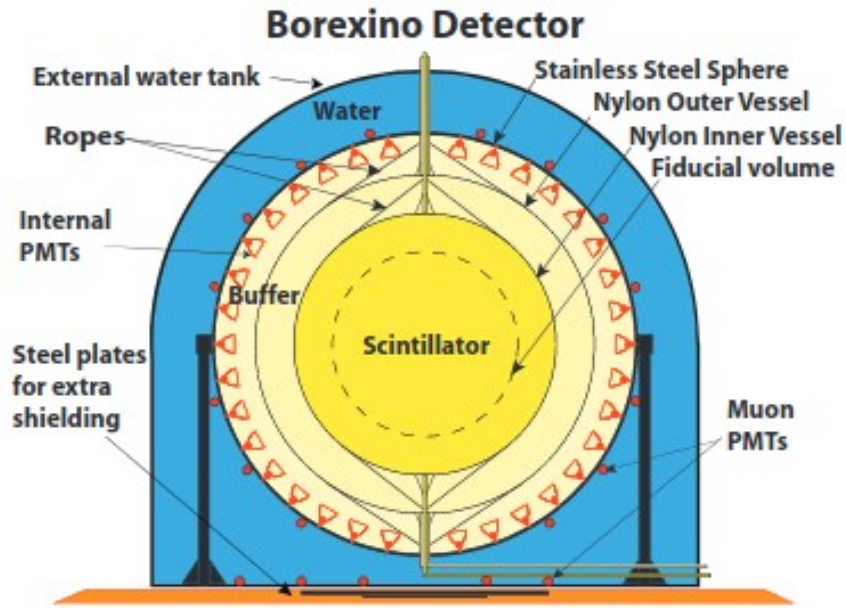


The visible energy for this interaction:

$$E_{vis} = E_{\bar{\nu}_e} - 0.789 MeV$$



PMTs in Astroparticle: Borexino

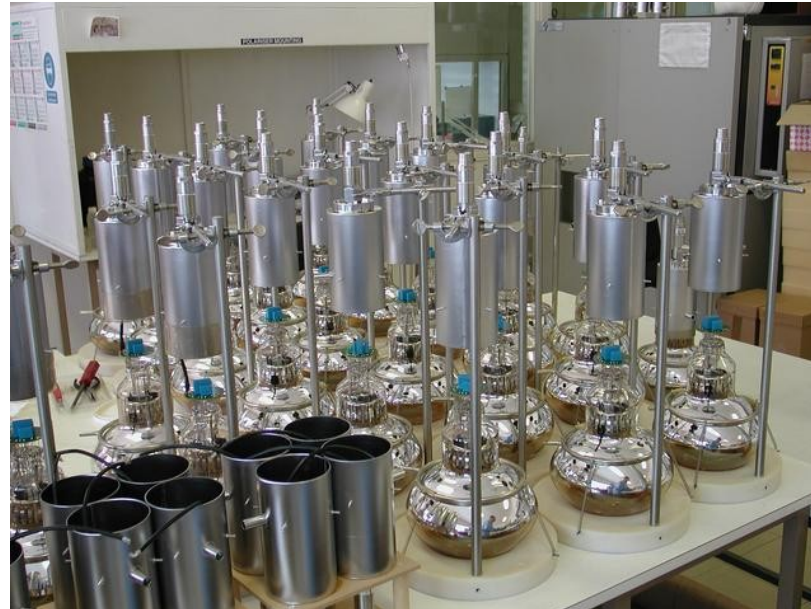
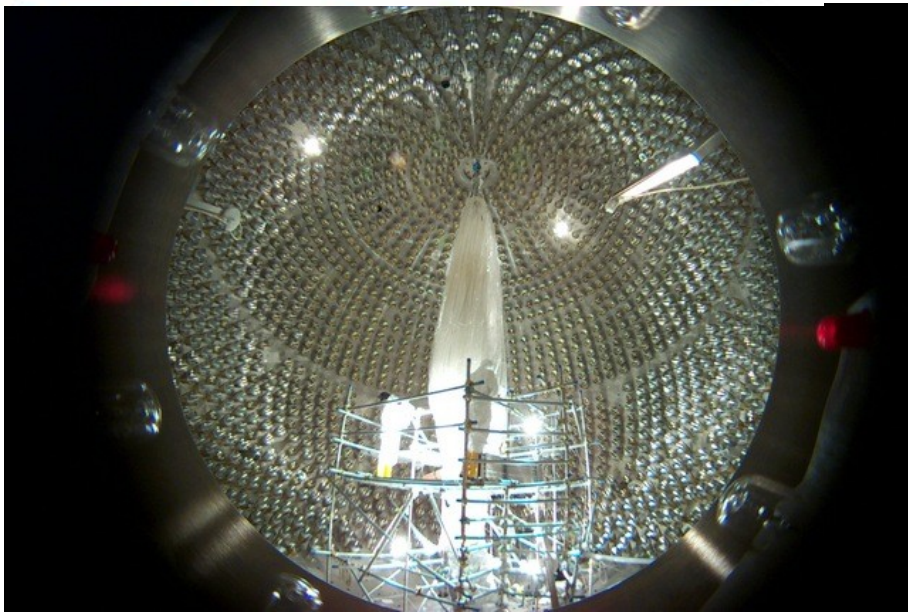


- Detects **solar neutrinos** through elastic neutrino scattering on electrons.
- **Graded shielding** form outside to inside
- **Inner scintillator mass** (pseudocumene+PPO) is **~300t**

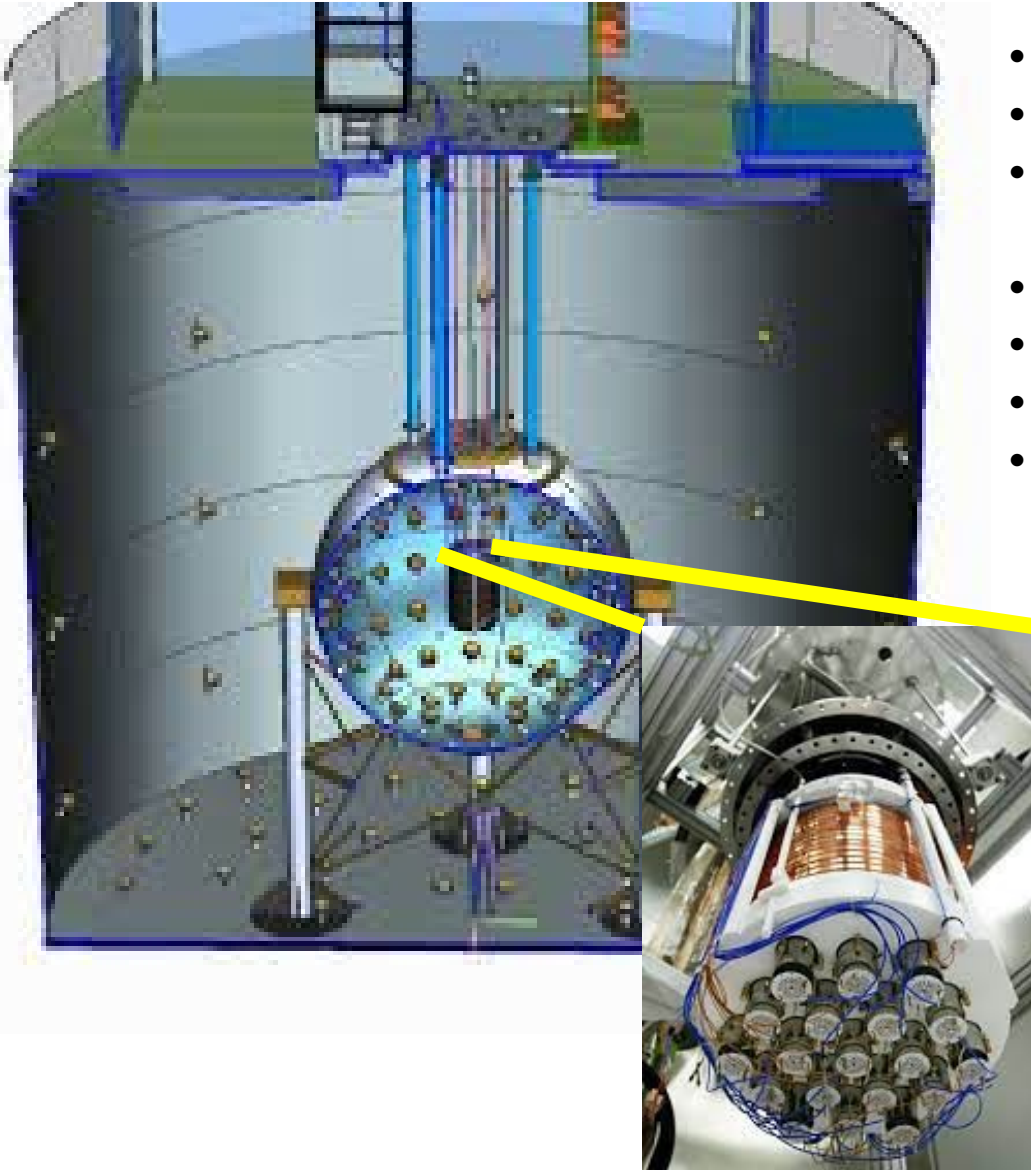
2200 ETL9351 => 8" PMTs

High gain => 10^7

Short TTS=> 1 ns



PMTs in Astroparticle: DarkSide50



- Experiment for the *direct detection of Dark Matter*
- **Dual phase depleted Ar (from ^{39}Ar) TPC**
- **38 PMTs** in the inner LAr detector=> *Hamamatsu 3" R11065 cryogenic*
- **High quantum efficiency > 35%**
- **Very low radioactive background**
- *110 Hamamatsu R5912 (8")* in the liquid scintillator of the veto
- *80 ETL 9351 8" PMTs* in the water Cherenkov muon veto.



ETL 9351



HAMAMATSU R11065

PMTs in Astroparticle: XenonNT



- *Dual phase Xe experiment **for direct Dark Matter detection***
- *XenonNT **uses 8 ton of Lxe readout by 494 PMTs***
- **Hamamatsu 3" R11410-21**
- **Cryogenic**
- **High QE ~ 35% -UV sensitive**
- **Ultra low background**



KM3NeT multi-PMT optical module

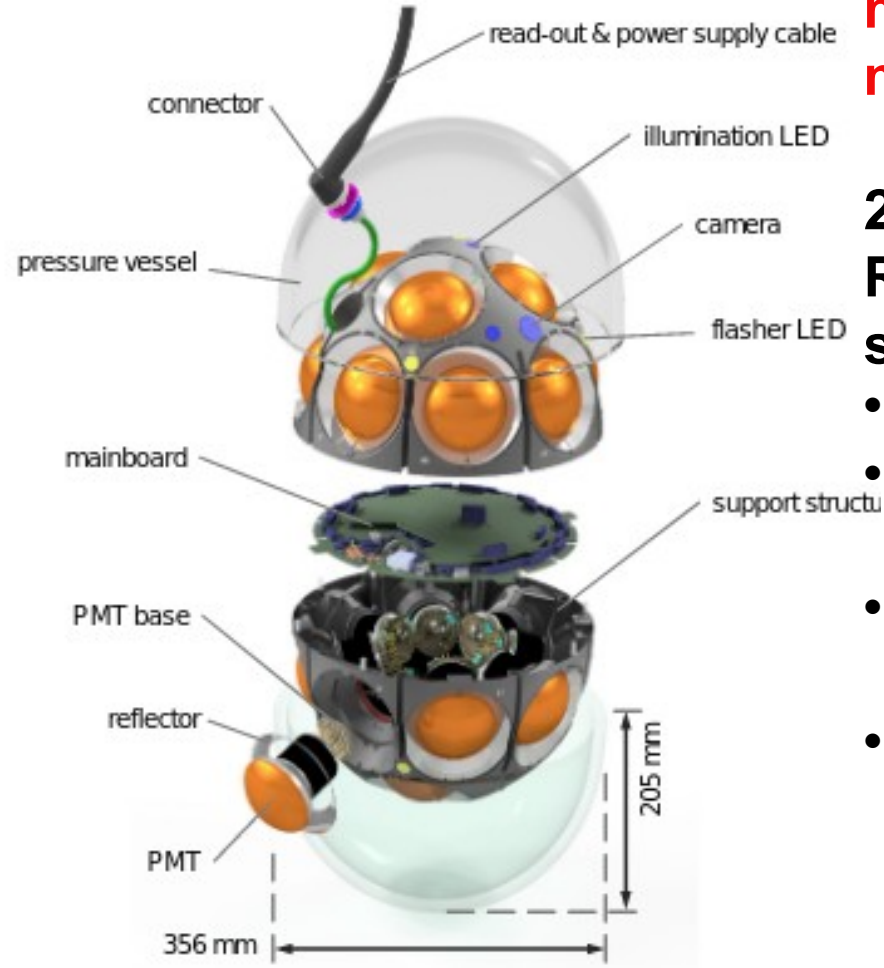


Undrsea experiment for atmospheric and high energy neutrinos: two sites in the Mediterranean Sea

Optical module is made of a **glass sphere containing 31 3" PMTs, calibration and readout electronics**

- A **Photocathode area of about 1300 cm^2** three times the area of a single 10" PMT,
- **Uniform angular coverage**
 - *Sensitivity to the incoming direction of detected photons*
- Good photon counting performance;
- Possibility to define **local triggers** (implemented onshore) **based on the pattern of PMT signals** => *background suppression*

ICECUBE mDOM



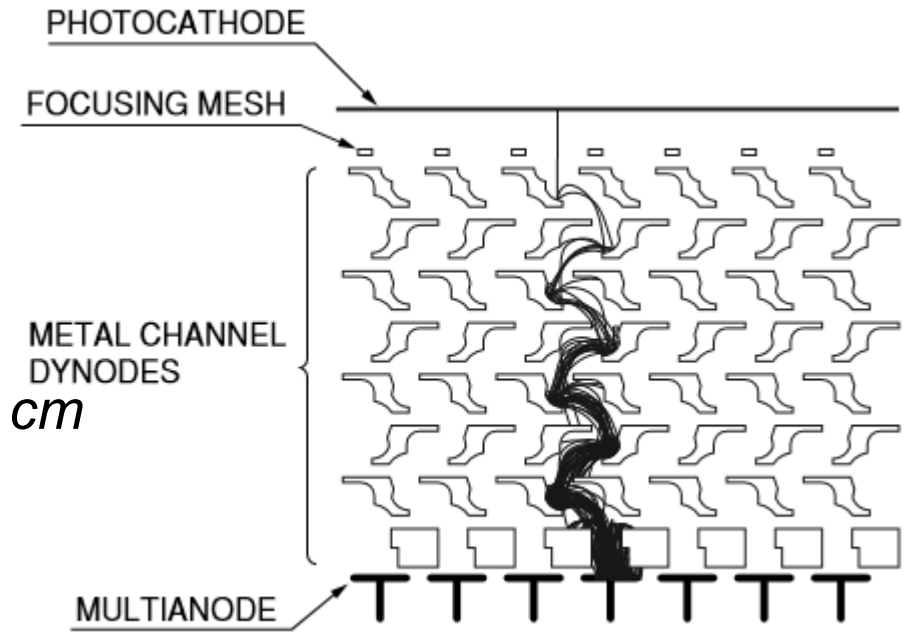
The *ICECUBE upgrade* foresees the installation of ~**400 new multiPmt digital optical modules**

24 small (3") Hamamatsu R15458-02 PMTs arranged in a spherical geometry

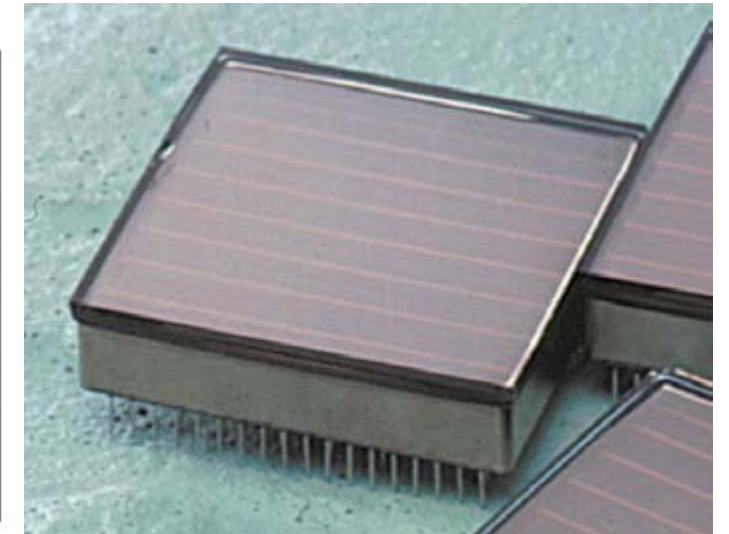
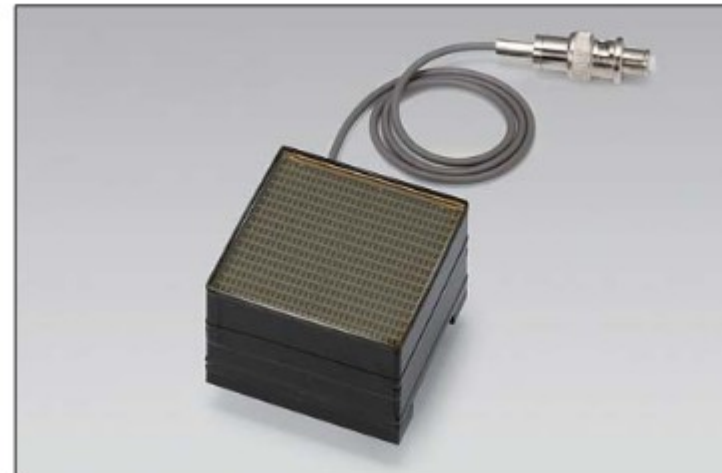
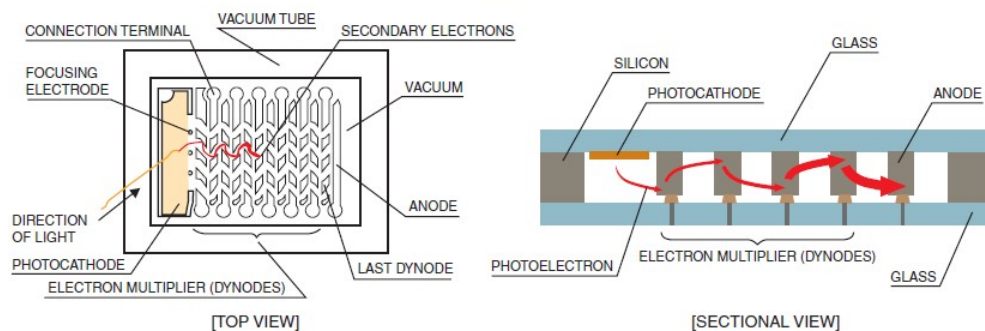
- Large optical coverage
- Homogeneous solid angle coverage
- Allows to access directional information
- Implement multiplicity triggers inside one module

Multi Anode PMT

- **Electron multiplication in narrow, independent channel**
 - The read-out is performed with a **segmented anode**
 - *Position sensitive*
 - *Tolerance to modest B field*
- *Exist in many anode segmentation. Dimensions ~5 cm x 5 cm*
- **High gain, high QE**
- Limited cross talk <2%
- **MicroPMT**: very small, flat single channel devices

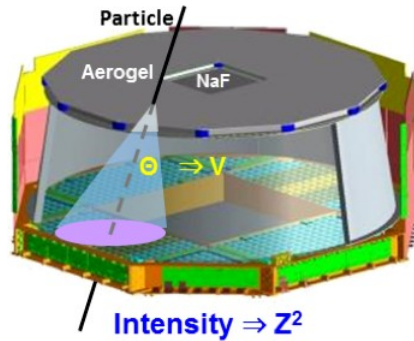
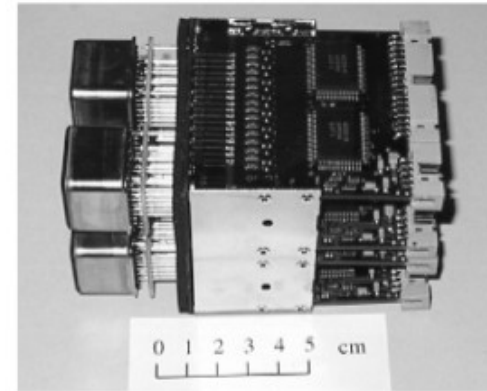


Micro PMT internal structure

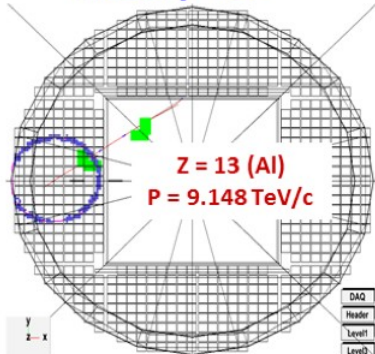
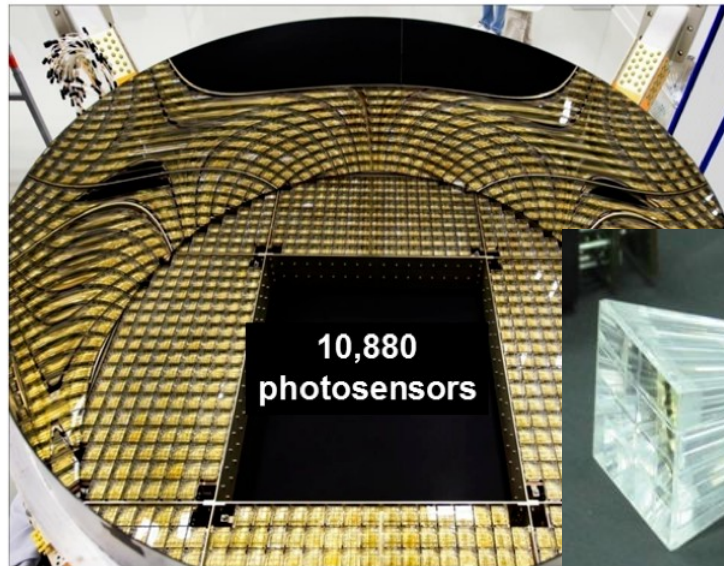


Multi Anode PMTs: Applications

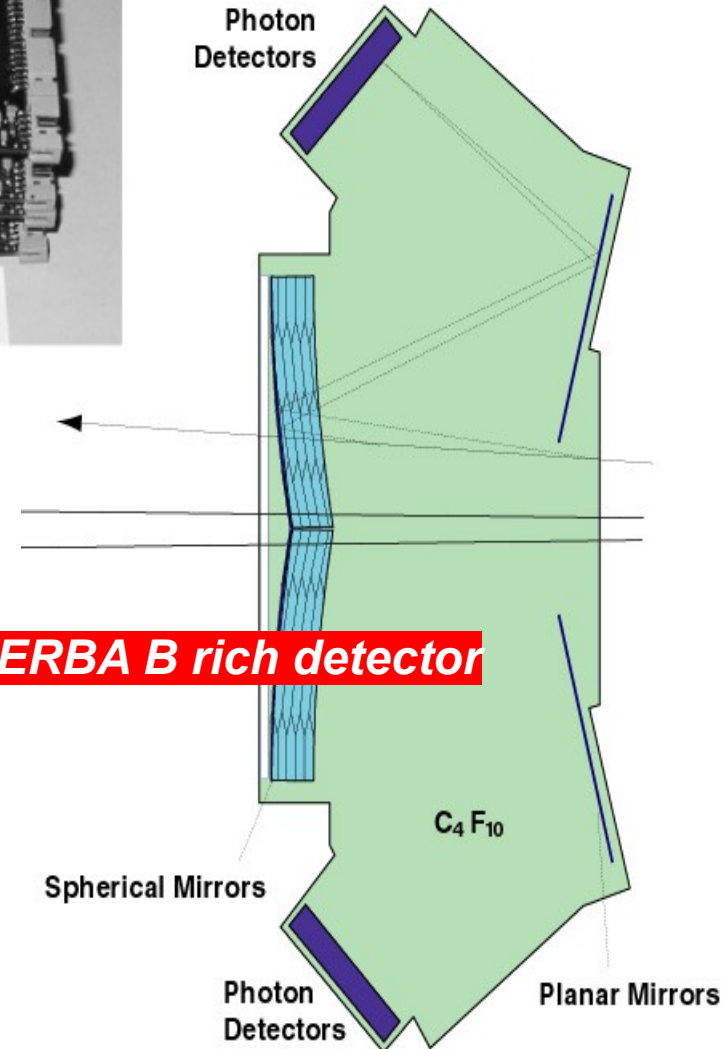
- **RICH detectors** (HERA-B first with MaPMTs)
- **Positron Emission Tomography**



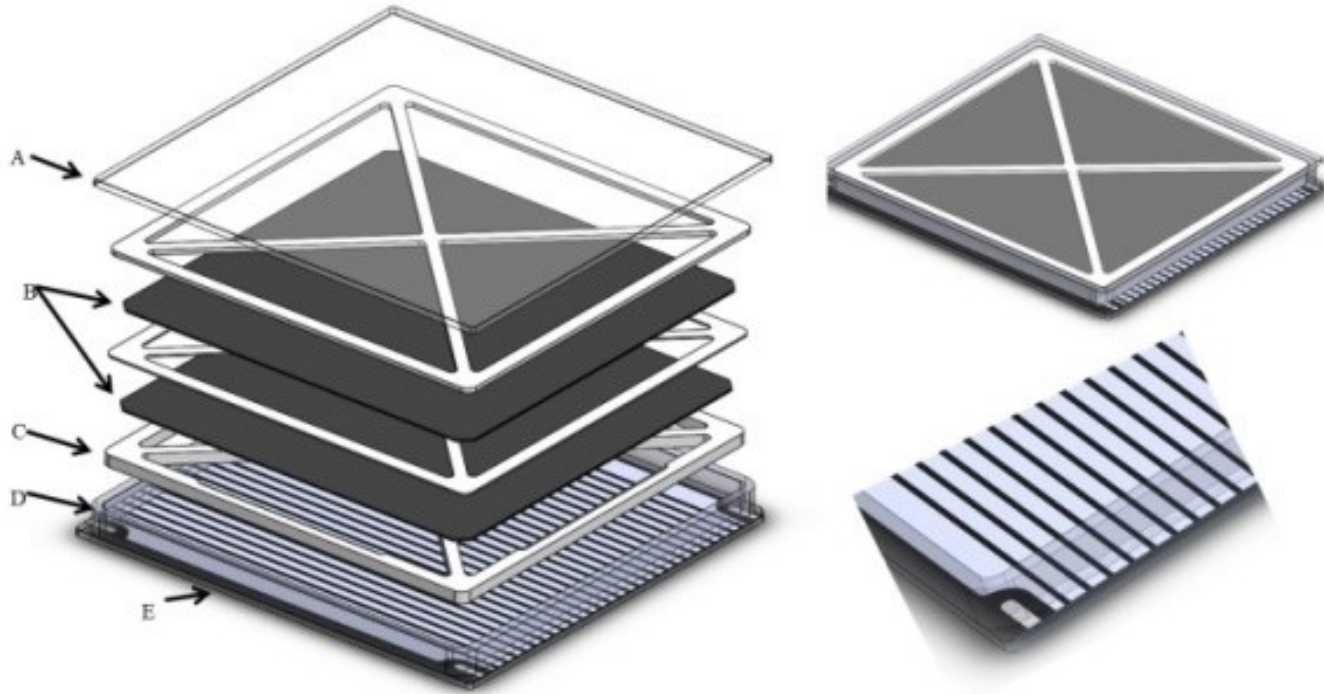
AMS Rich detector



HERBA B rich detector

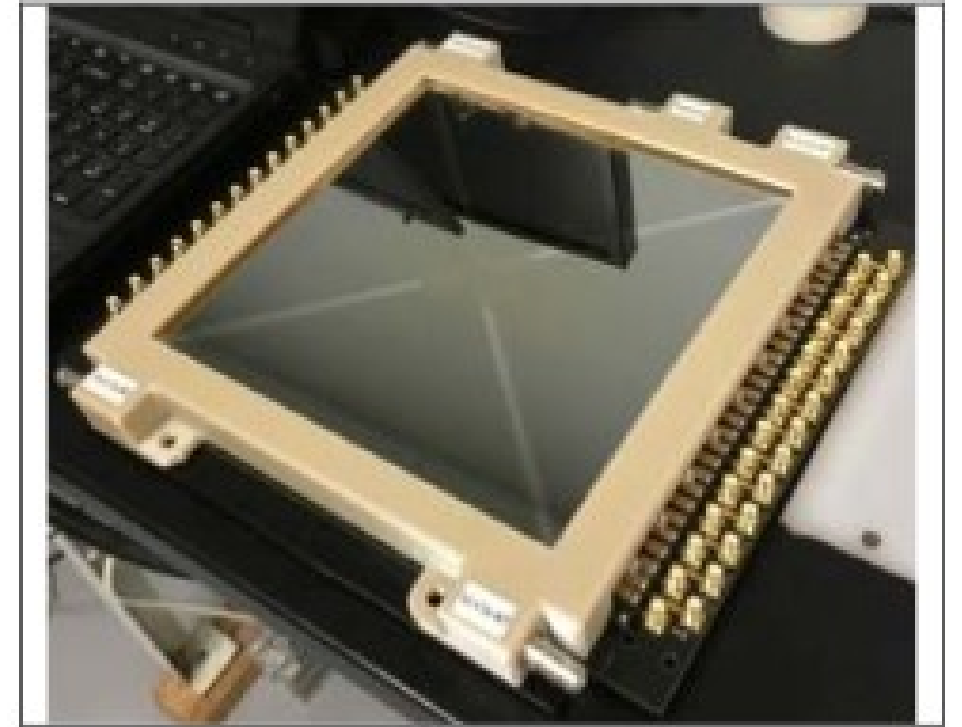


LAPPD Large Area Picosecond Photodetector



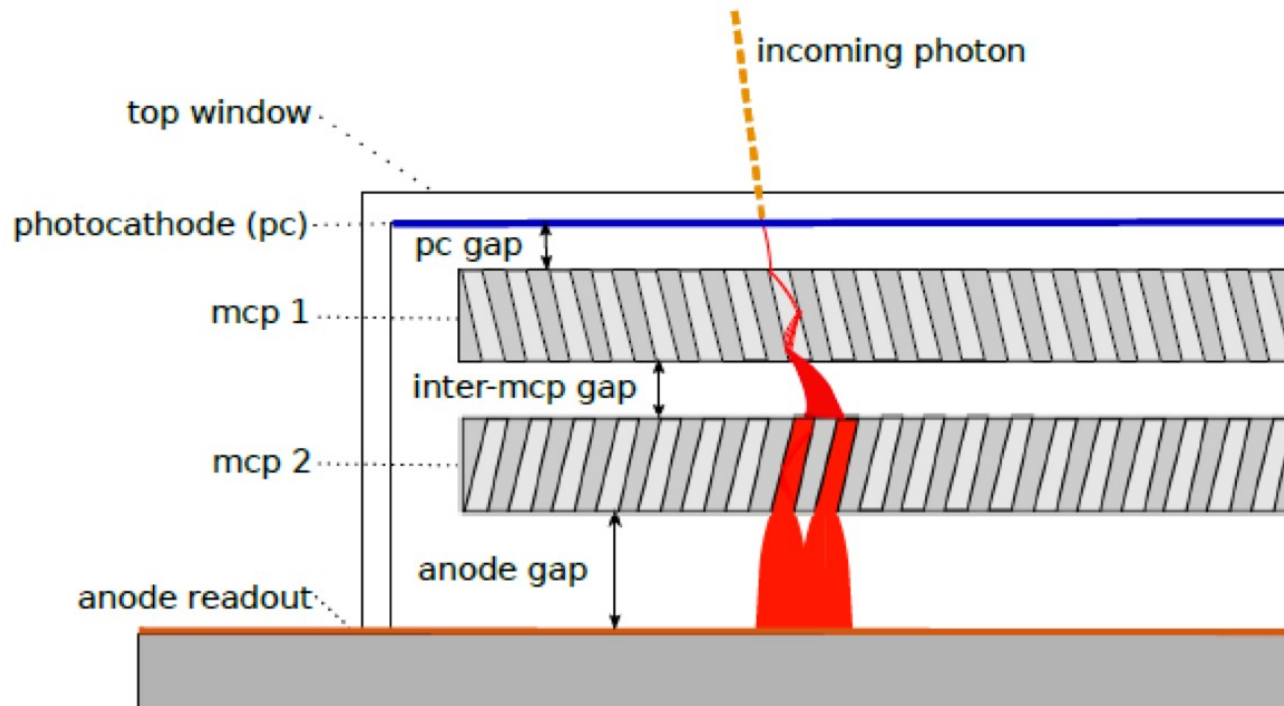
- Large area (20 cm X 20 cm) **vacuum device**
- Fused silica window with MultiAlkali photochatode on the inside
- Two stages of electron multiplication through **microchannel plates**
- **Strip anode** => spatial reconstruction of the hit

- QE ~20%
- **Time resolution < 100 ps for single photon events**
- **Space resolution < 1 mm** in both directions
- Gain 10^7 @ 1 kV
- Dark noise ~20 Cts/s/cm²



LAPPD Large Area Picosecond Photodetector

Micro Plates Channel



New generation large-area high performance MCPs - enabled by two technological breakthroughs

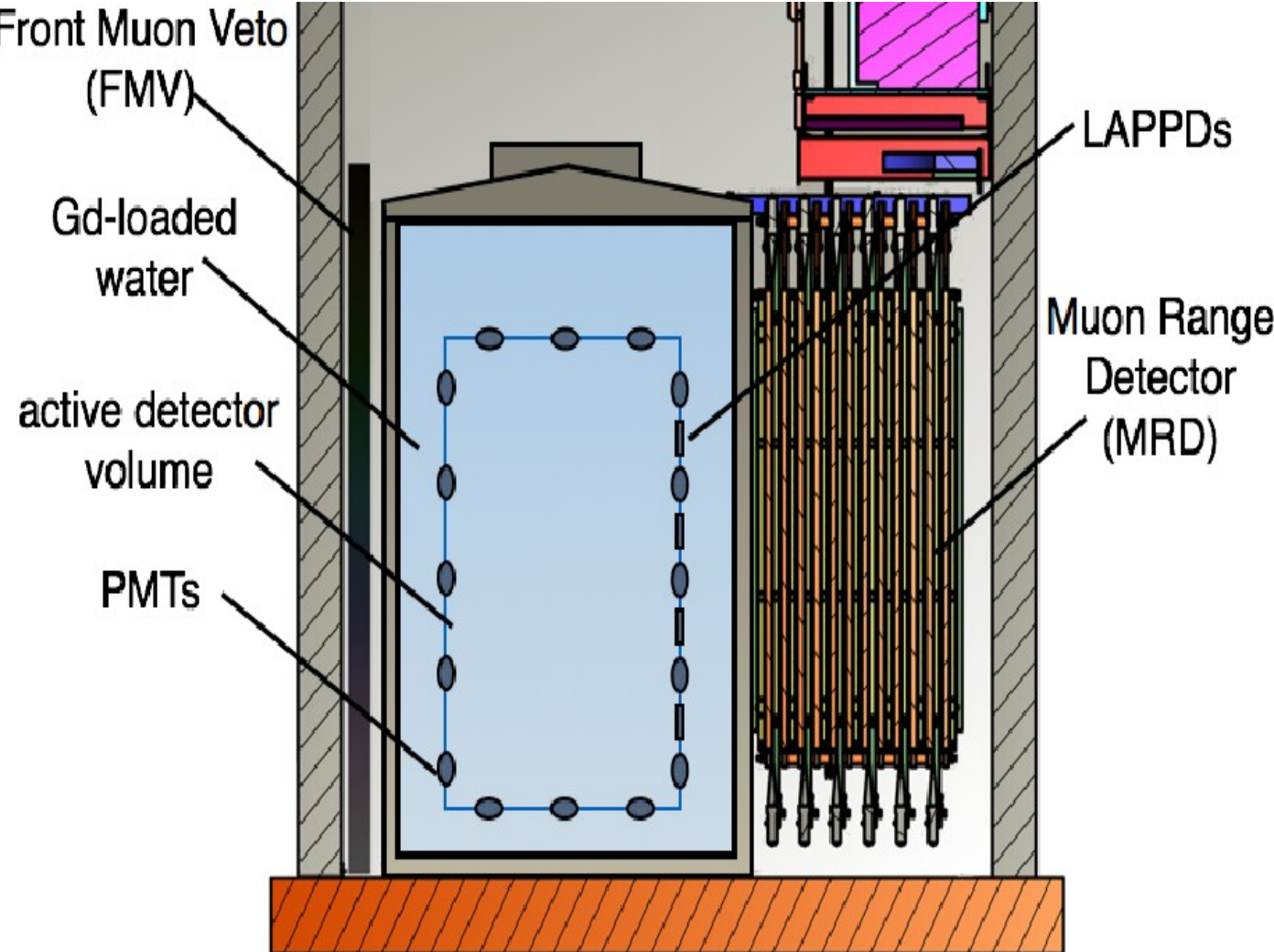
Produce **large blocks of low cost, hollow, glass capillary arrays with micron-sized pores** (Incom Inc). No need of chemical etching

Atomic layer deposition coating methods to impart the necessary resistive and secondary emission properties for high electronic gain and robust performance

LAPPD: ANNIE detector

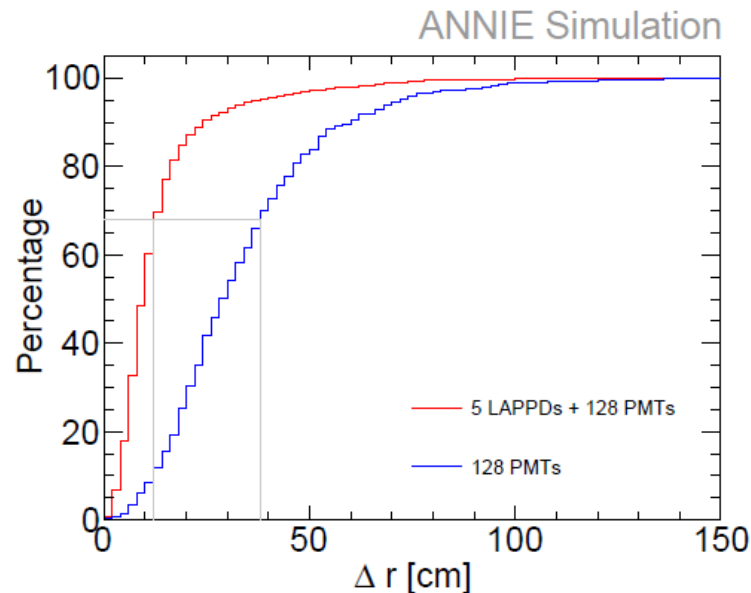
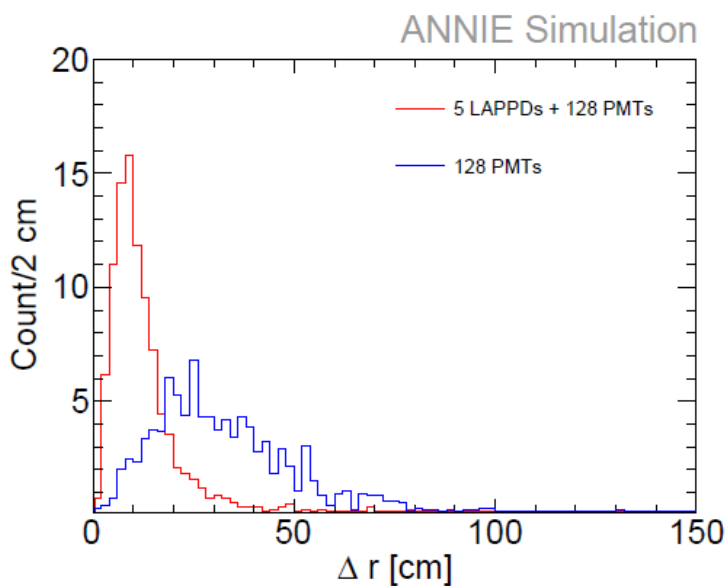
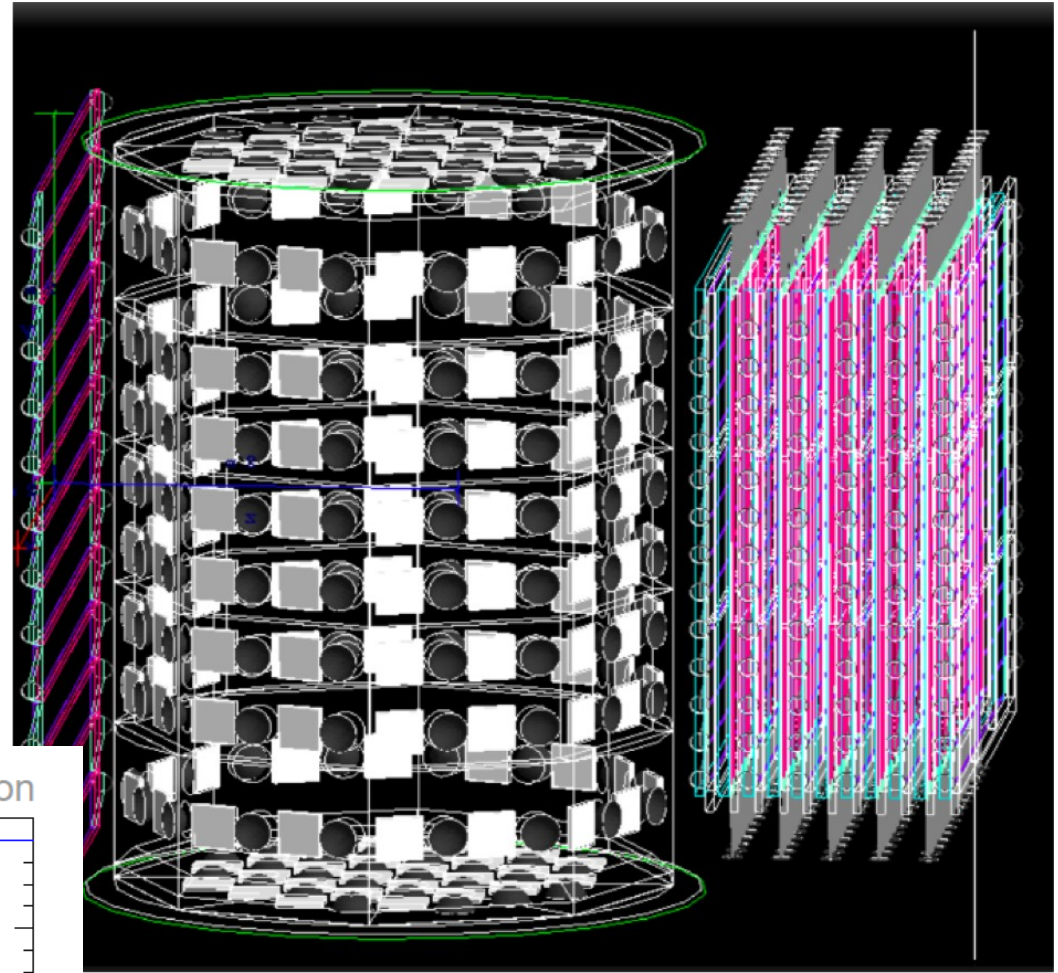
- **A**ccelerator **N**eutrino **N**eutron Interaction **E**xperiment
- **26-ton Gd-doped water Cherenkov** detector installed in the *BNB* at *Fermilab*
- **Study the neutron multiplicity** in *CC neutrino-nucleus interaction in water*
- **Demonstrate the use of LAPPD**

Identifying and counting final state neutrons is important to understand and reduce the systematic uncertainties of the neutrino energy reconstruction in oscillation experiments

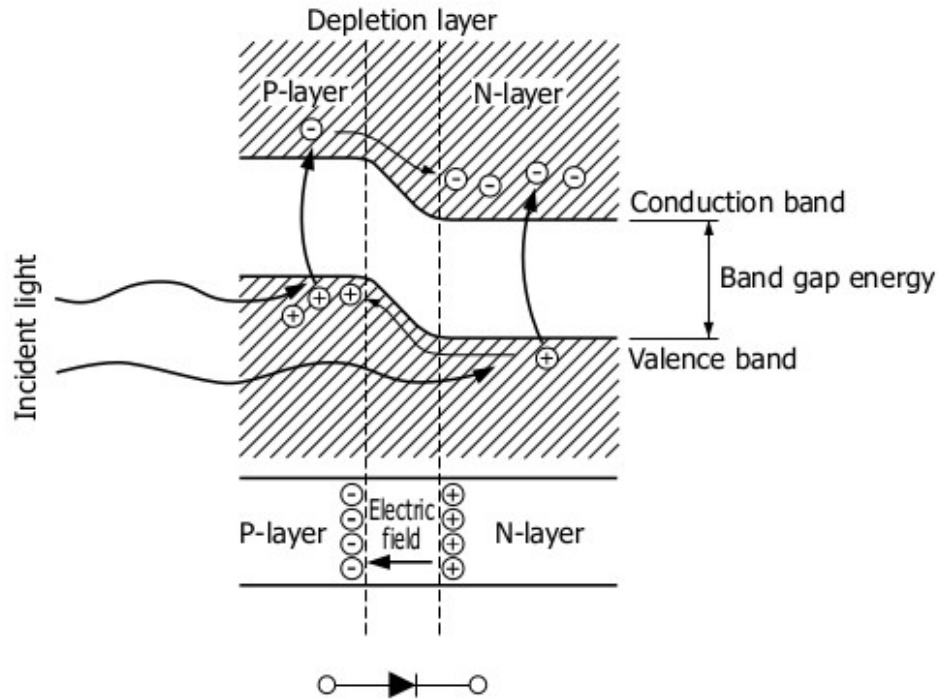


LAPPD: ANNIE detector

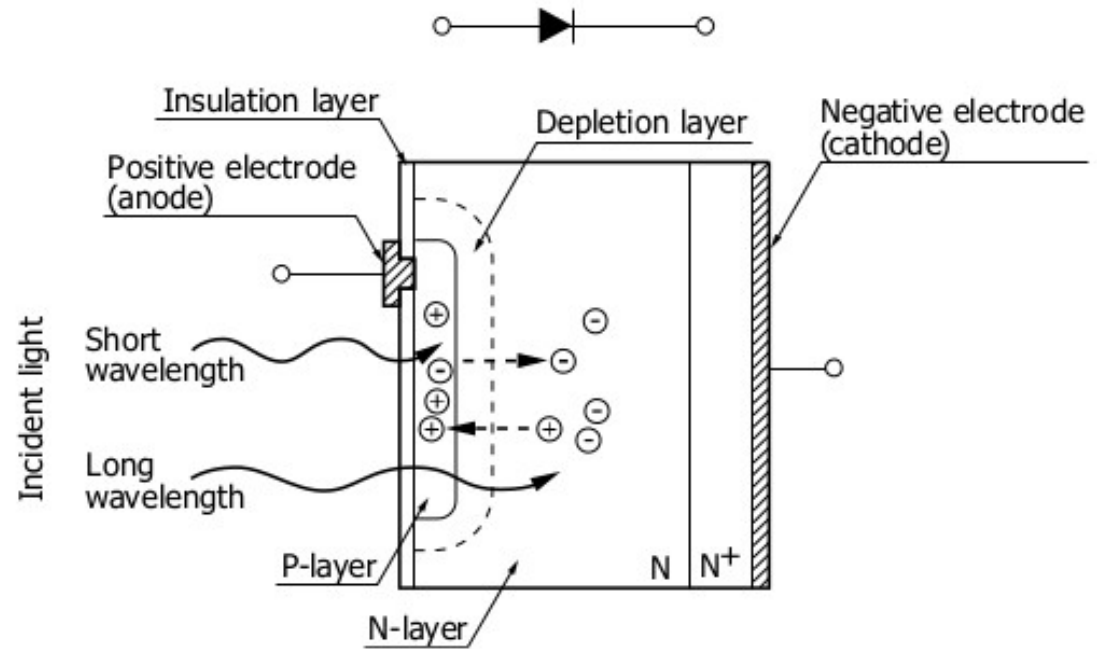
- **Fundamental measuring with precision the interaction vertex** of the neutrino to **fiducialize the active volume** => *maximize the capture prob. of neutron by Gd after thermalization*
- Using just **a small coverage of LAPPD**, complementing standard PMT (5 over 128) **significantly improves the localization of the vertex** (factor 3)



Silicon devices: PN junction



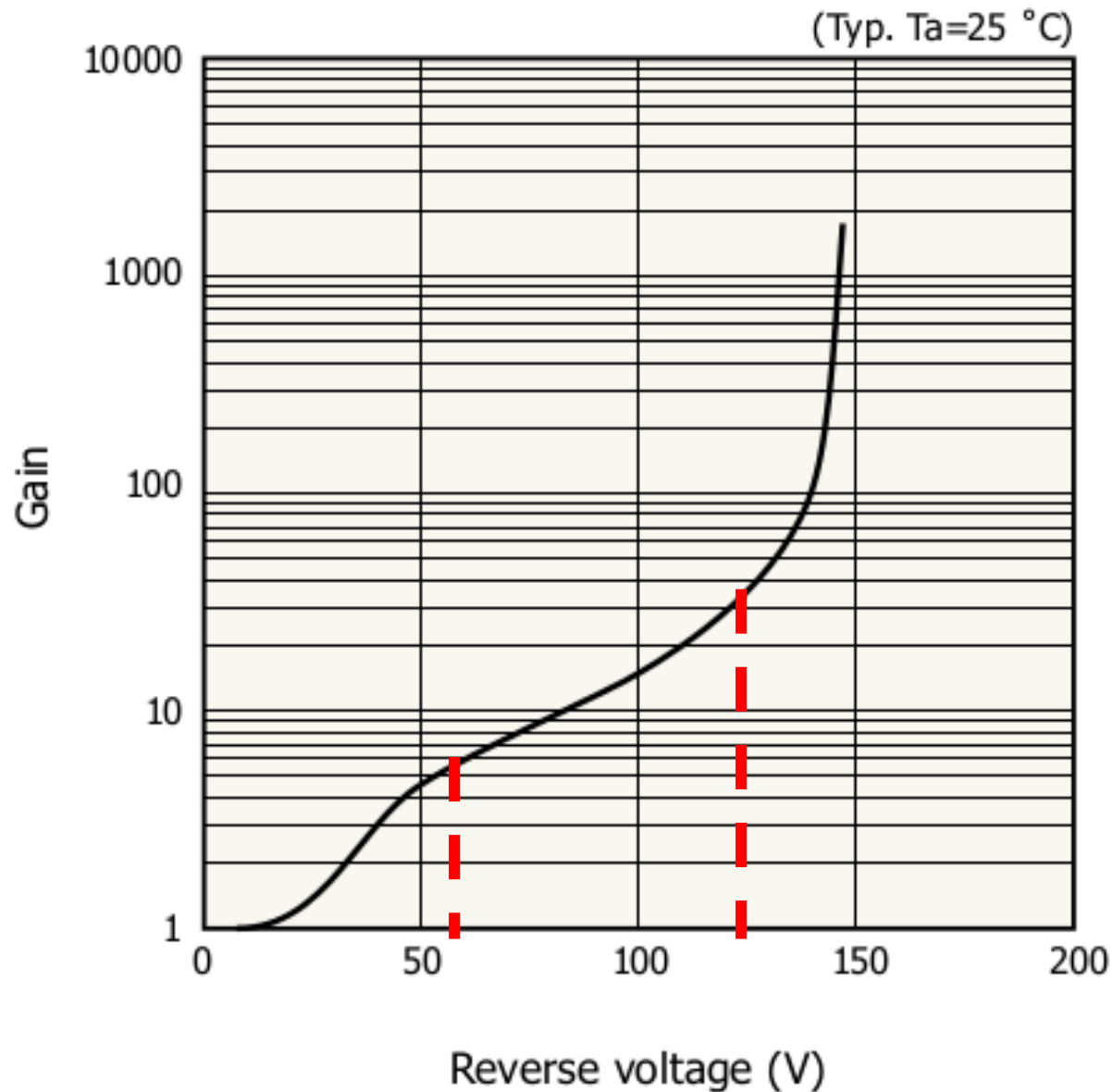
KAPDC0071EB



KPDC0002EA

Members of a larger family with PIN diode and APD (Avalanche Photo Diode). They differ for the amplification mechanism

APD

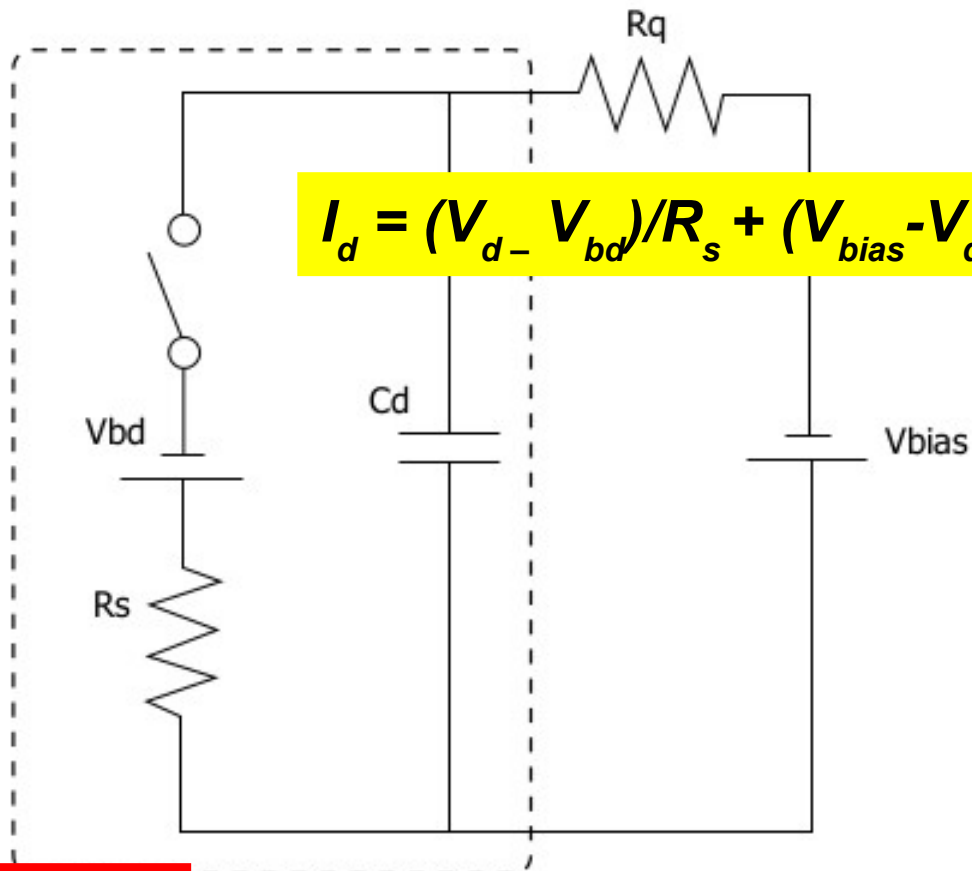


- **Depletion layer can be deepened** biasing the PN junction **in reverse**
- Increases the electric force on charge carriers => *more kinetic energy between collisions*
- If E is high enough => mean energy of carriers can exceed the silicon band gap energy between collisions => ionize lattice atoms upon impact and **release at least another electron-hole pair into conduction and valence bands per impact**

$$G = 2 + 2P^2 + 2P^3 + \dots = \sum P^i = \frac{1}{1-P}$$

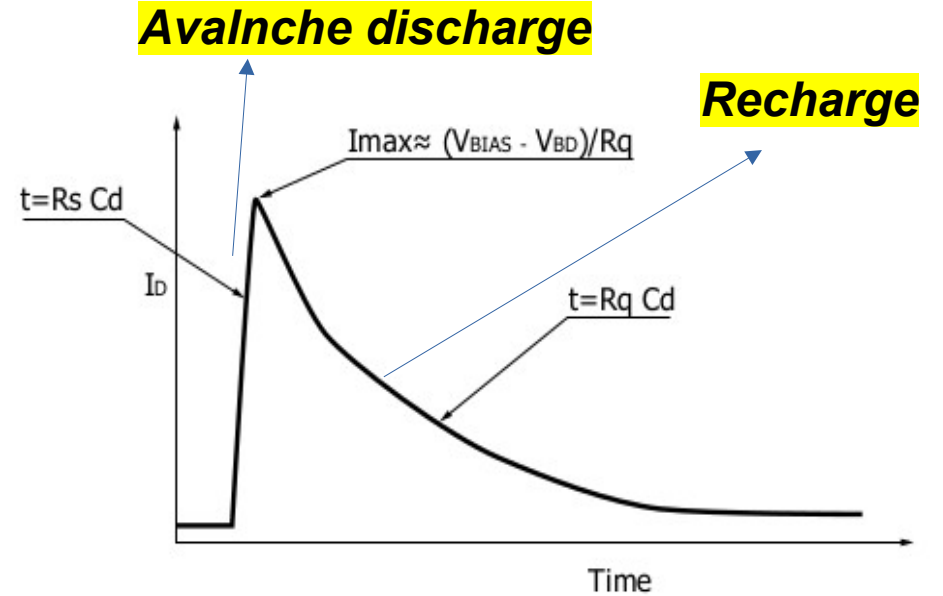
Geiger Mode APD (GAPD)

APD working in Geiger mode → digital device



$$I_d = (V_d - V_{bd})/R_s + (V_{bias} - V_d)/R_q$$

single cell



$$G = C_d (V_{bias} - V_{bd})$$

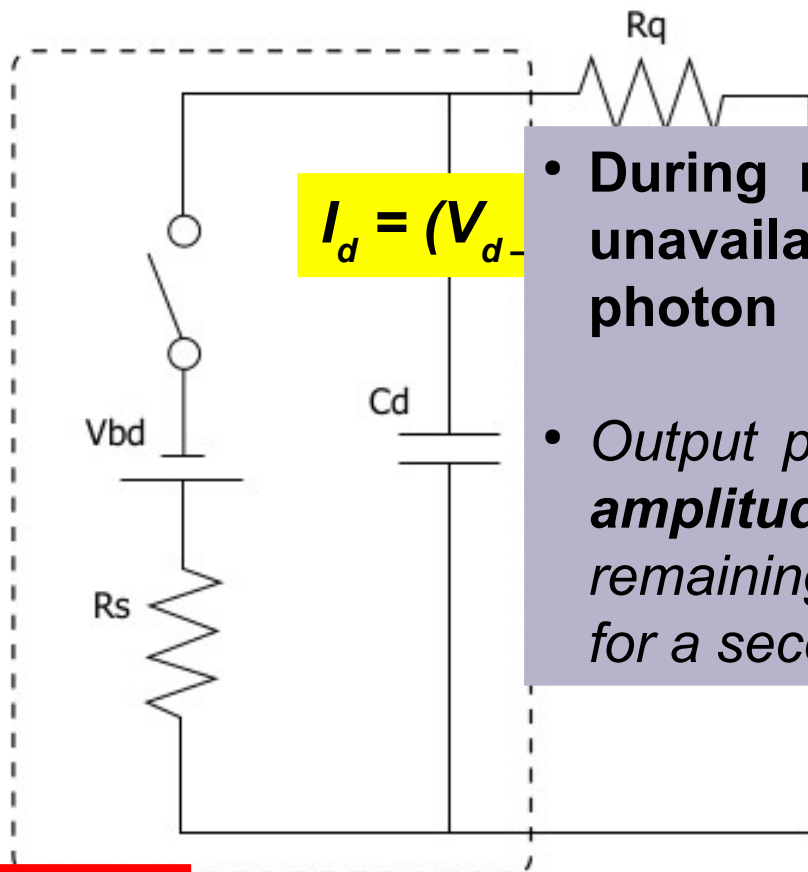
Rise time is fast ~ ns (good for timing)
Decay time slower ~ hundreds of ns

KAPDC0074EA

KAPDC0073EA

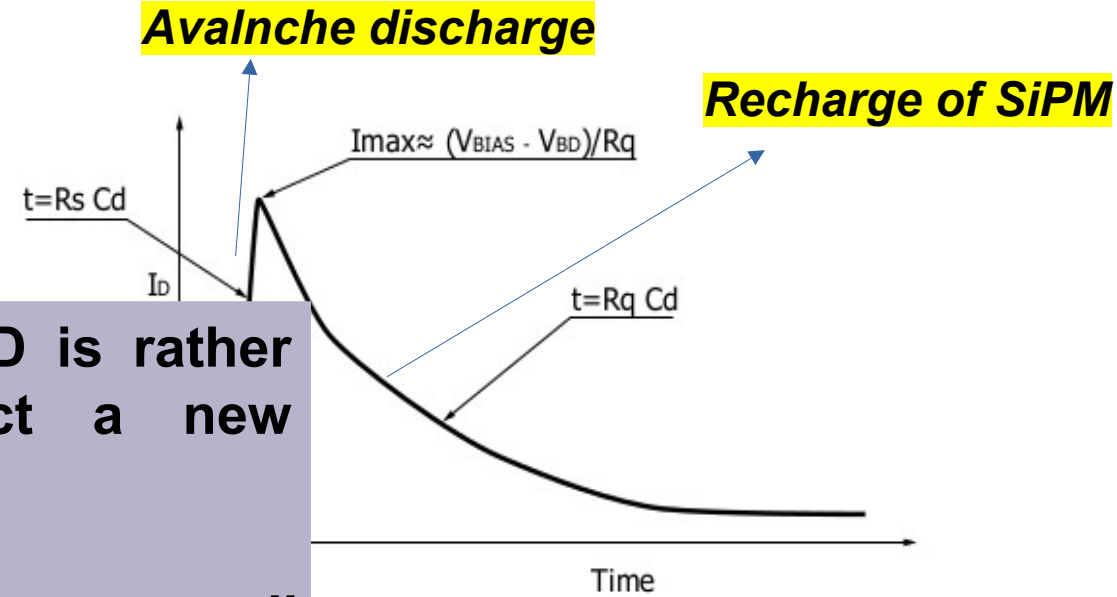
Silicon Photomultipliers equivalent circuit

APD working in Geiger mode → digital device



$$I_d = (V_{bd} - V_{d-}) / R_q$$

- During recovery GAPD is rather unavailable to detect a new photon
- Output pulse would have a **small amplitude** (depending on the remaining charge that is available for a secondary discharge)



Avalanche discharge

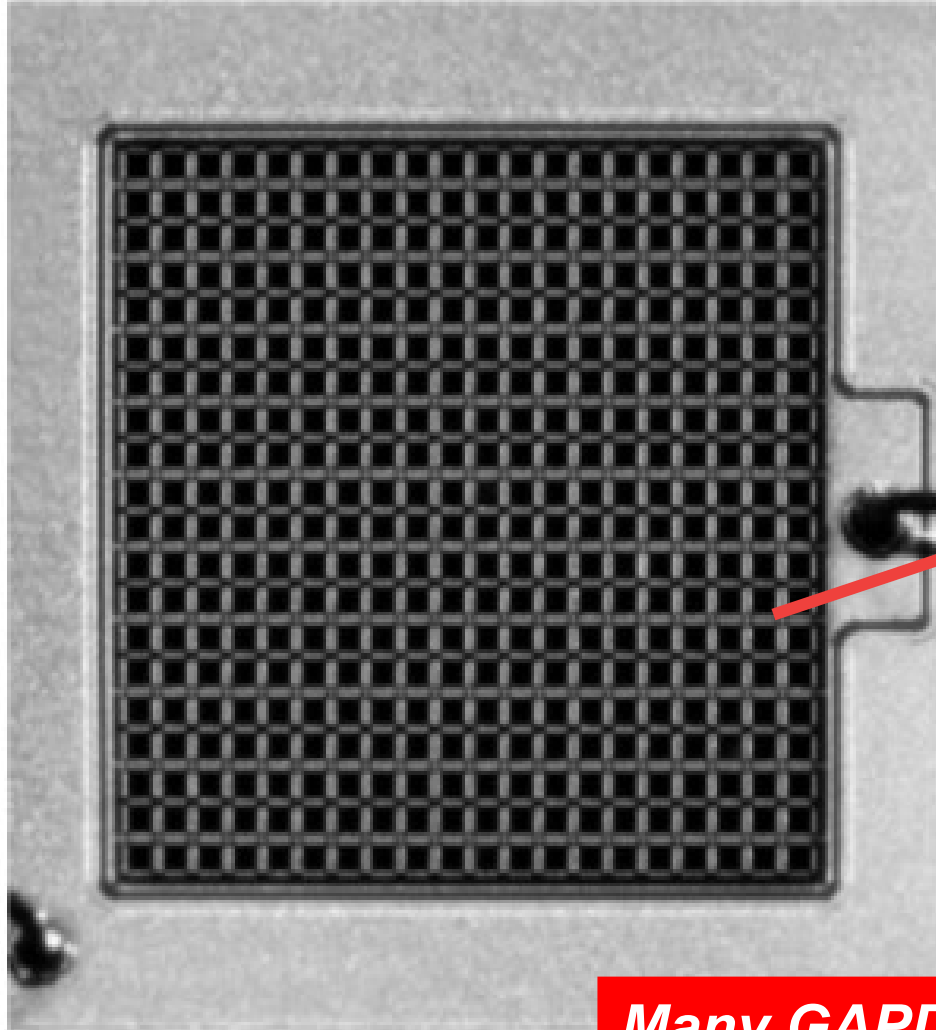
Recharge of SiPM

KAPDC0074EA

Recovery time is fast ~ ns (good for timing)
Decay time slower ~ hundreds of ns

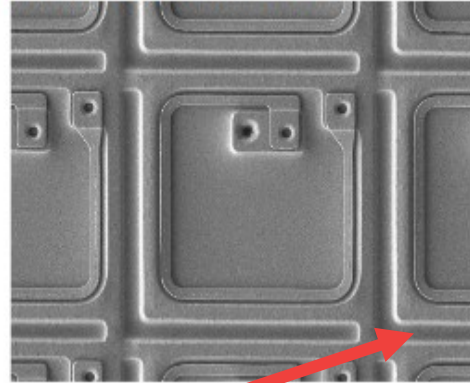
single cell

Silicon Photomultipliers (SiPM)

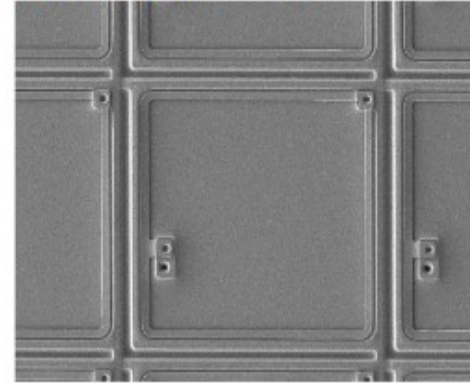


**Many GAPD
in parallel**

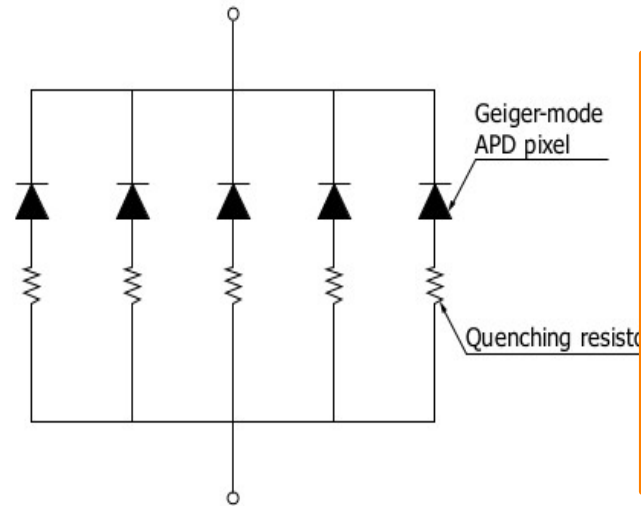
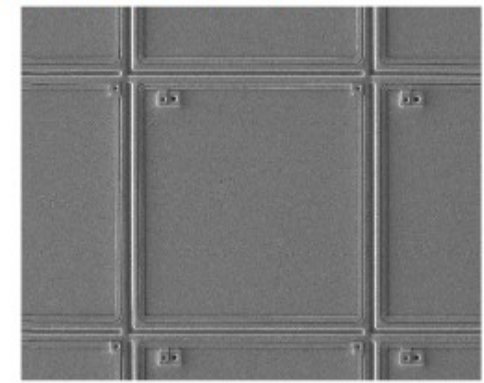
(a) Pixel pitch: 25 μm



(b) Pixel pitch: 50 μm



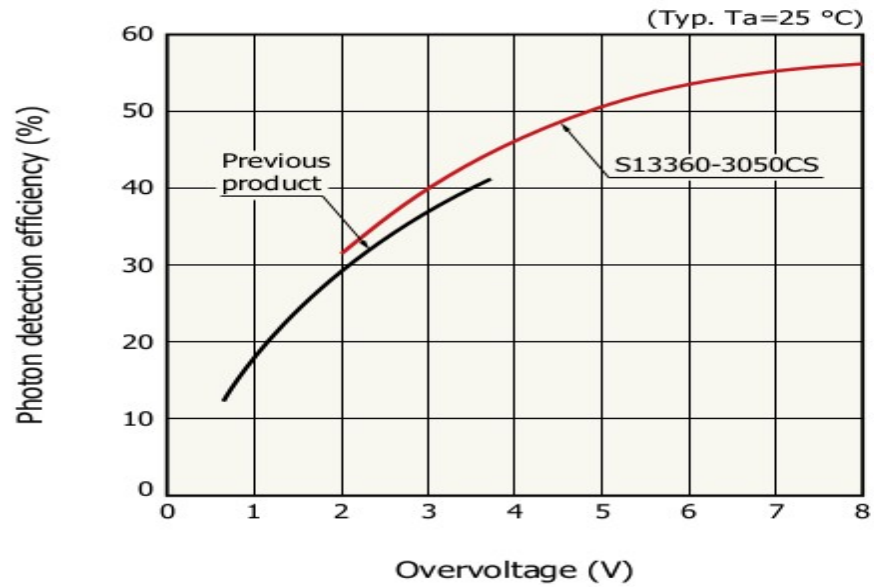
(c) Pixel pitch: 75 μm



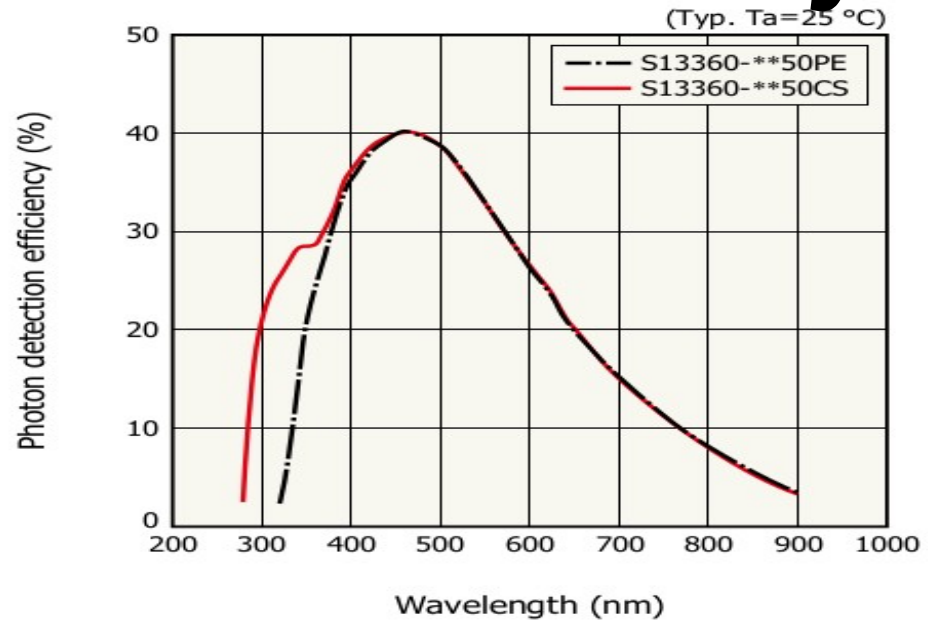
$$\text{PDE} = \text{QE} \times \text{F} \times \text{P}_a$$

QE quantum efficiency
F fill factor
 P_a probability of triggering an avalanche

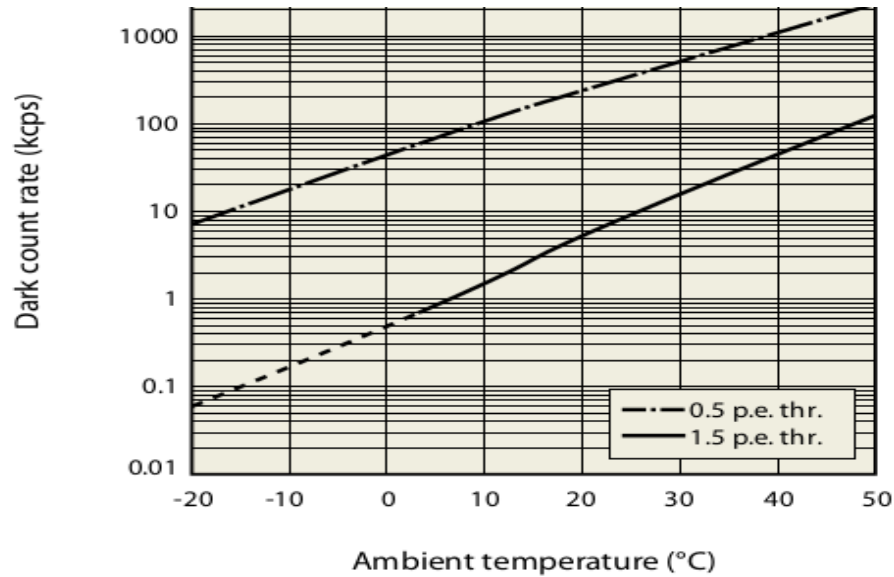
Gain and Photon Detection Efficiency



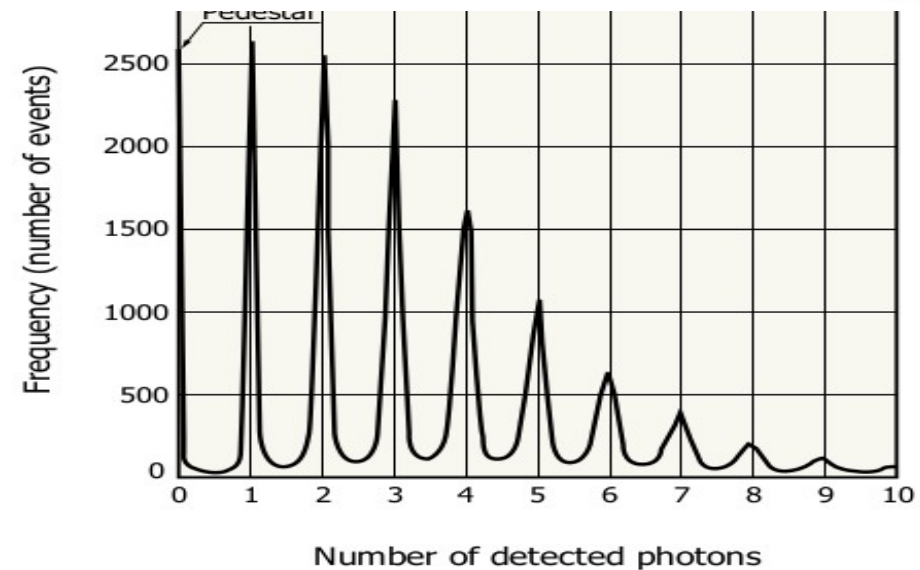
KAPDB0308EB



KAPDB0322EA

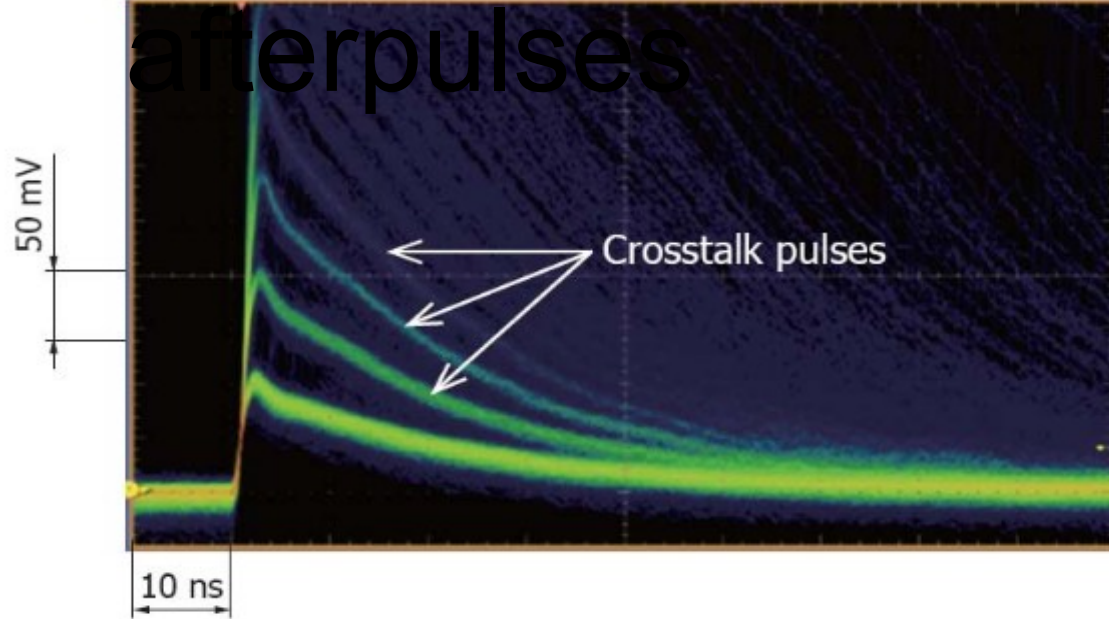


KAPDB0141EB

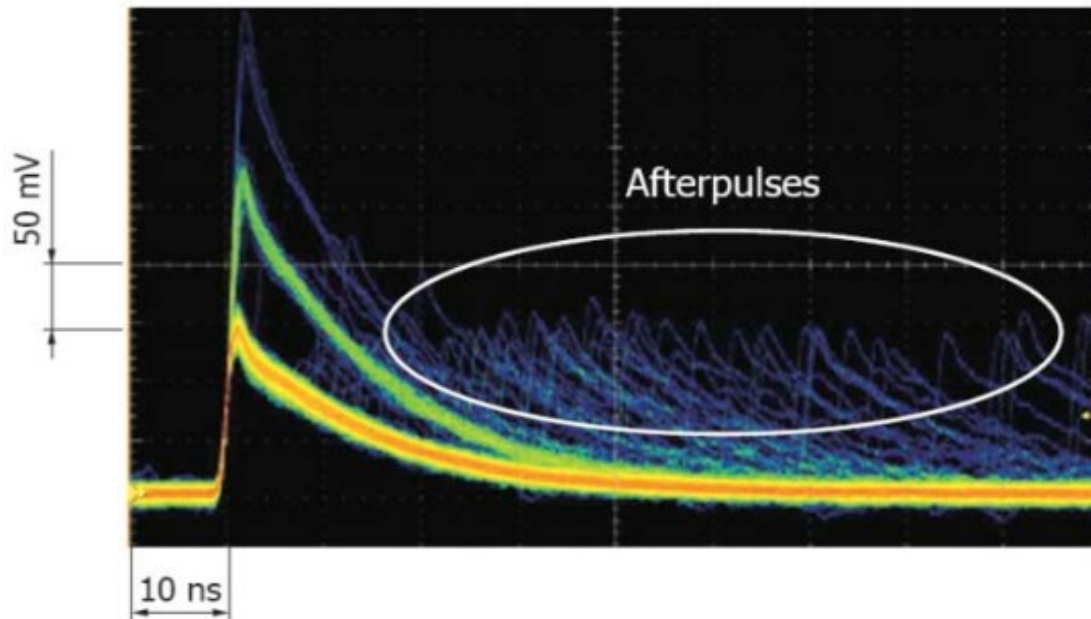


KAPDB0133EA

Cross talk and afterpulses

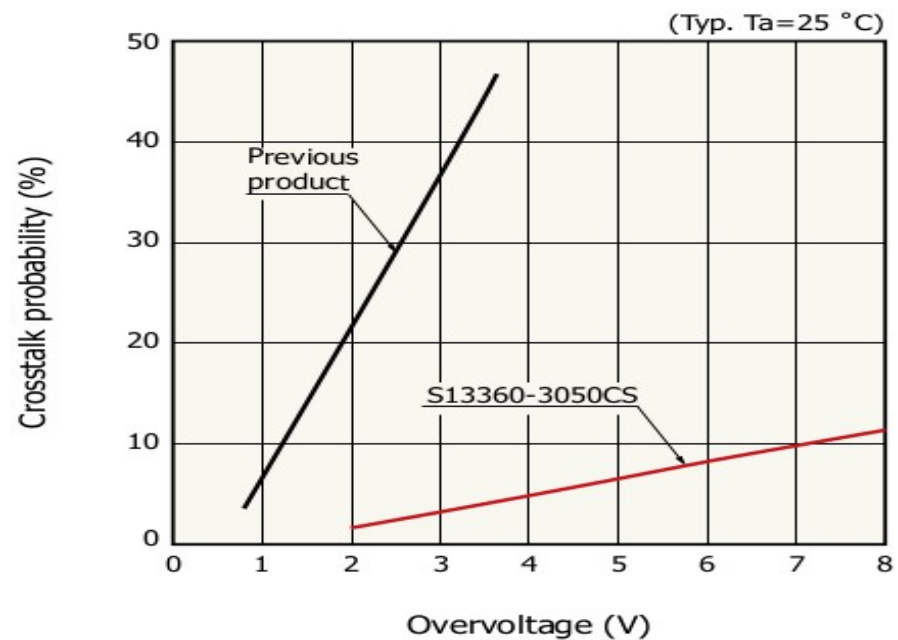
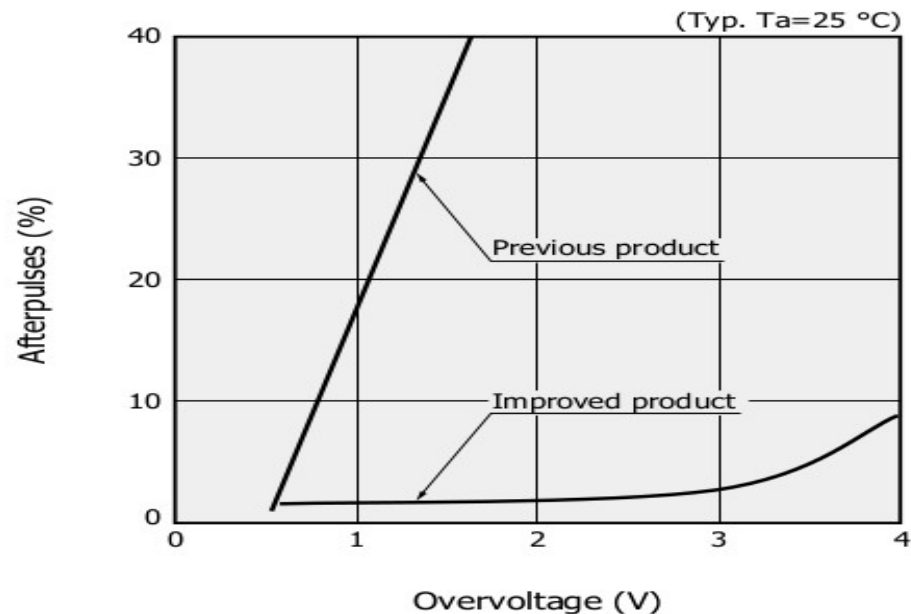
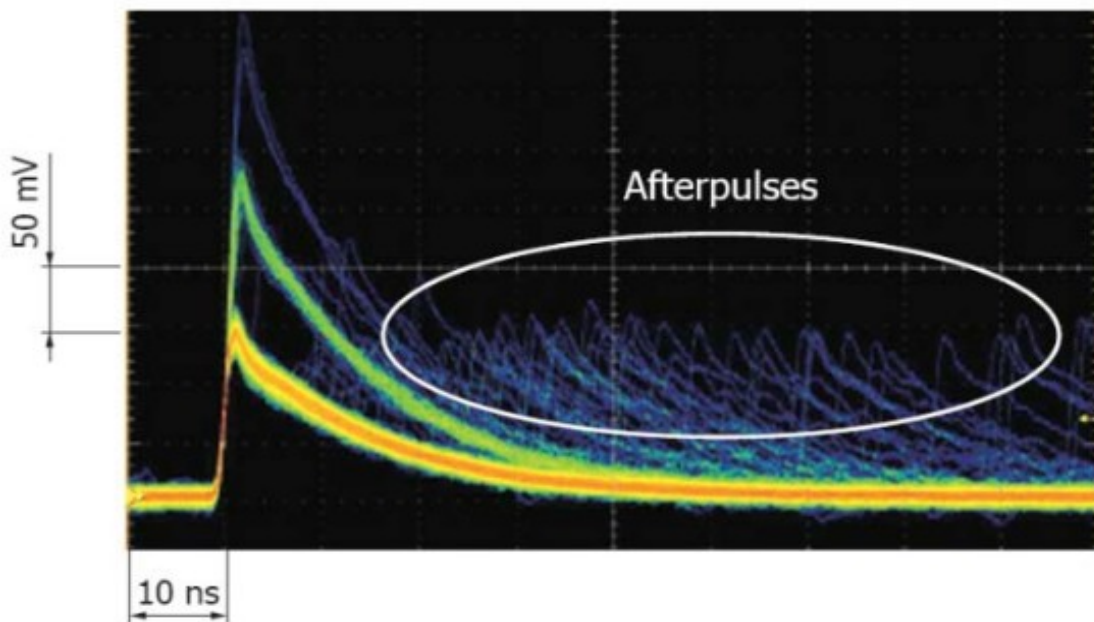
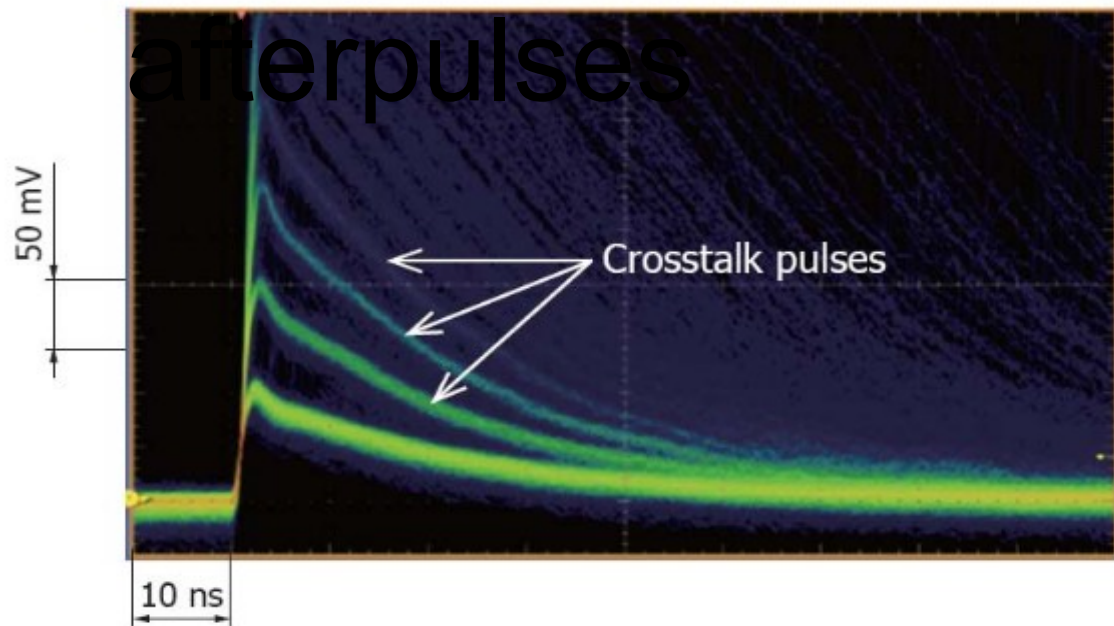


- During avalanche process, kinetic energy of avalanching carriers can be lost **through photon emission**
- Photons **can travel to the neighboring pixels and initiate avalanches**



- During avalanche process a small fraction of avalanching carriers can be **trapped in impurity energy levels**
- **Released after short delays**

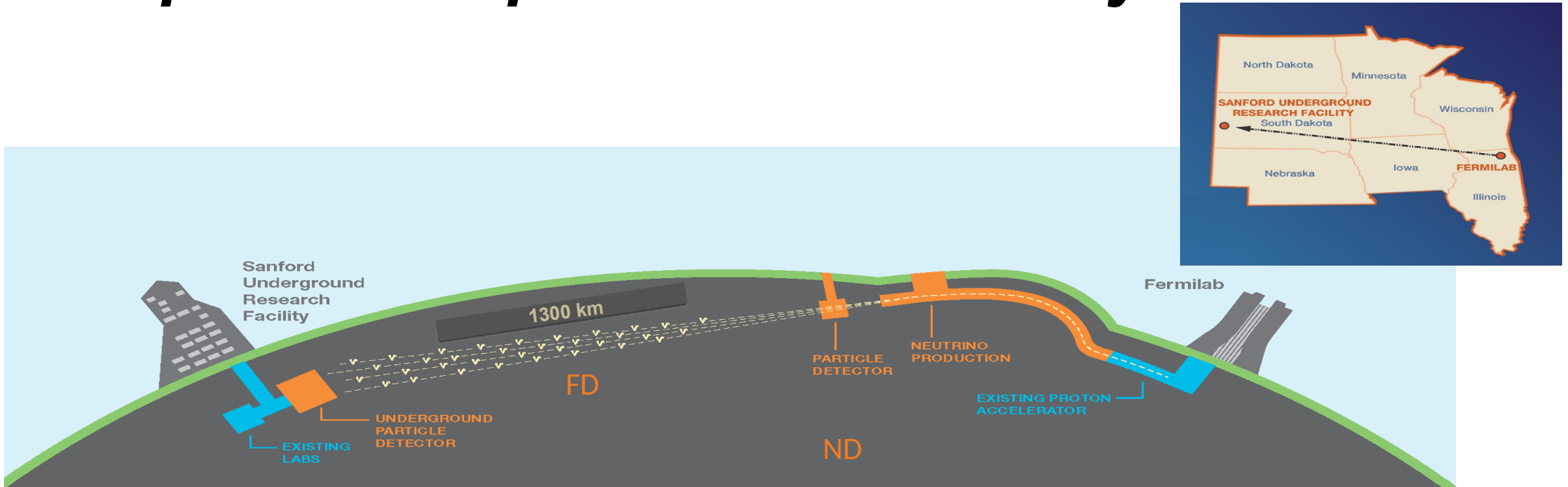
Cross talk and afterpulses



Silicon Photomultipliers – pros and cons

- ***Low bias voltage $O(50 \text{ Volt})$***
- ***Digital detectors***
- ***High gain → Single Photo electron reconstruction capability***
- ***Small amount of material => Good for low background experiments***
- ***But small active area $O(1 \text{ cm}^2)$ each***
- ***High Dark count rate at room temperature***
- ***Need of ganging schemes to reach the coverage of a standard PMT***
- ***and/or coupling with passive photon collectors***

Example: DUNE photon detection system

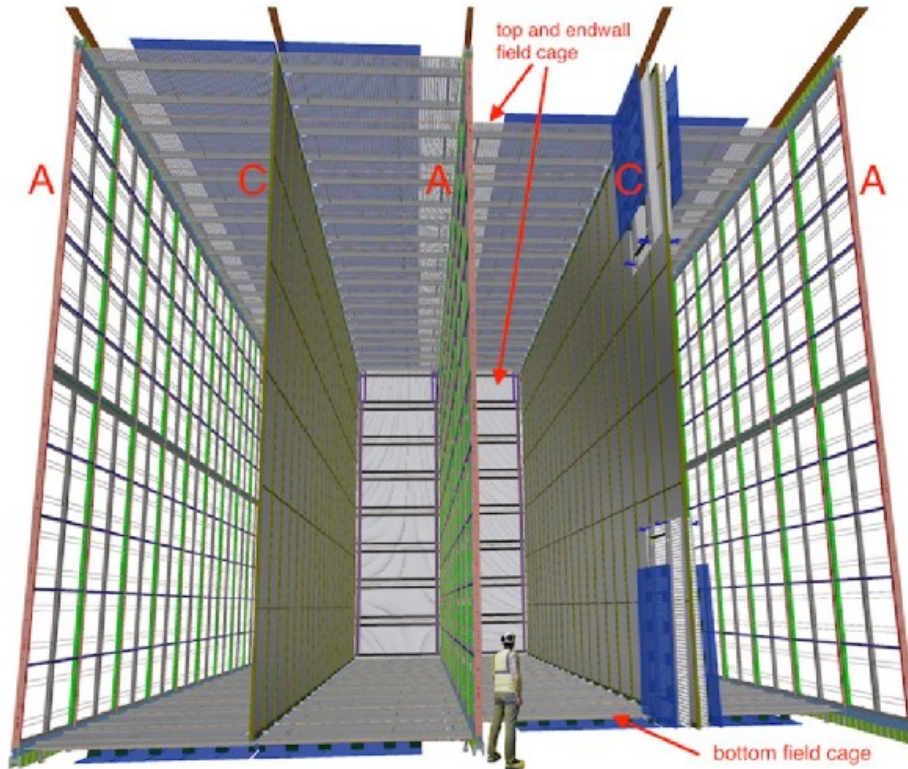
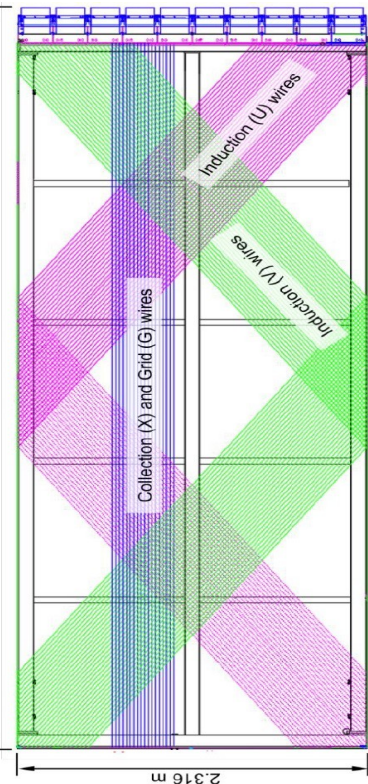


1. A high-power, wide-band **neutrino beam** (~ GeV energy range).
2. A ≈ 40 kt liquid-argon **Far Detector** in South Dakota, located 1478 m underground in a former gold mine.
3. A **Near Detector** located approximately 575 m from the neutrino source at Fermilab close to Chicago.

LAr read-out technologies

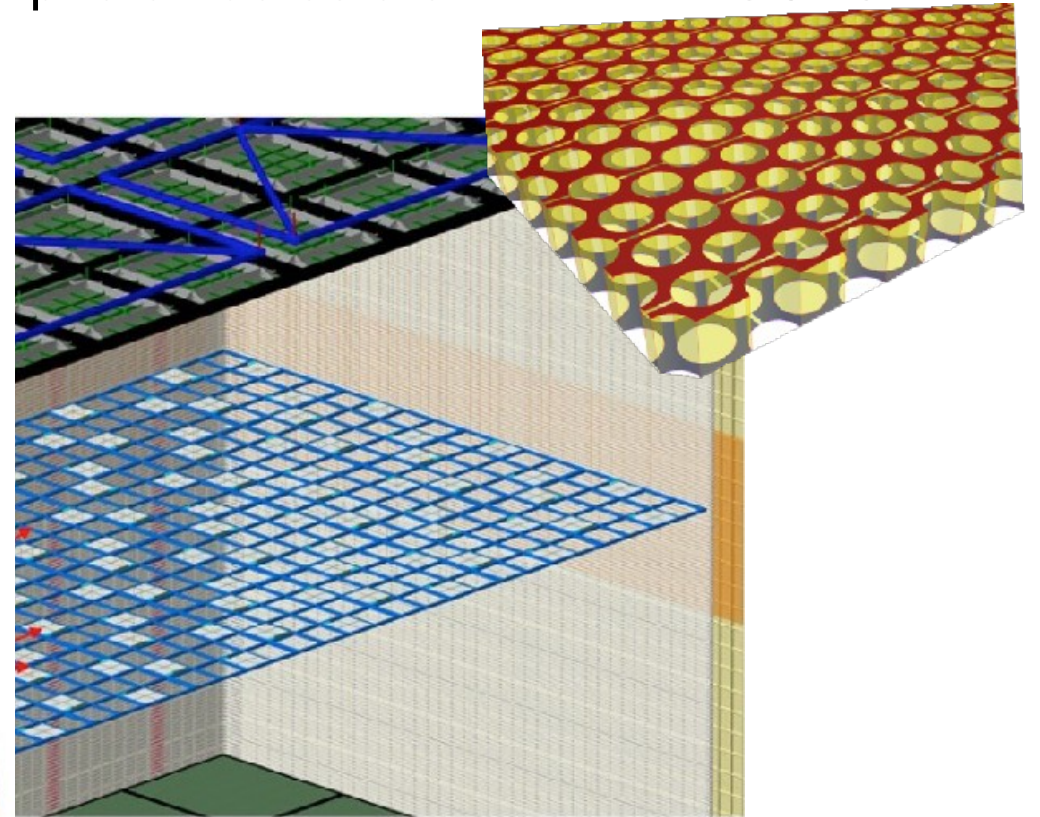
Module #1

- 3.6 m horizontal drift
- vertical anode wire planes
- vertical resistive cathode photon detectors → **XARAPUCAs**



Module #2

- 6.5 m vertical drift
- horizontal PCB anode readout (CRP)
- horizontal grid cathode photon detectors → **XARAPUCAs**

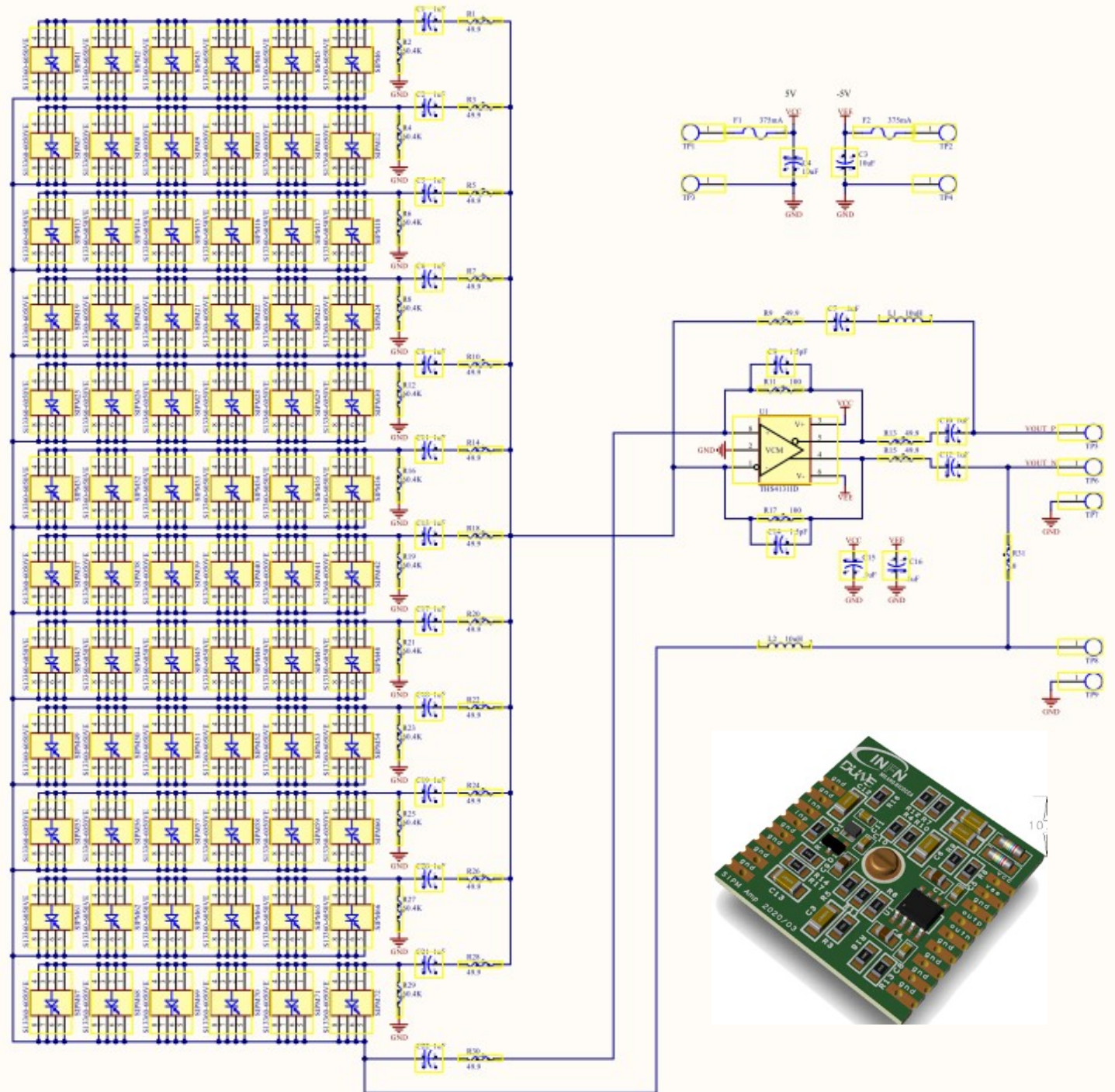


48 6x6 mm² ganged together in a single electronic channel

Ganging scheme:

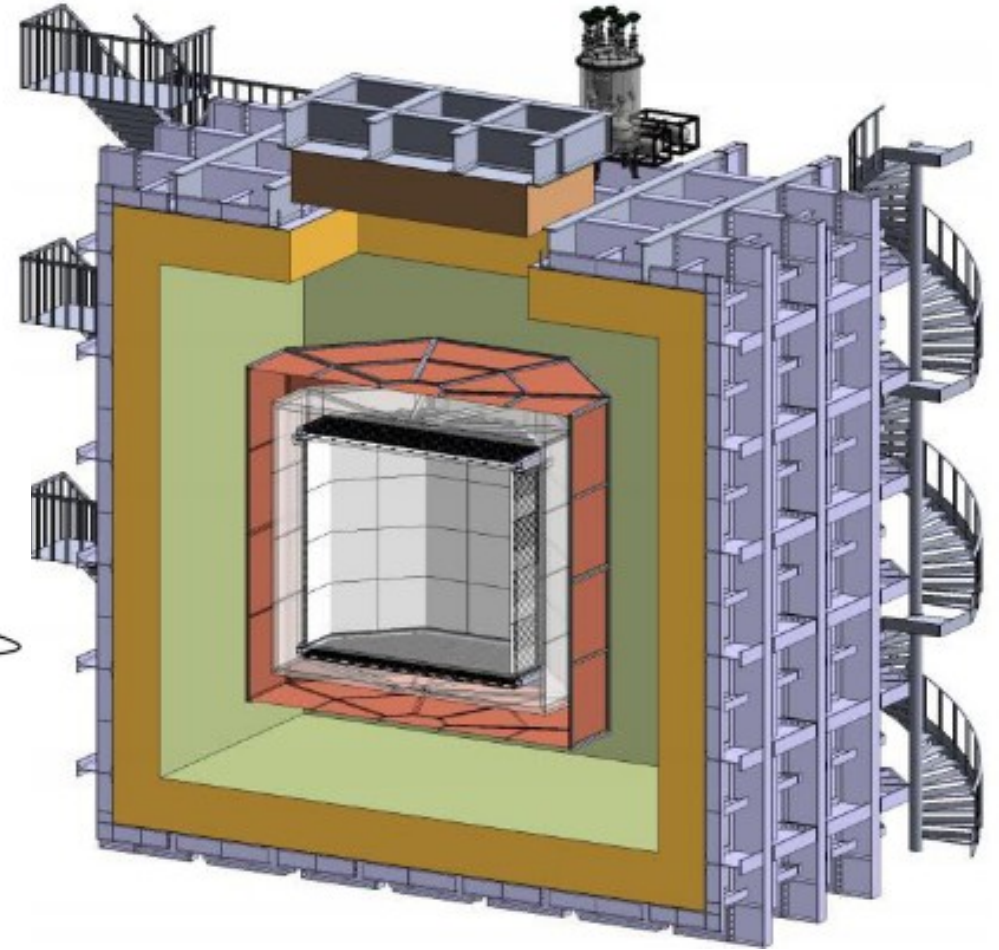
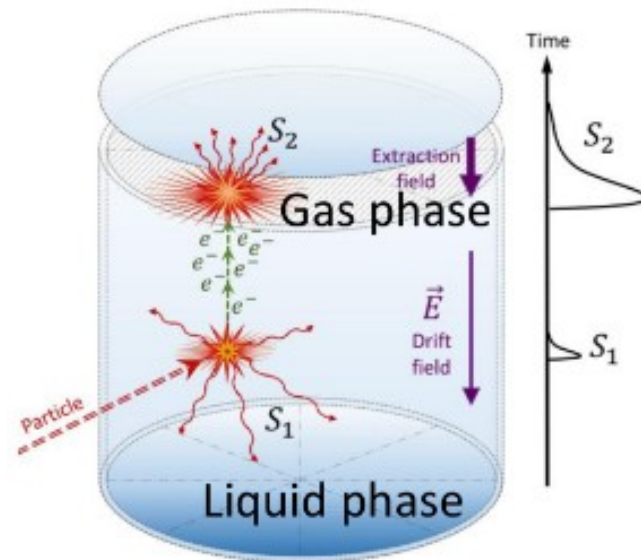
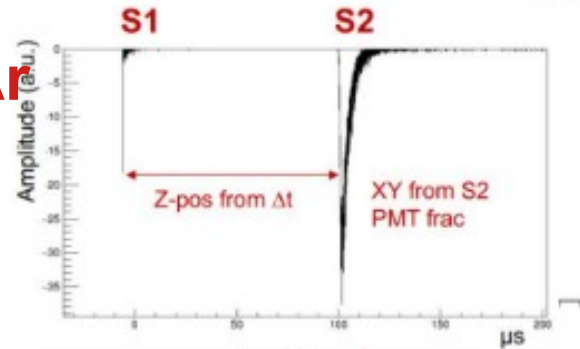
- SiPM **passively ganged in parallel in groups of 6**
- 8 groups of 6 SiPMs **ganged actively together through an OpAmp**
- *Passive ganging of SiPM reduces the amplitude of single photon signals given the increased overall capacitance*
- Active ganging **does not affect the amplitude** but adds electronic noise

Total number of SiPM ~ 300,000



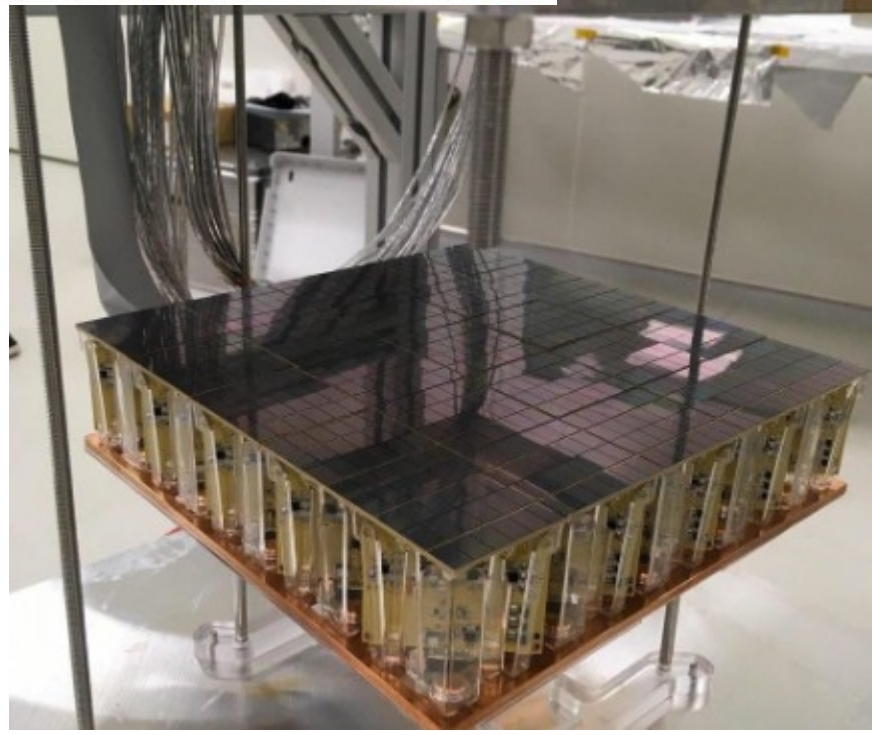
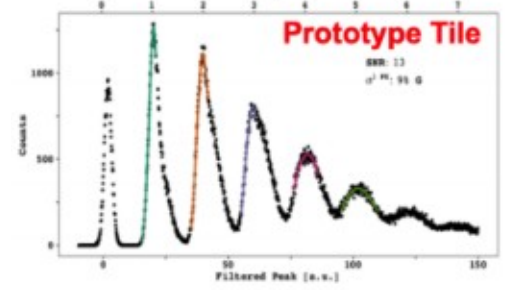
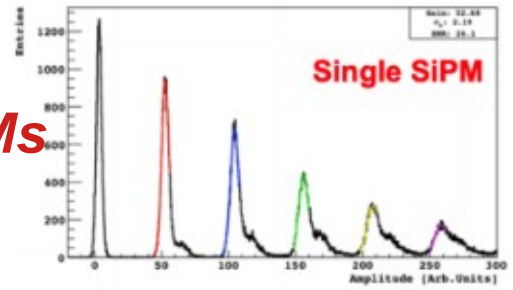
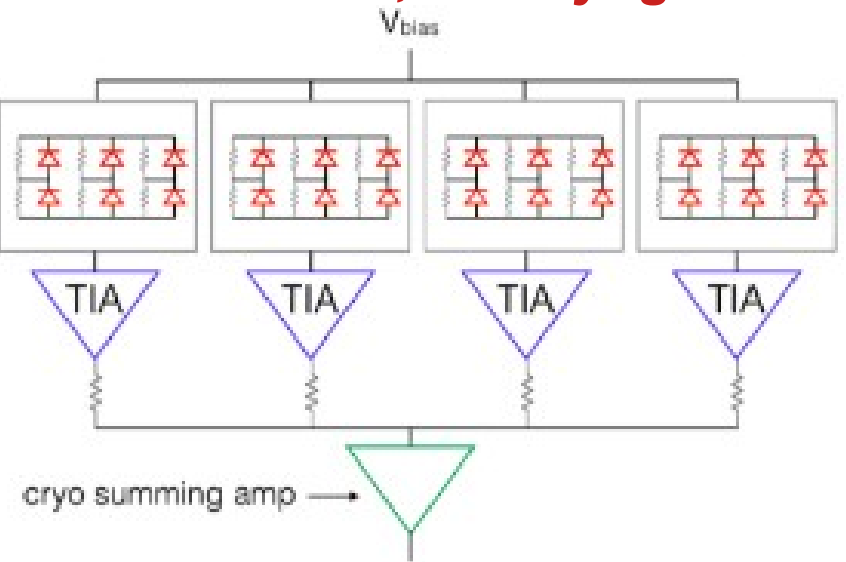
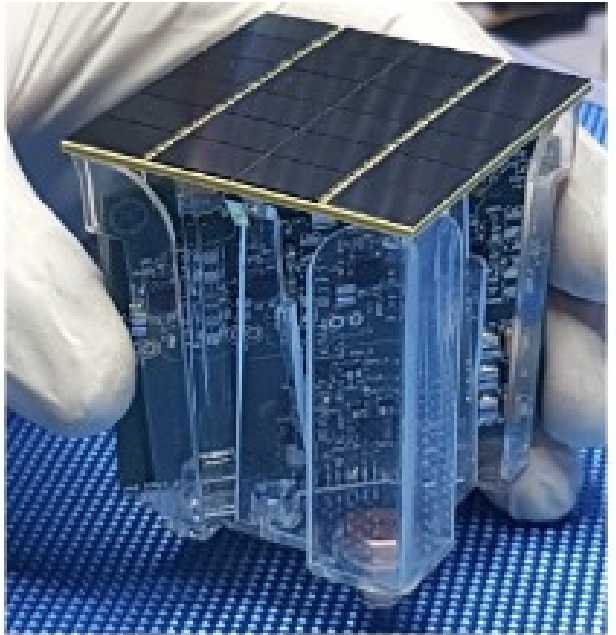
Example: DarkSide 20k

- **50t of Ultrapure depleted Ar**
- Primary (S1) and secondary (S2) scintillation and electroluminescence signals detected by **two planes of SiPM arrays**
- SiPM allow for a **denser coverage** of the surfaces, **higher PDE** and **improved radiopurity**



Example: DarkSide 20k

- Basic photo-detection module is an array of **24 SiPM => PDM**
- SiPM *passively ganged in groups of 6 – mixed series/parallel* and *actively ganged in 4 groups of 6*
- **25 PDMs** arranged in a **Motherboard**
- **8,200 PDMs => 196,800 cryogenic SiPMs**



Hybrids: HPD, HAPD, QUPID, VSIPM, ABALONE

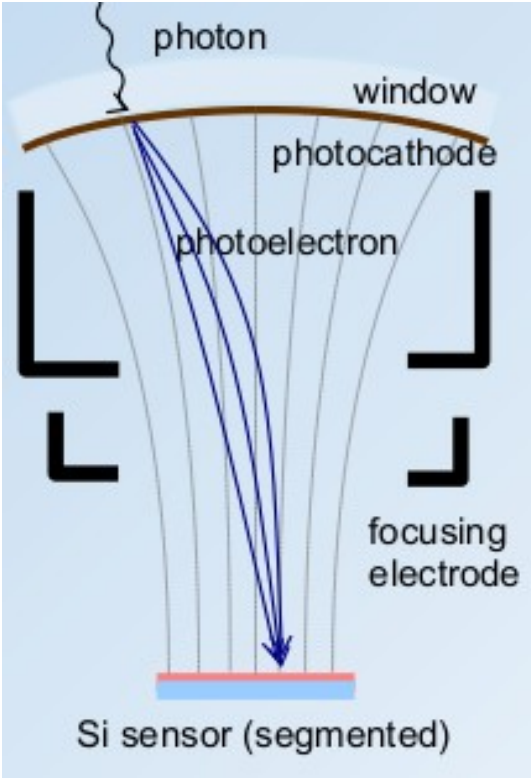
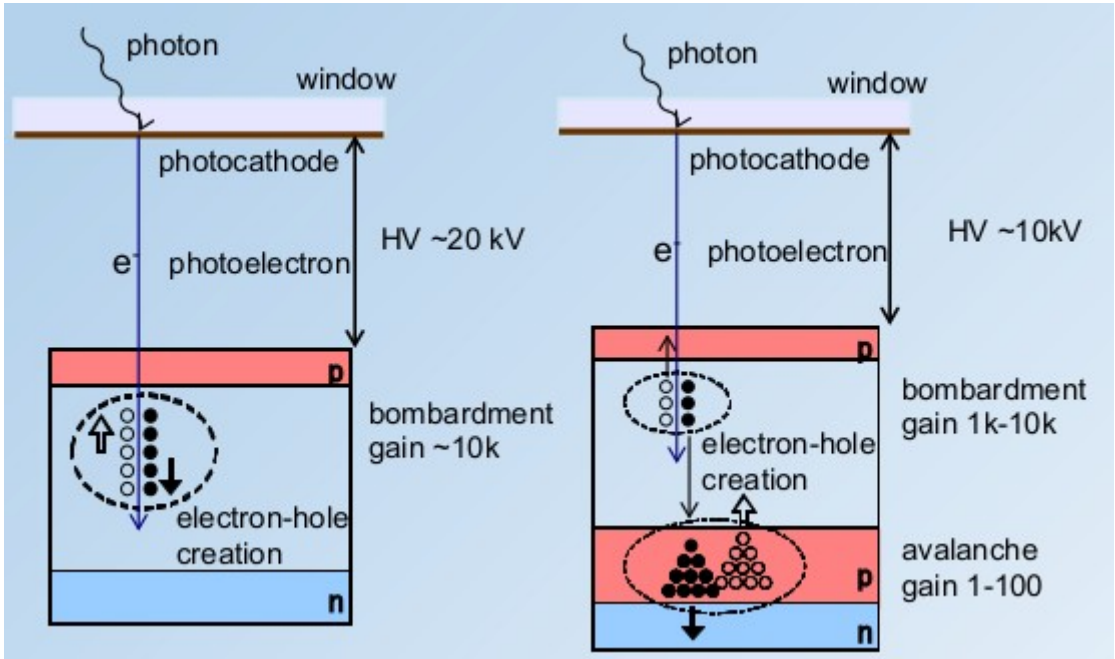
- Hybrid detectors are **cobinations of vacuum and silicon devices**
- They have **large photocathode** which ensure a large photoelectron conversion area
- Photoelectrons are accelerated by a strong high field (10-20 kV) and **focused on a silicon device**
- Photoelectrons loose energy **prodcing a number of electron-hole pairs proportional to the electron kinetic energy**, eventually multiplied by the intrinsic gain of the silicon device

- **$G = e G_{Si}(\Delta V - V_{th})/W_{Si}$ $W_{Si} = 3.6 \text{ eV for silicon}$**

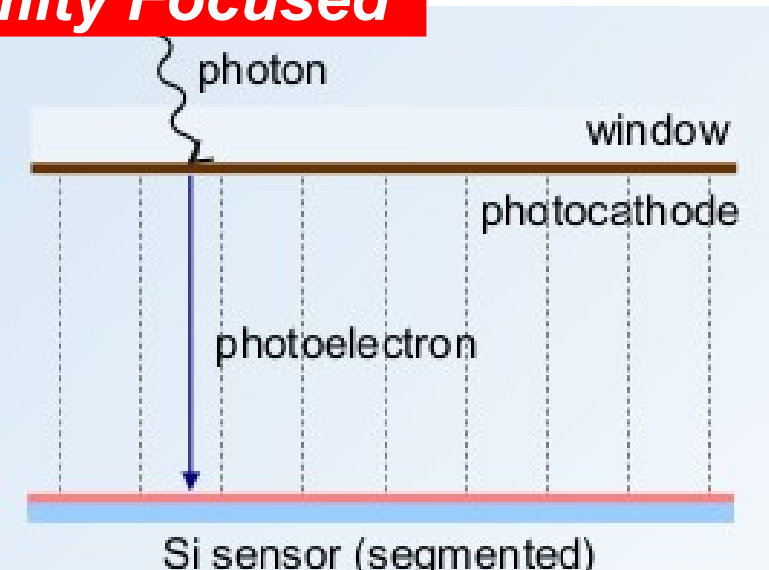
- Very low fluctuation in the Gain => Fano factor of Si ~ 0.12 $\sigma = \sqrt{F G}$

Hybrids: HPD

Cross Focused

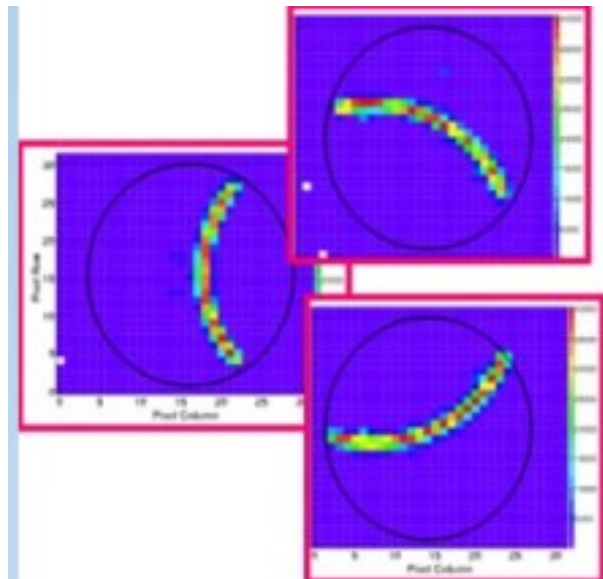
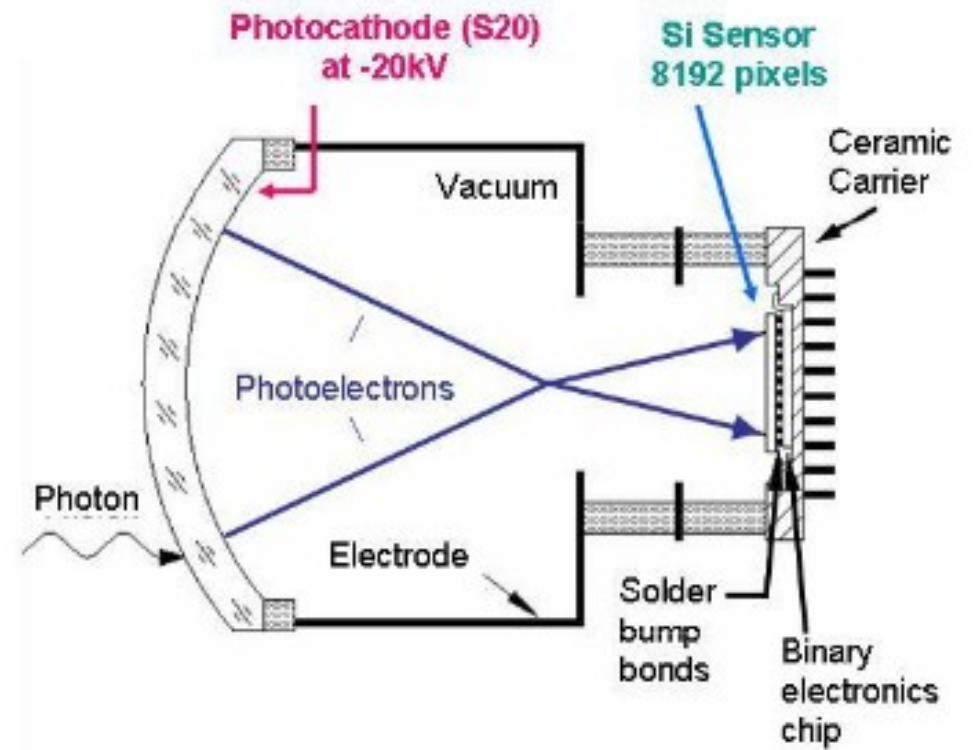


Proximity Focused



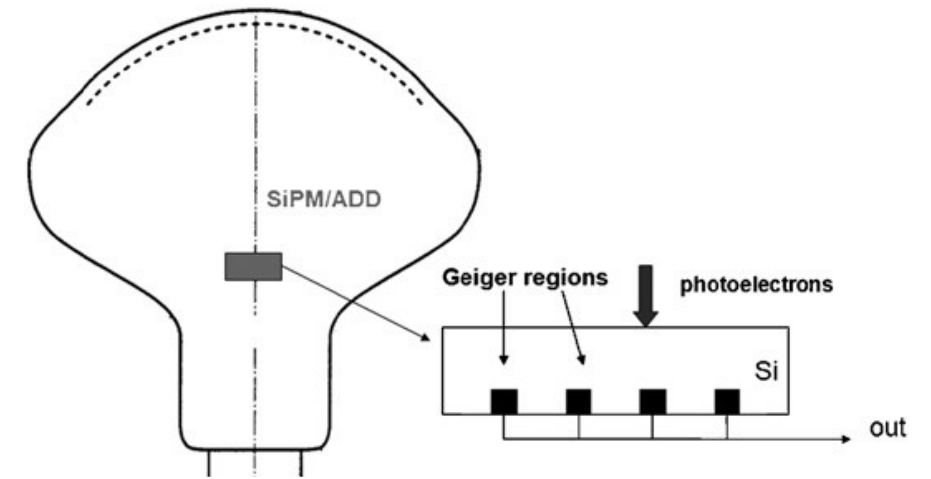
LHCb HPD

- Used in the **RICH detector of LHCb**
- *Cross focused HPD* – $HV = 20kV$, $G = 5,000$
- **8192 pixels of size $500\mu m \times 62.5\mu m$**
- **QE $\sim 30\%$ @ $350nm$**
- Vacuum degradation causes ion feedback and aging of the device

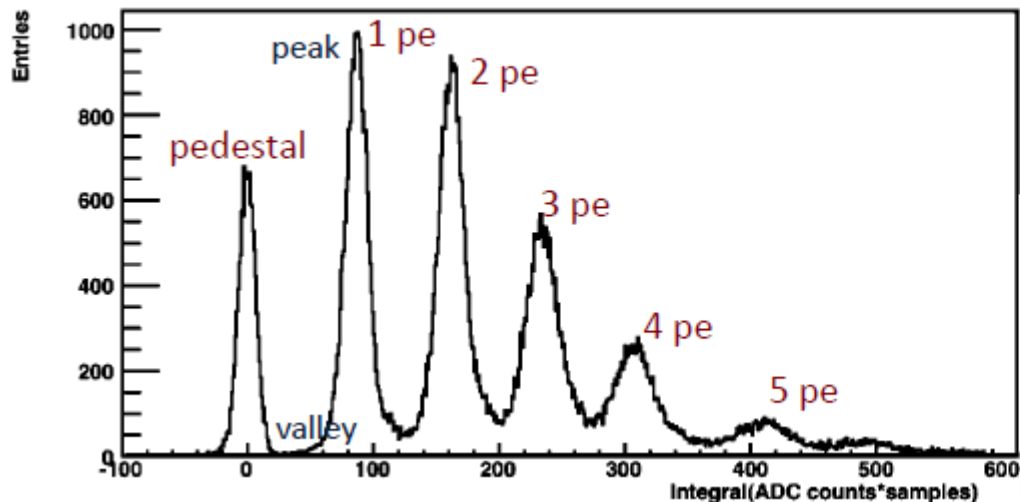


Hybrids: Vacuum SiPM - VSiPM

- Vacuum device coupled to a Silicon Photomultiplier
- Good photo detection efficiency
- Gain $\sim 10^5 - 10^6$
- Good Spe resolution



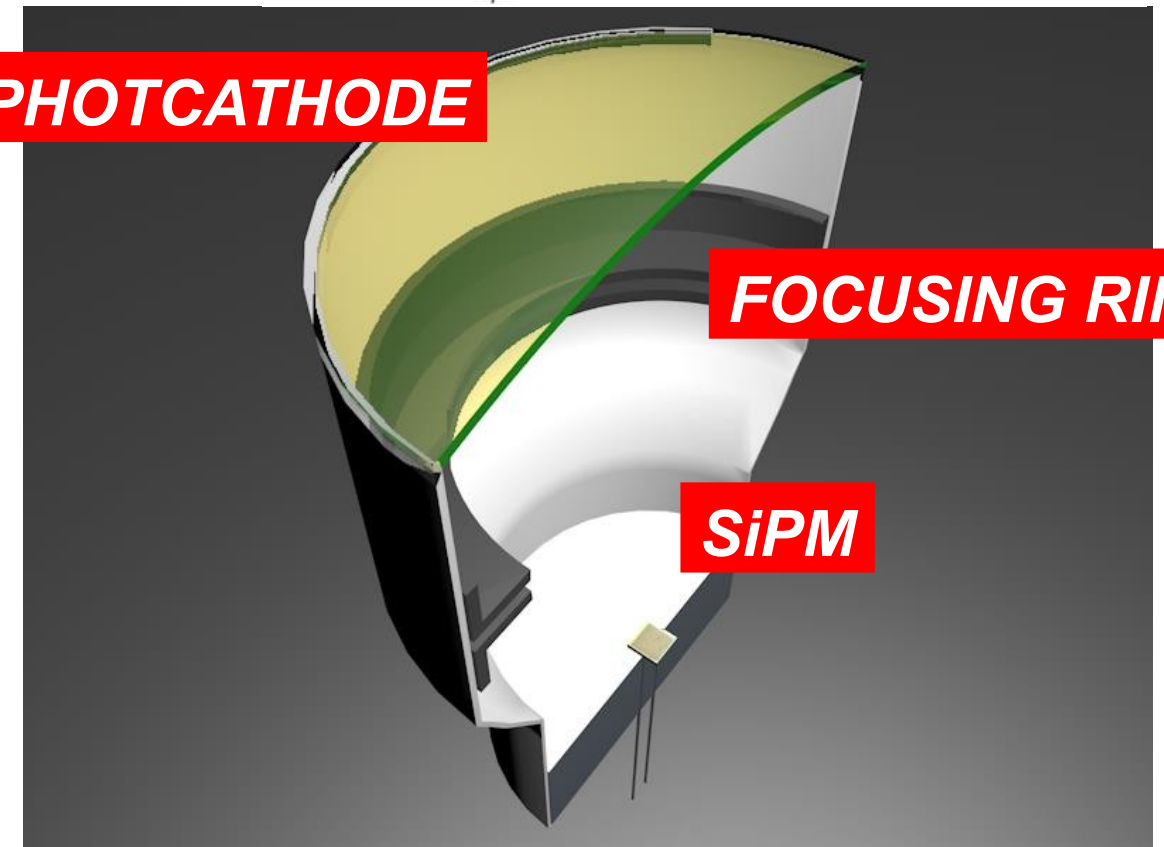
G. Barbarino et al. NIM-A594(2008)326



PHOTOCATHODE

FOCUSING RING

SiPM

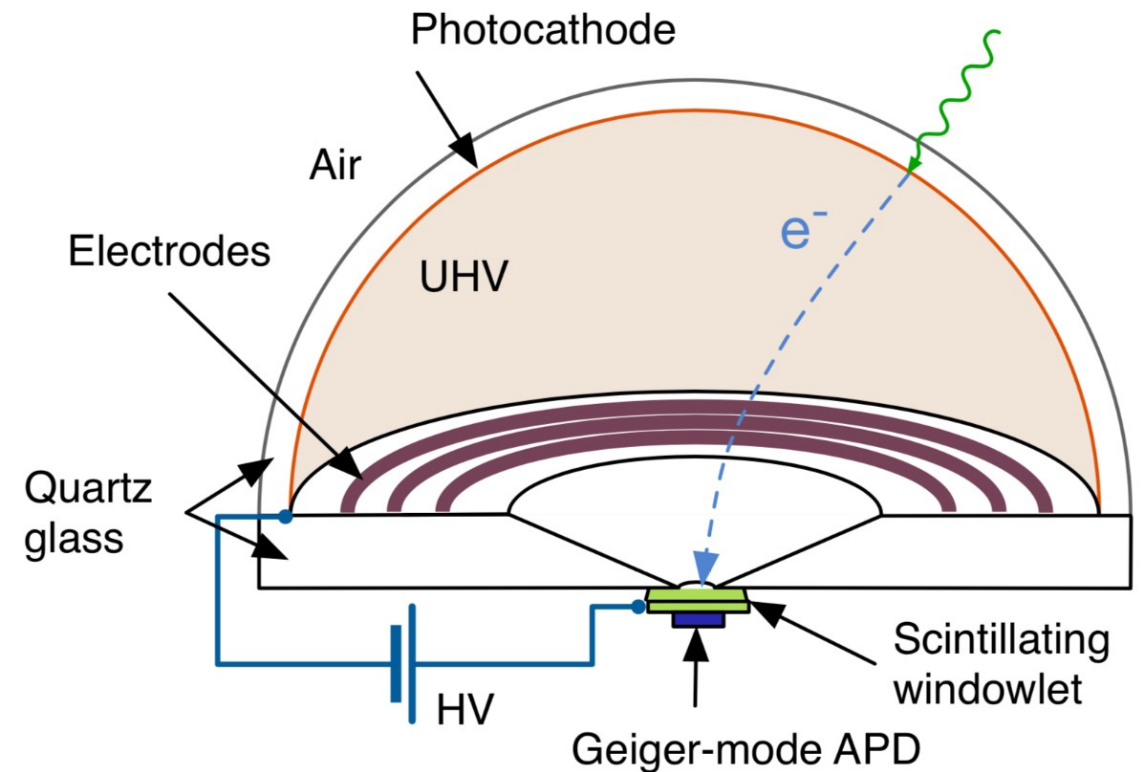
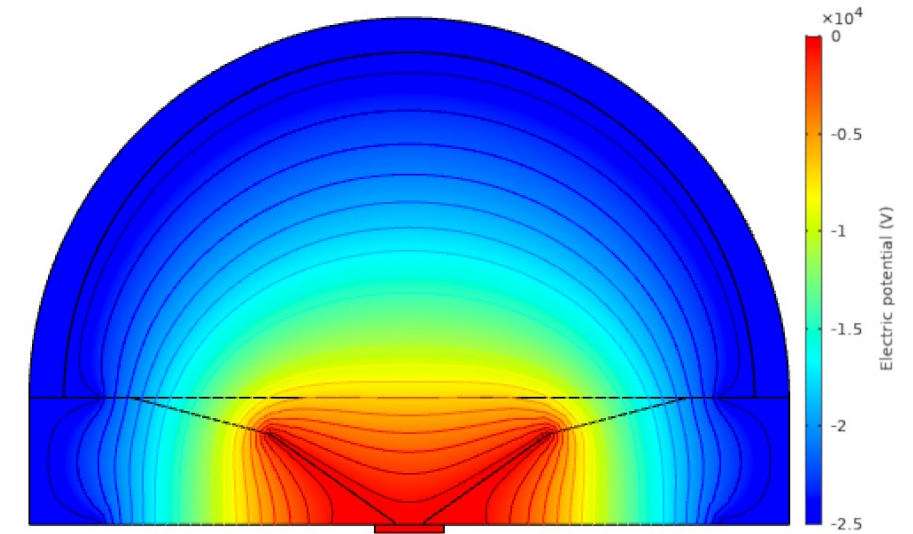


Hybrids: ABALONE

- *Ultra high vacuum device*
- Photocathode coupled to a **scintillator read-out by a SiPM**
- **Great optical aperture $\sim 2\pi$**
- QE determined by the photocathode
- **Excellent gain $\sim 10^8$**
- Proposed as photosensor for the *future dark matter experiment DARWIN*

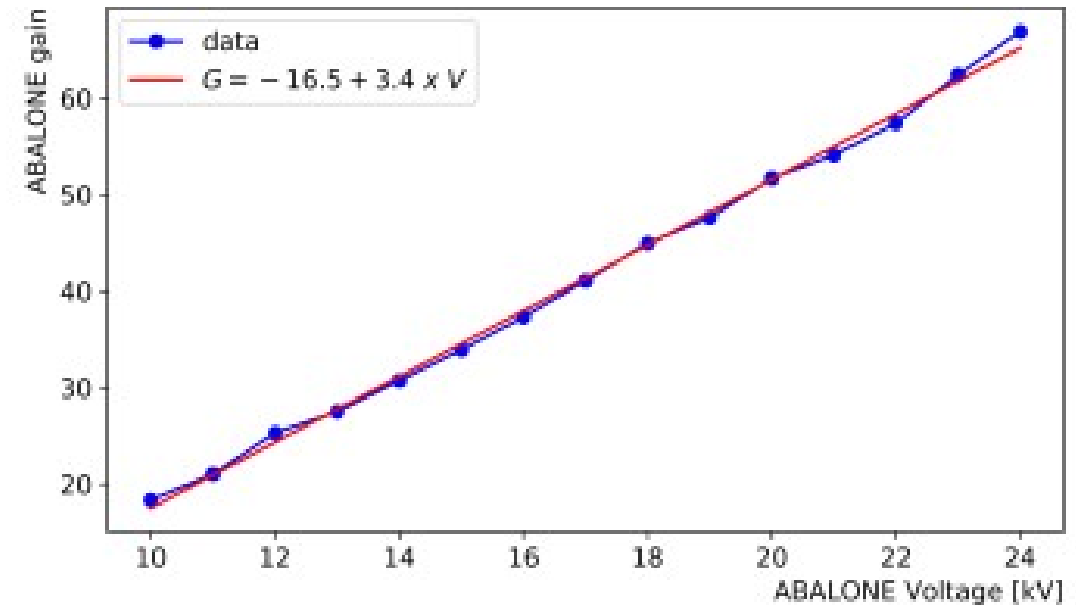
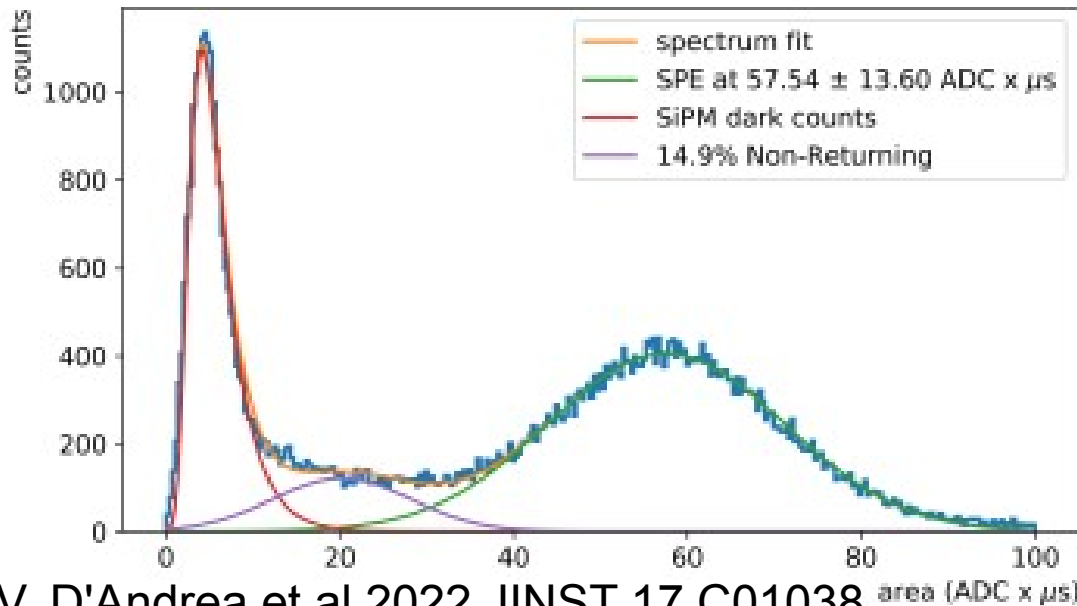
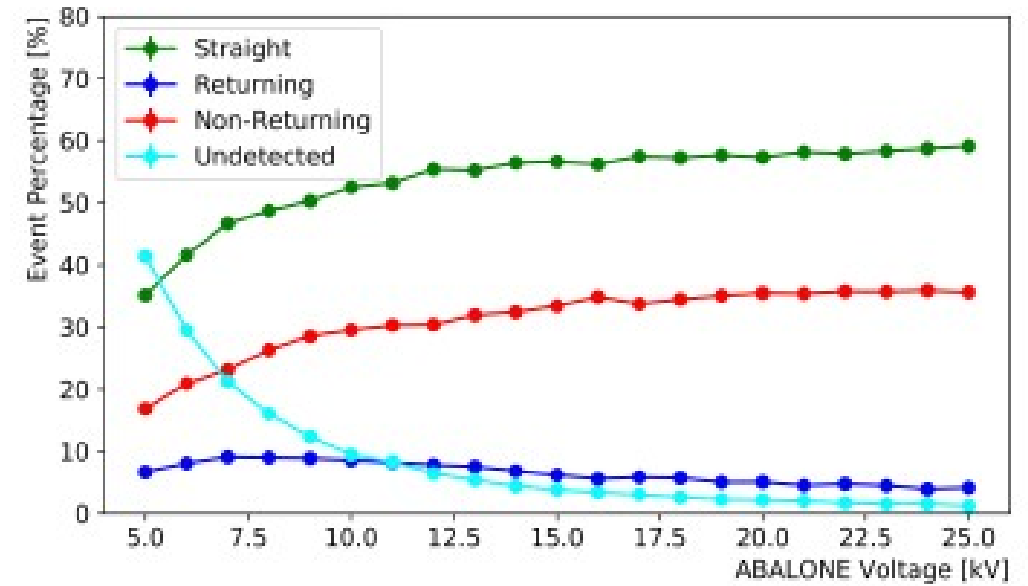


V. D'Andrea et al 2022 JINST 17 C01038

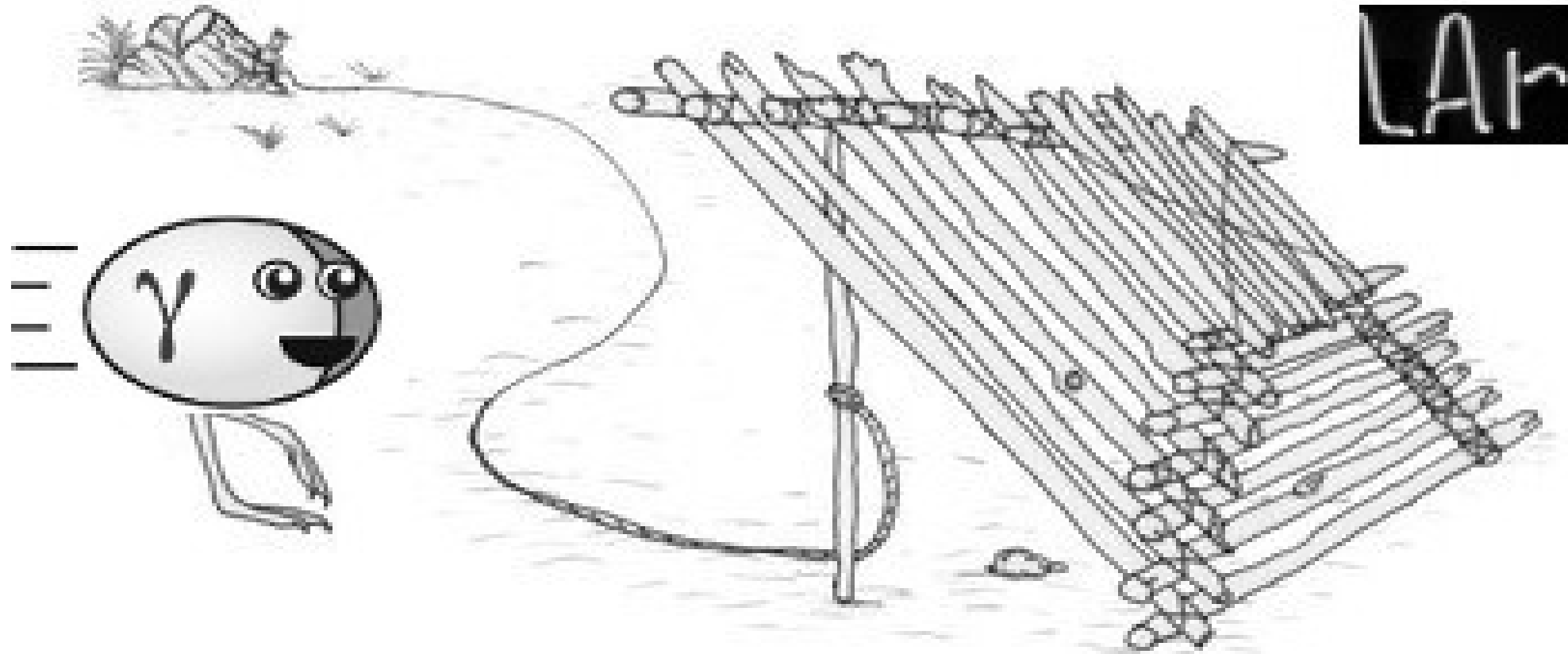


Hybrids: ABALONE

- Operated **at 25 kV**
- *LYSO scintillator*
- Gain of the Scintillator ~ 100
- **Overall gain $\sim 10^8$**
- Non negligible fraction of electrons **escapes from the crystal and does not deposit entire energy** (non-returning)
- *A dedicated R&D program to minimize this effect*



ARAPUCA concept



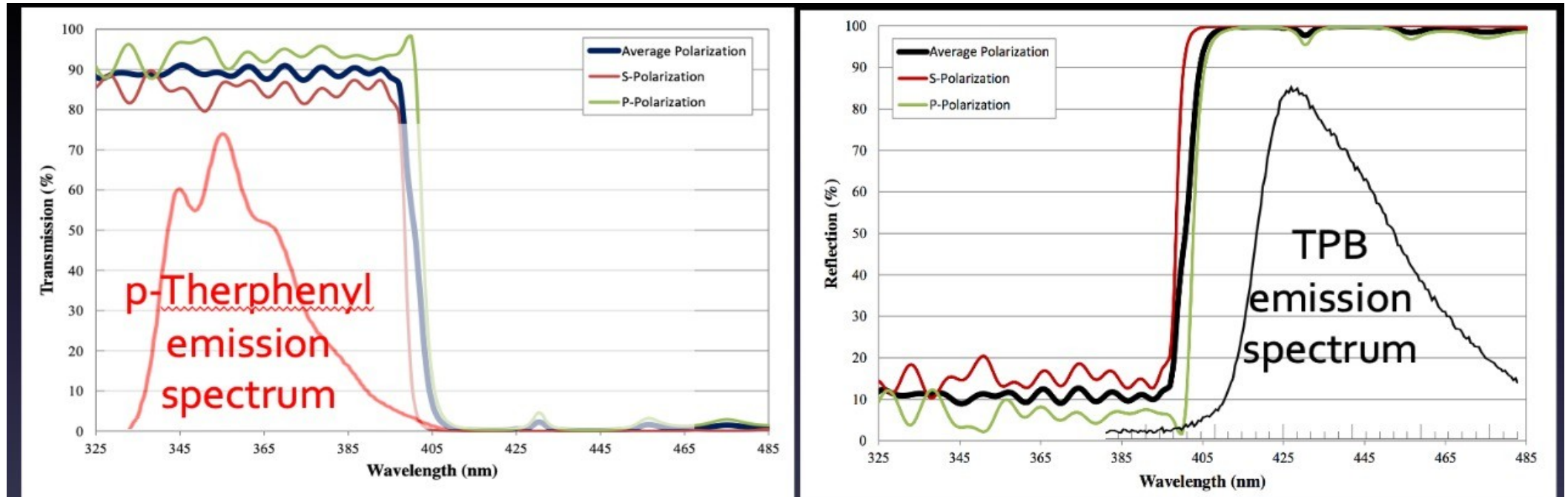
ARAPUCA concept



- **ARAPUCA** in the language of *native Brazilian* means **trap** for birds
- **Trap photons** inside a **box with highly reflective internal surfaces** => Increase detection efficiency even with a limited active coverage of its internal surface
- Detection efficiency can be **tuned by varying the number of SiPMs (ratio between acceptance window and SiPM areas)**..
- **Baseline DUNE design of Photon Detection System of 2 far detector modules**

Dichroic filter

- The core of the device is a **dichroic filter**. It is a dielectric interference film deposited on a fused silica substrate.
- It has the property of being **highly transparent** for wavelength **below a cutoff** and **highly reflective above it**.

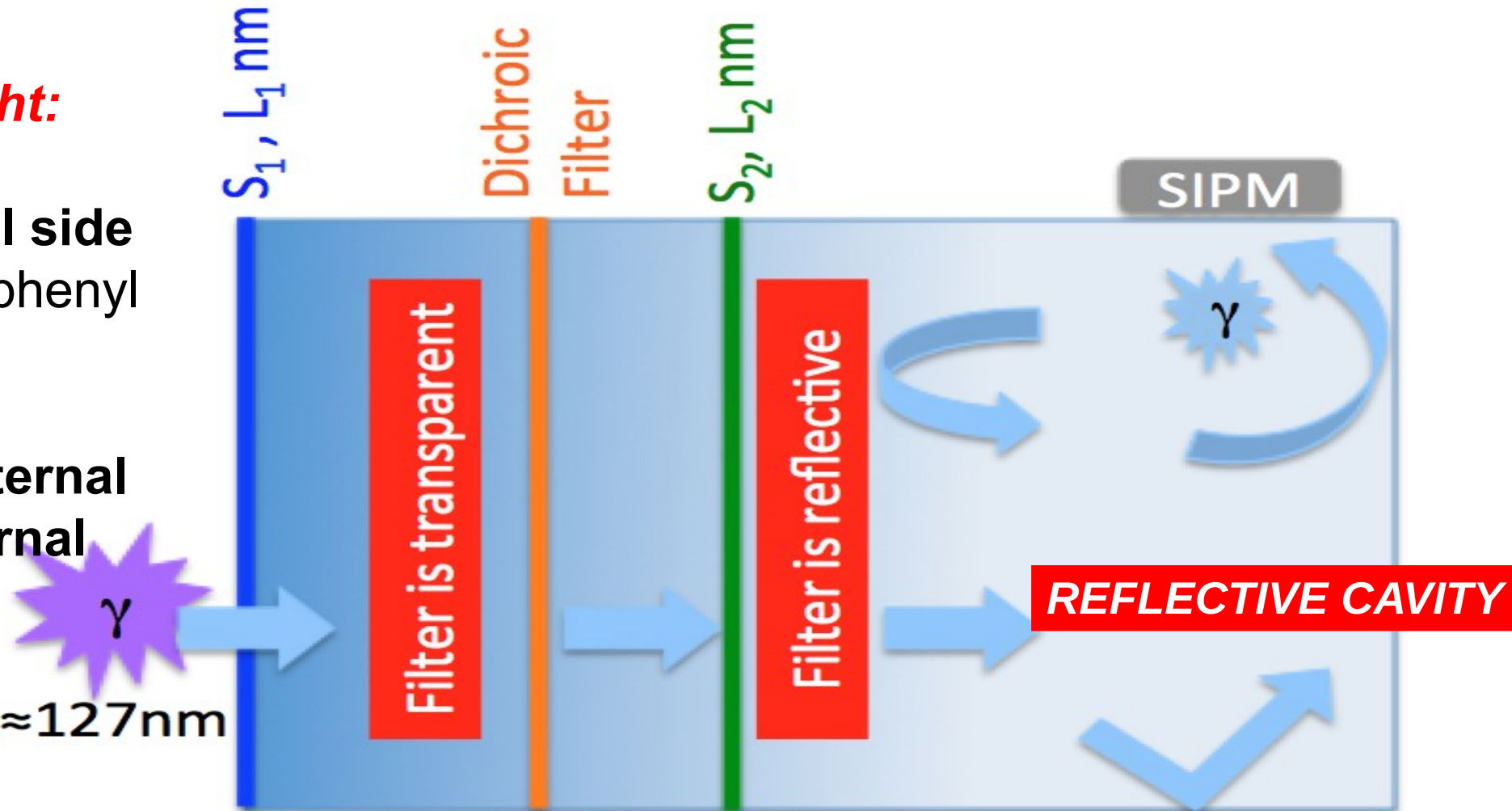


Foton VUV 128nm → p-Therphenyl → 350nm → Filtro cutoff 400nm → TPB → 430nm

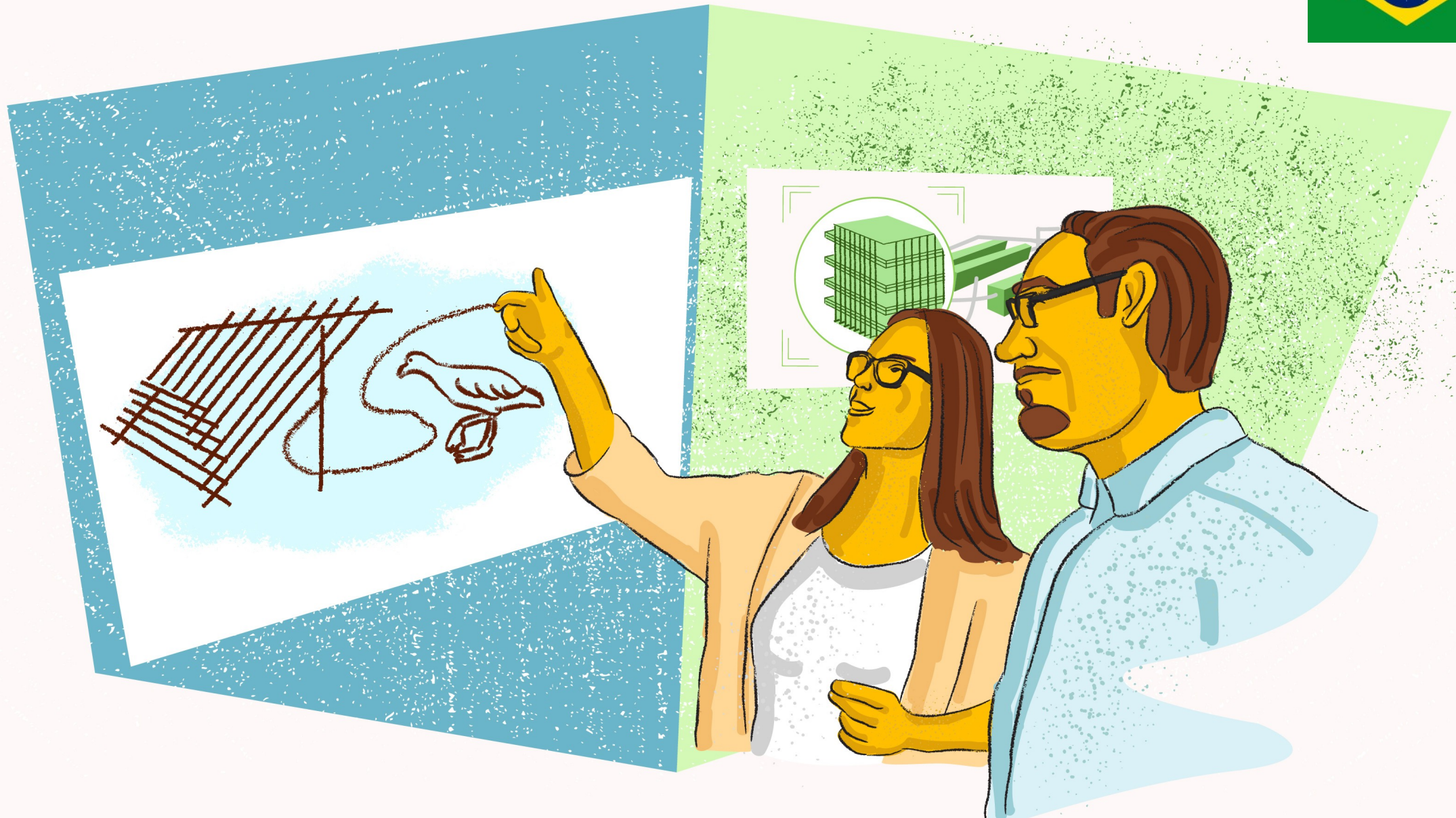
ARAPUCA Operating Principle

Two shifts of the light:

- One on the **external side of filter** (Para-Therphenyl 127nm => 350nm)
- The other on the **internal side or on the internal walls** (Tetraphenyl-Butadiene 350nm=>430nm) $\lambda \approx 127\text{nm}$



ARAPUCA for neutrinos!



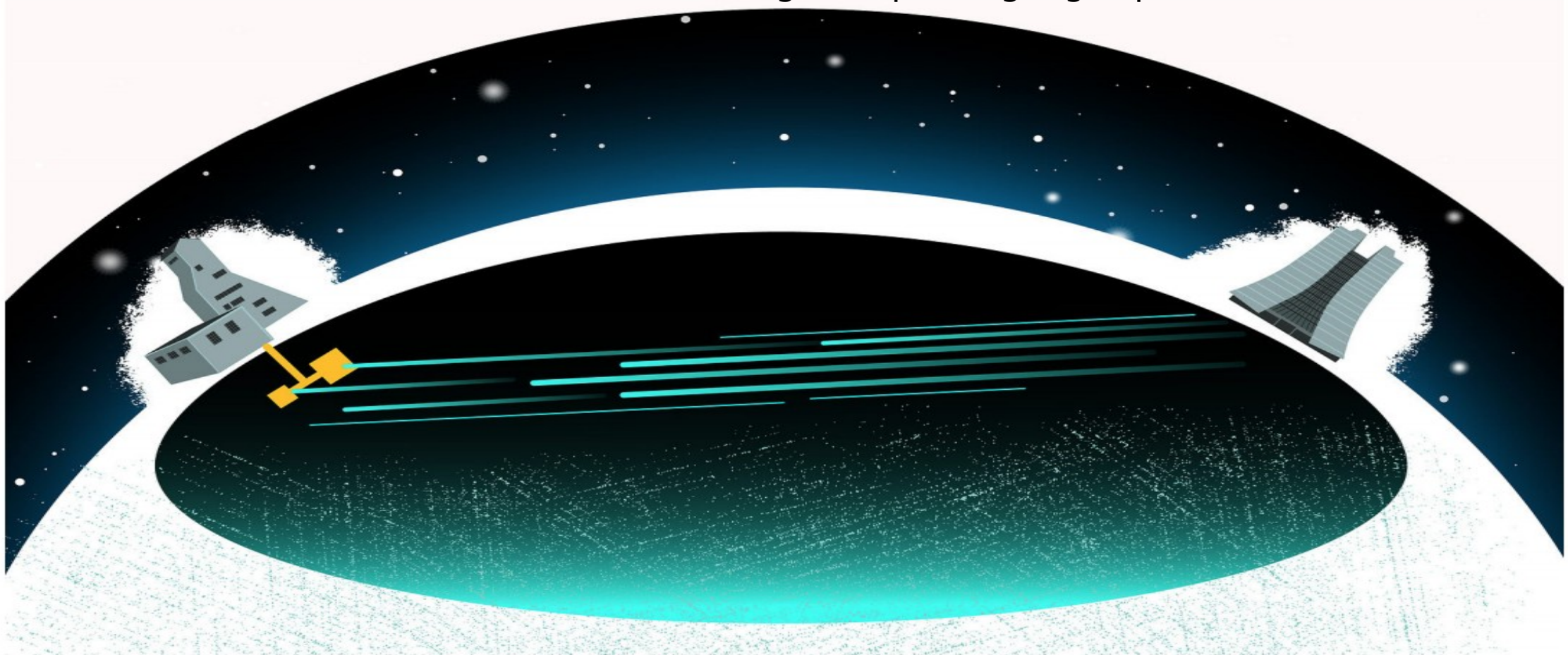


Illustration by Sandbox Studio, Chicago with Pedro Rivas

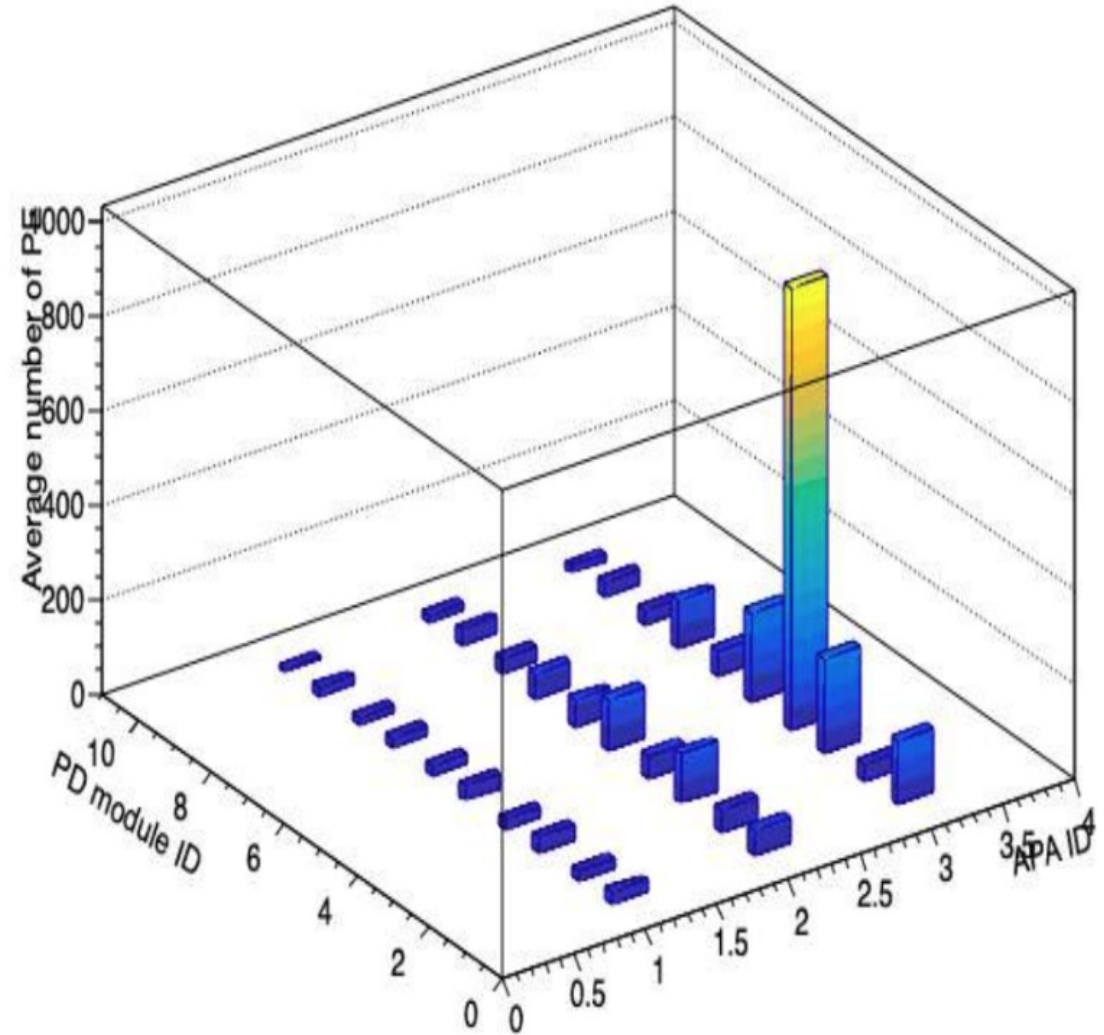
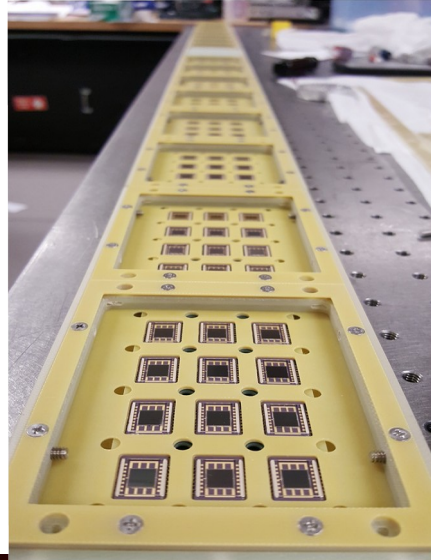
ARAPUCA: Façam-se armadilhas para a luz

10/24/19 | By Lauren Biron

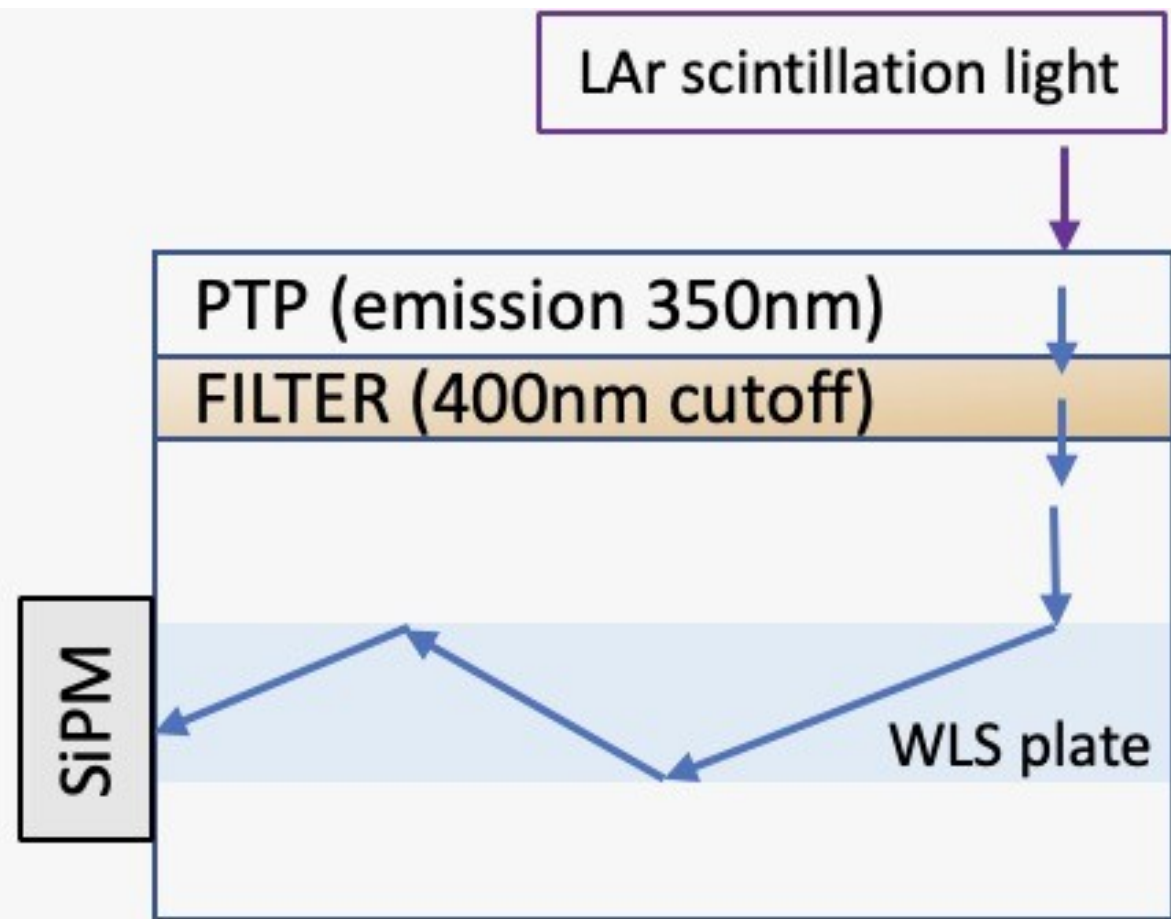
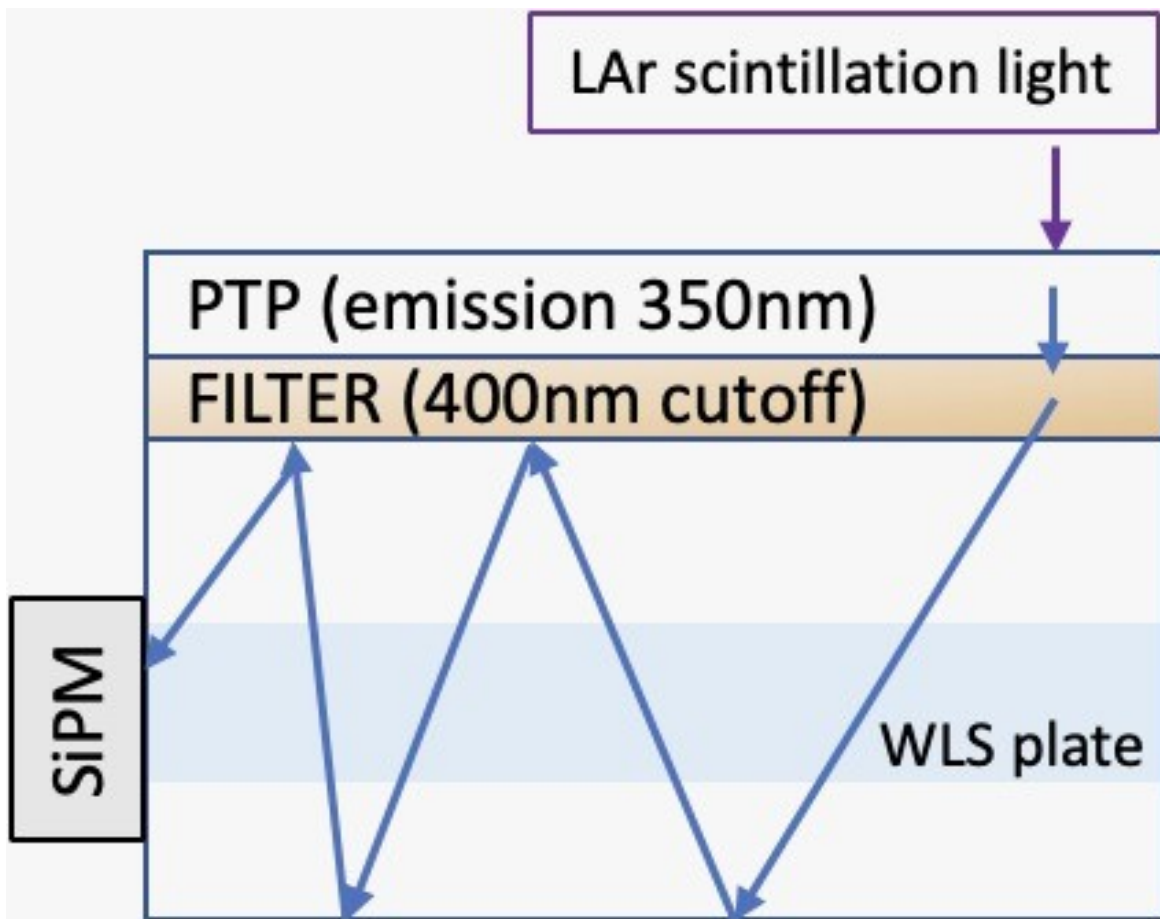
As instituições latino-americanas são imprescindíveis para a criação dos detetores de fótons usados na Experiência de Neutrinos em Grande Profundidade.

ARAPUCA in protoDUNE Run I (2018-2020)

Electrons



X-ARAPUCA



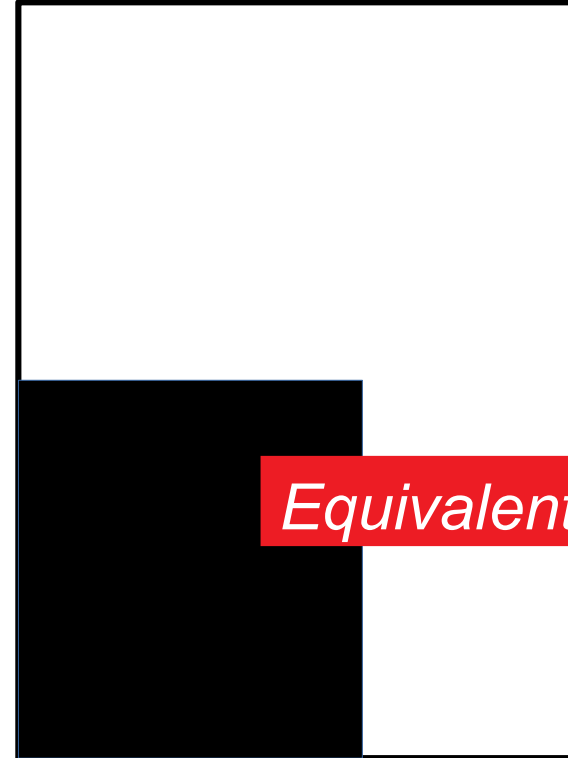
X-ARAPUCA detection efficiency

Gain factor between 7 and 10

X-ARAPUCA window



SiPM active surface



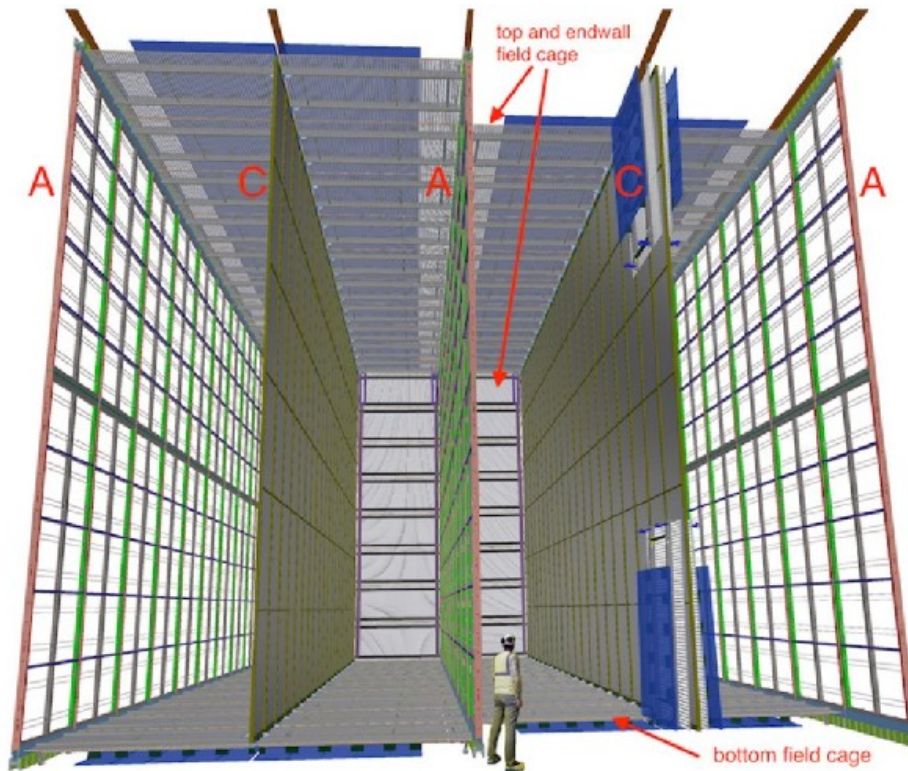
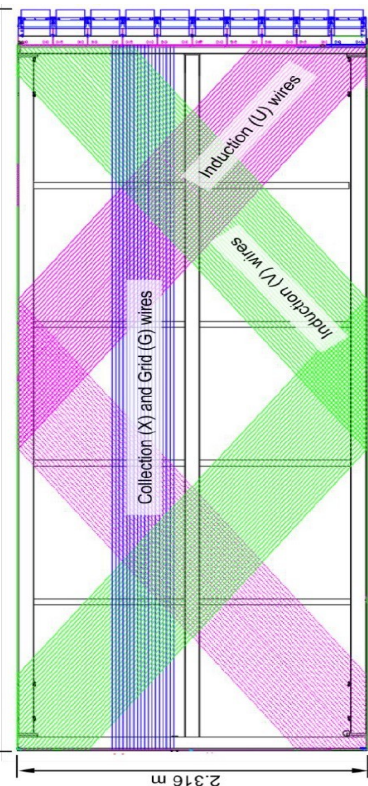
Equivalent active surface

In units of 8" PMT: 1 ***X-ARAPUCA bar*** is equivalent to **2.5 8" PMTs**

LAr Read-out Technologies of DUNE far detectors

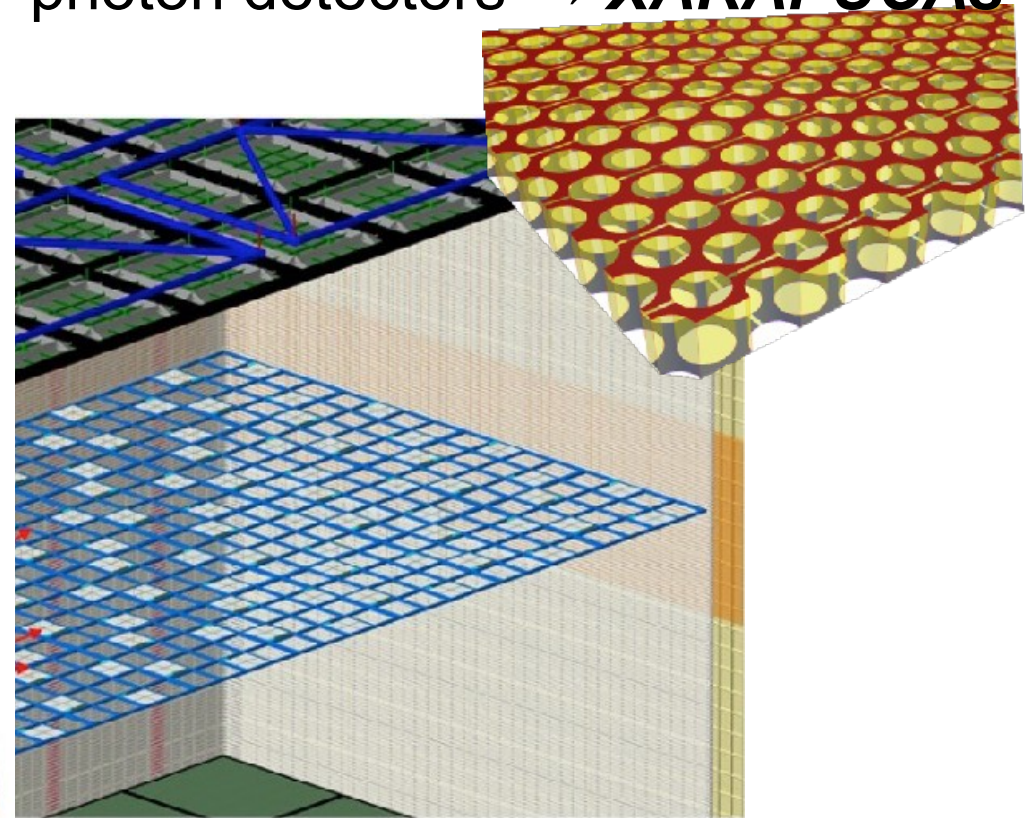
Module #1

- 3.6 m horizontal drift
- vertical anode wire planes
- vertical resistive cathode
- photon detectors → **XARAPUCAs**

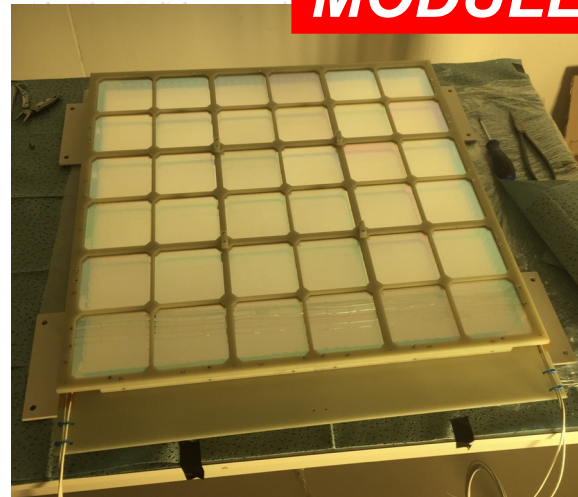
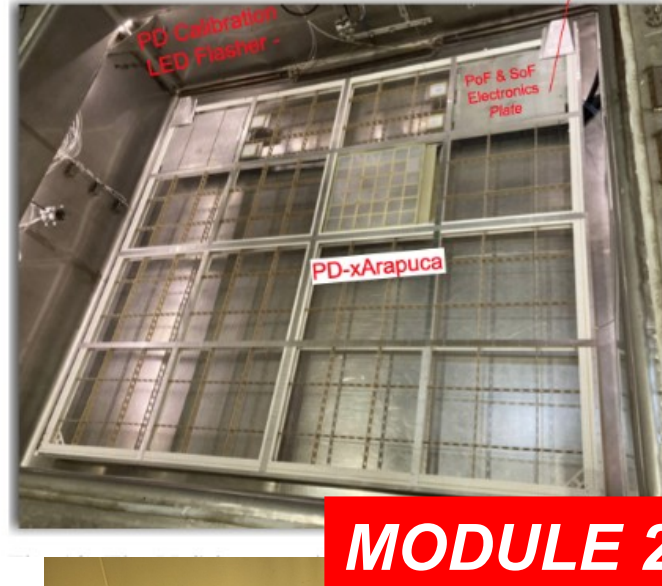
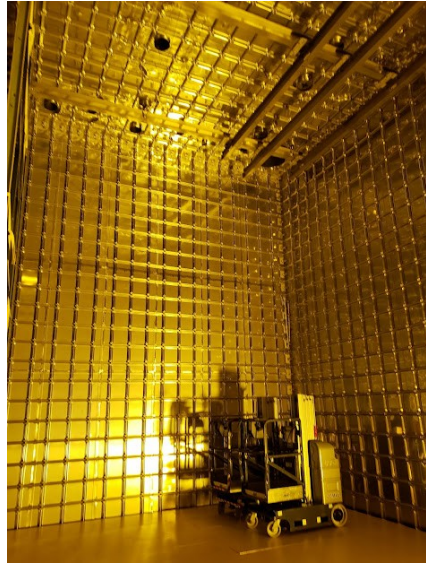


Module #2

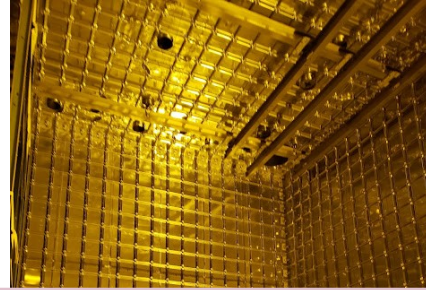
- 6.5 m vertical drift
- horizontal PCB anode readout (CRP)
- horizontal grid cathode
- photon detectors → **XARAPUCAs**



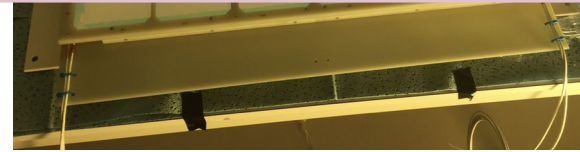
X-ARAPUCA in ProtoDUNE Run II (2022-2023)



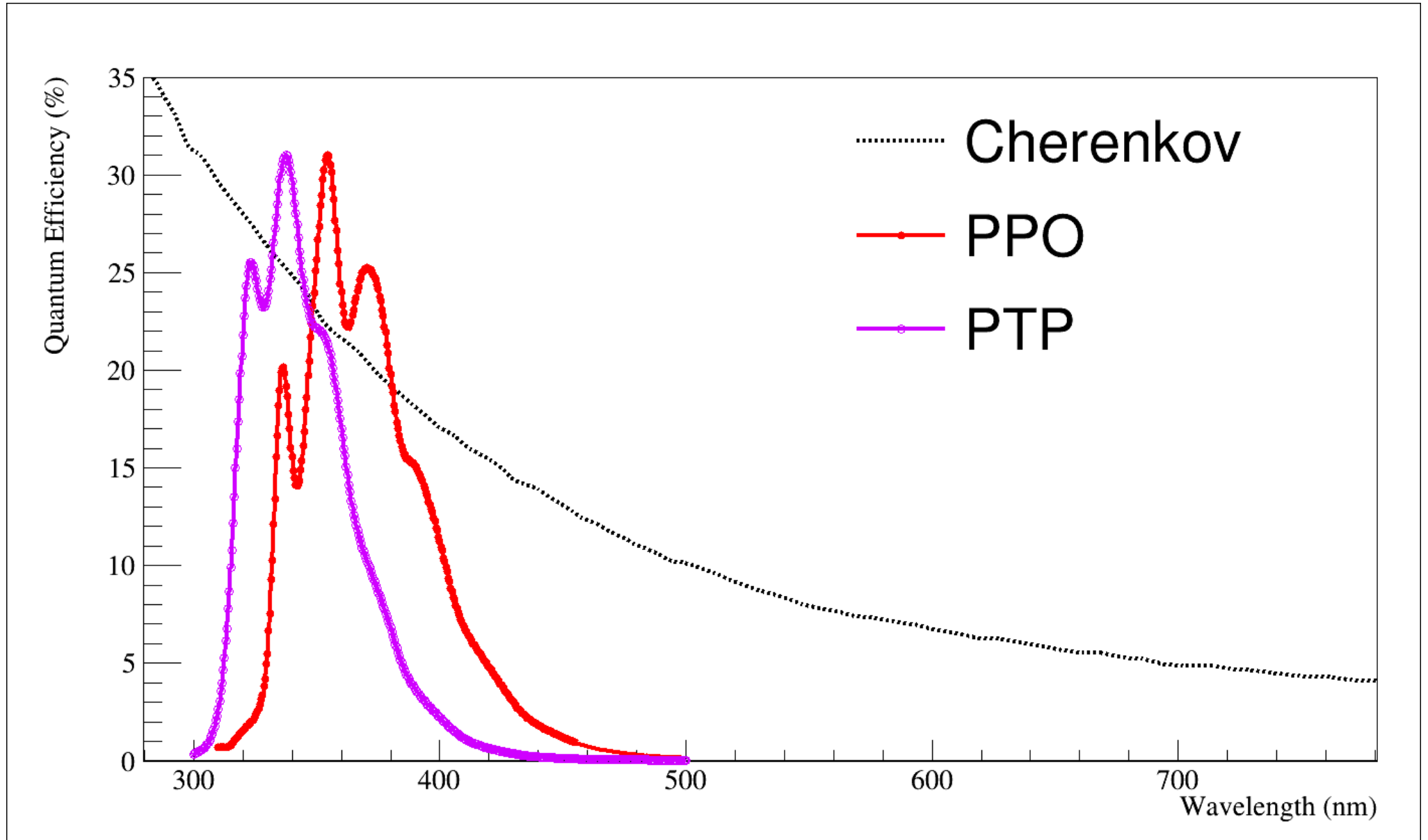
X-ARAPUCA in ProtoDUNE Run II (2022-2023)



- ***X-ARAPUCA is the baseline design for the two DUNE far detector modules***
- ***Design and construction managed by a Consortium of more than 50 Institutions in 3 continents***
- ***1,500 bar shaped modules in module 1 (Horizontal Drift) => 300,000 SiPMs ~10 m² area***
- ***640 square X-ARAPUCA modules for module 2 (Vertical Drift) => 100,000 siPMs 3 m² area***

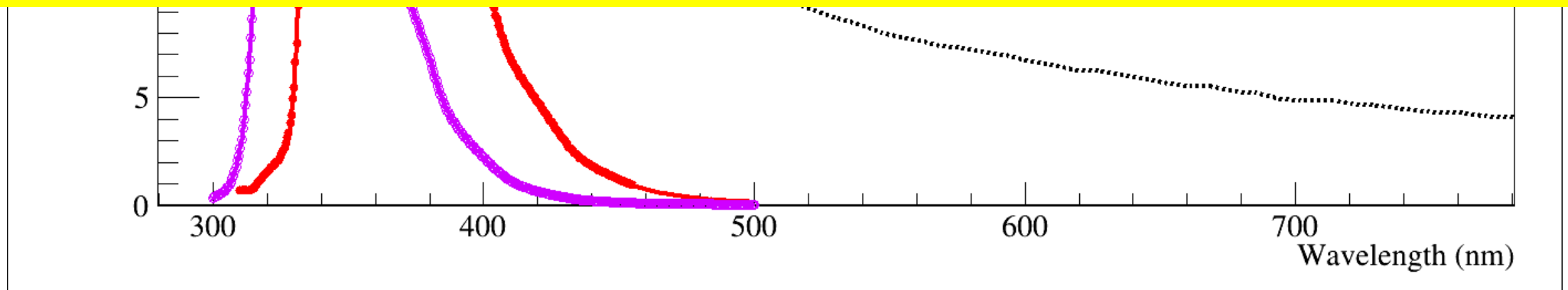


Dichroicon: sorting photons



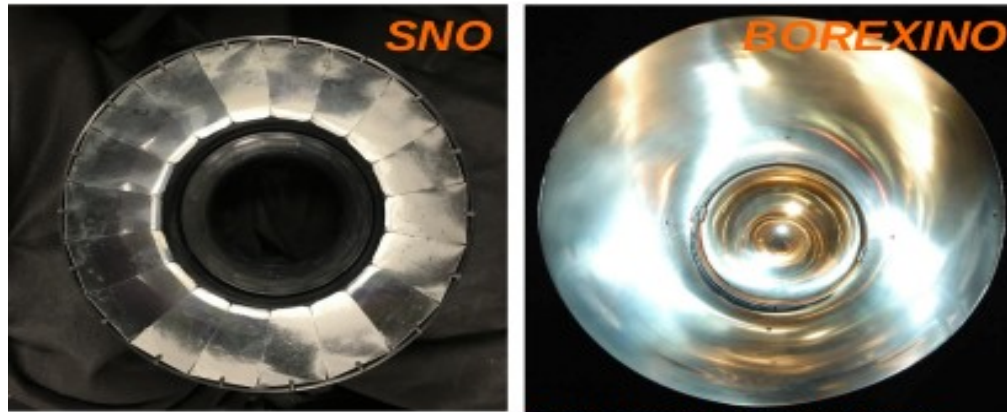
Dichroicon: sorting photons

- Charged particle traveling through liquid scintillator *creates both scintillation (~10,000 photons/MeV) and Cherenkov light (~100 photons/MeV)*
- **Challenge is to detect the Cherenkov light**, which provides the direction of the traveling particle. Typically use timing and directionality.
- *High light yield from scintillator provides excellent energy and position resolution and low energy thresholds*

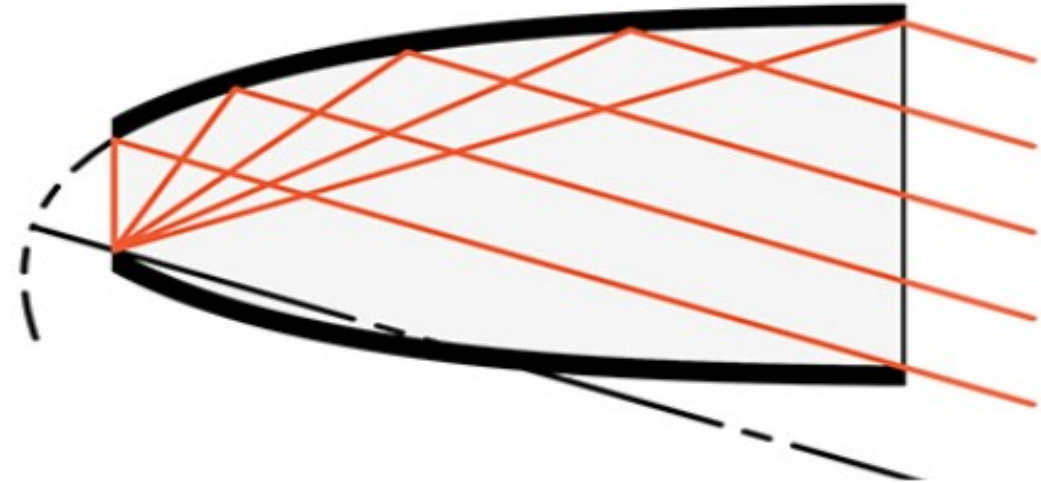


Dichroicon: combining two technologies

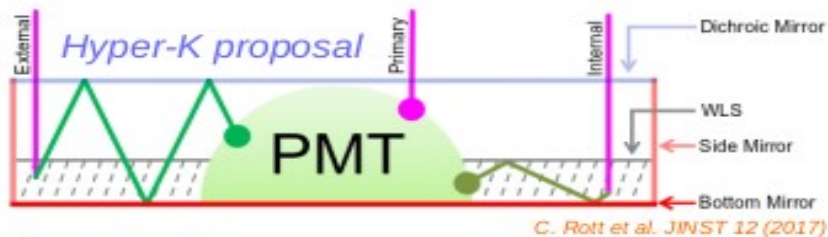
Winston Cones



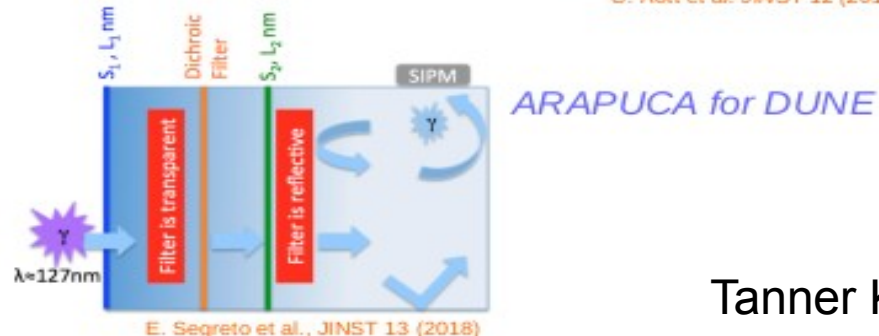
<https://arxiv.org/pdf/physics/0310076.pdf>



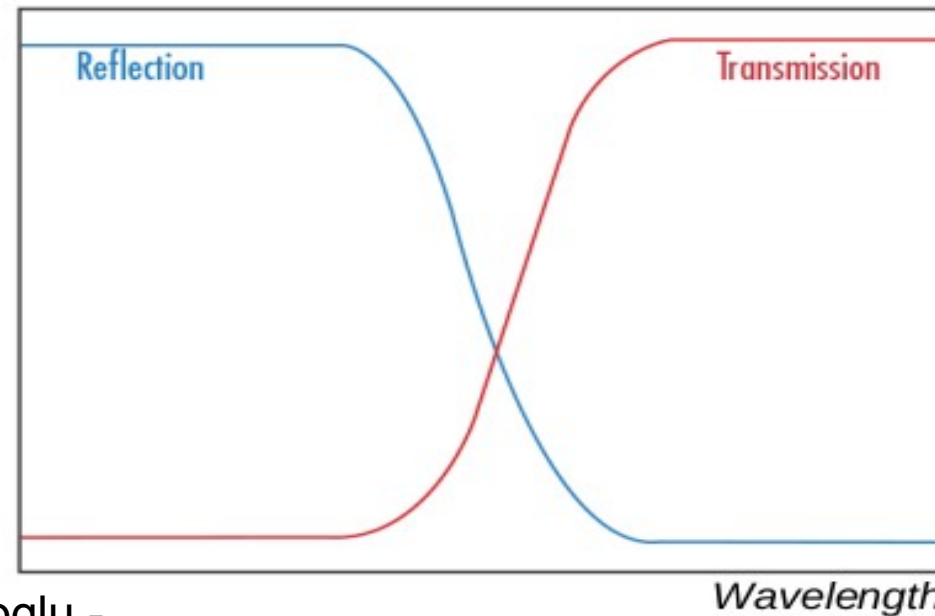
Dichroic Filters



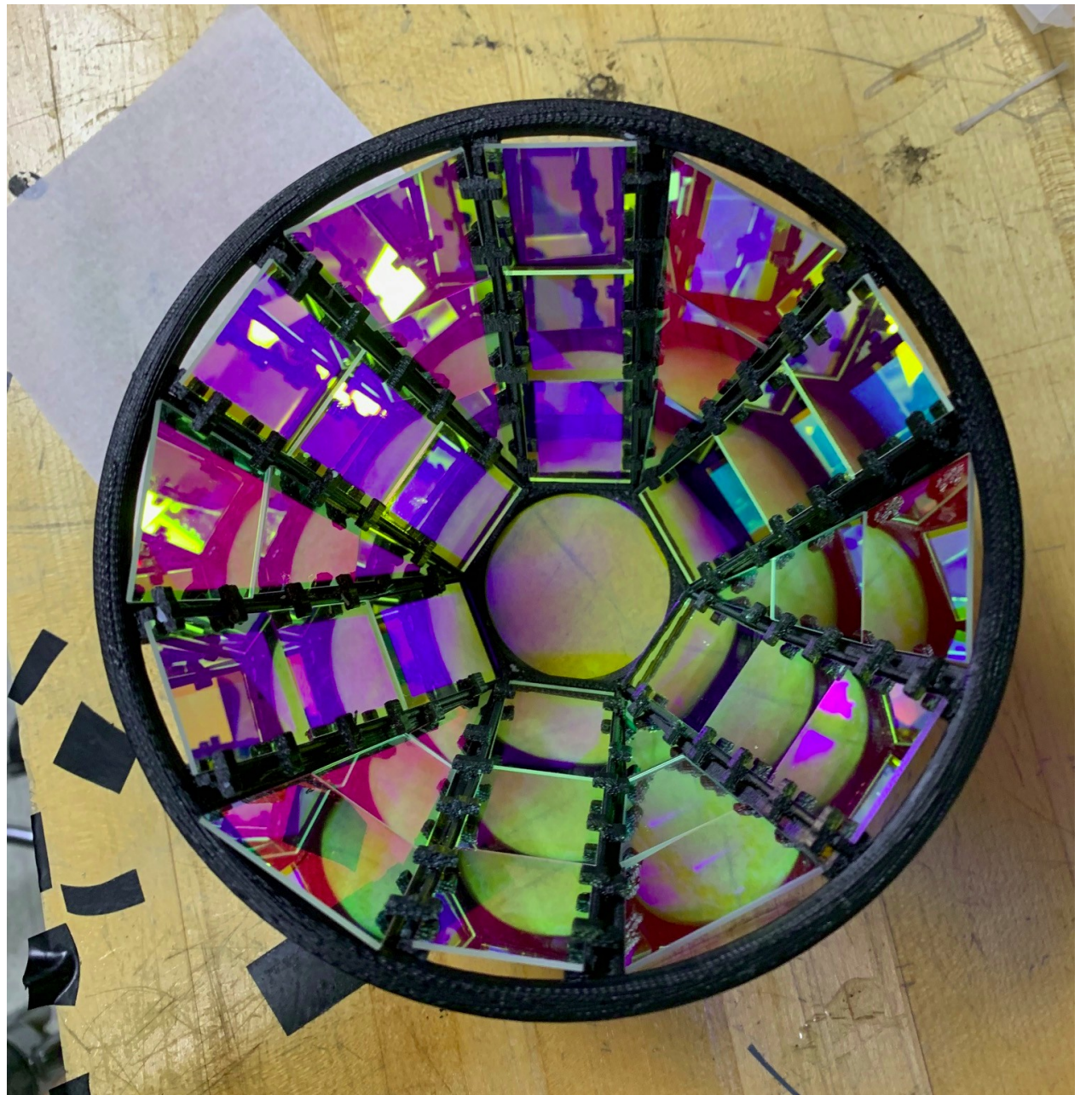
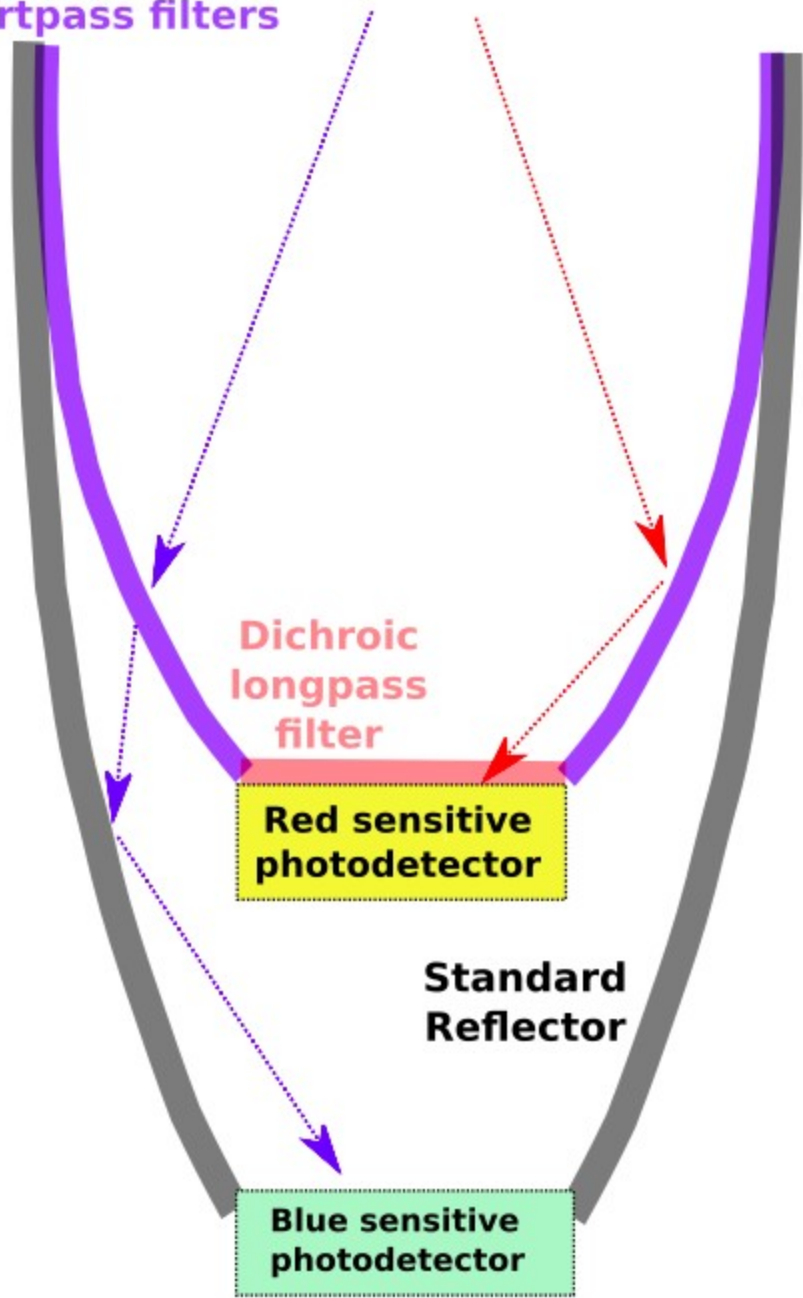
C. Rott et al. JINST 12 (2017)

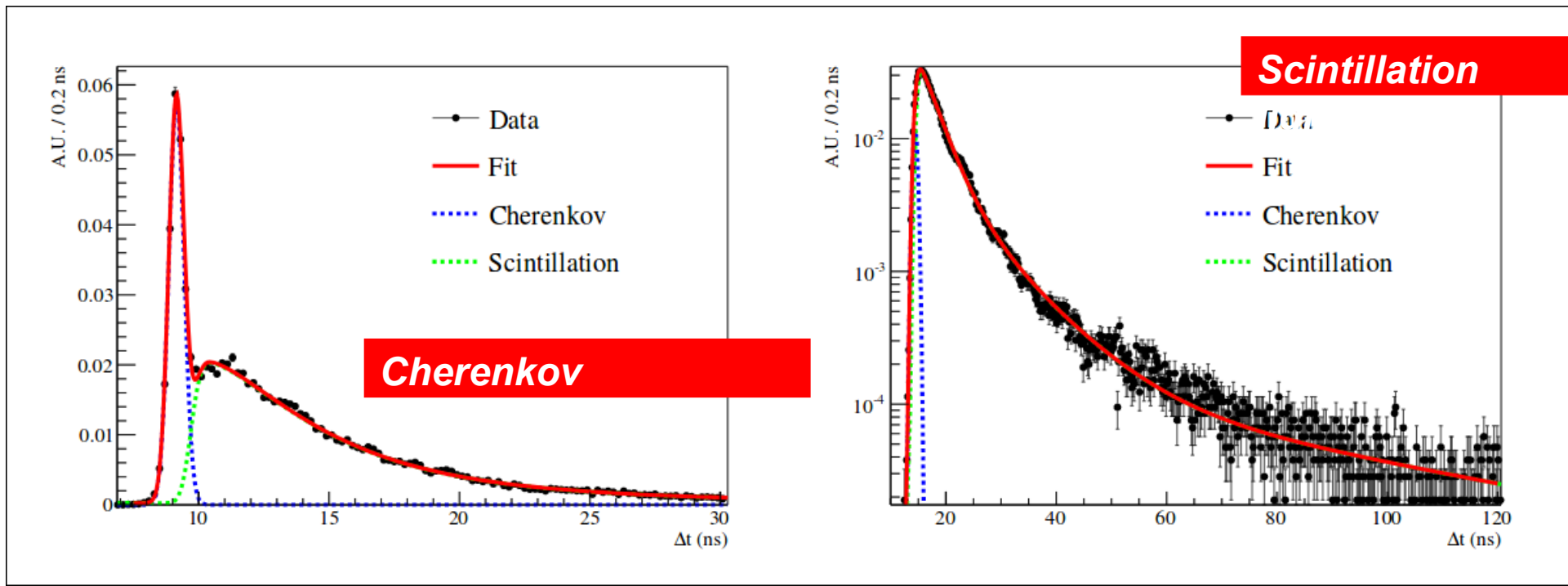
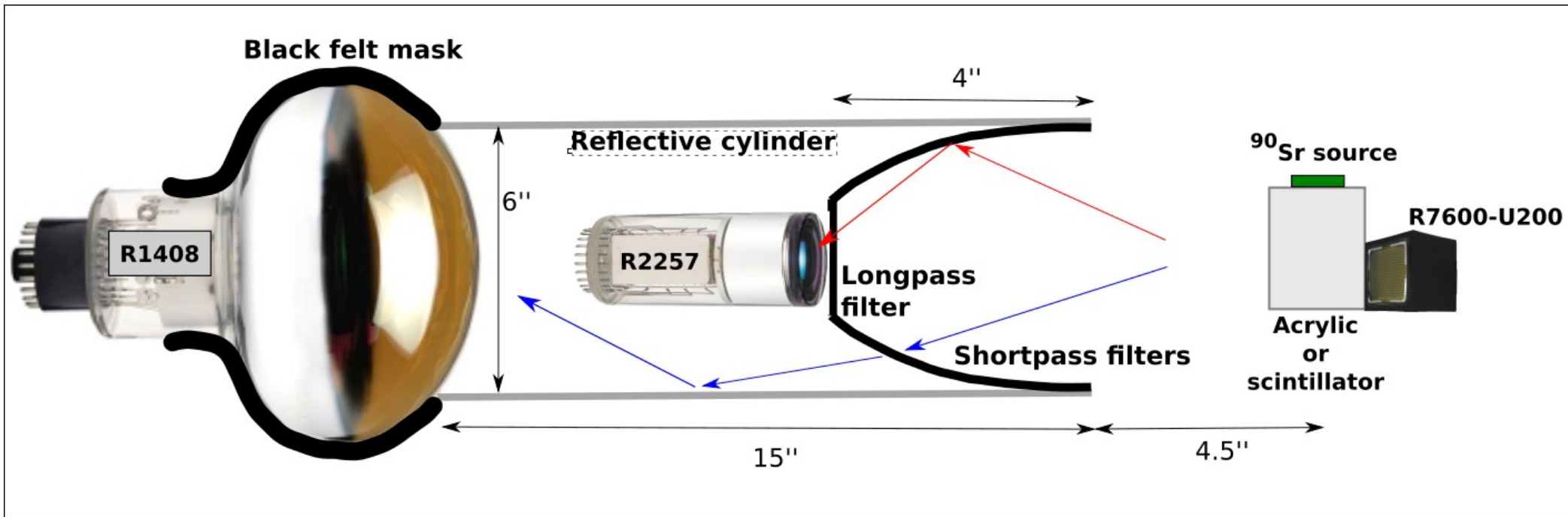


E. Segreto et al., JINST 13 (2018)

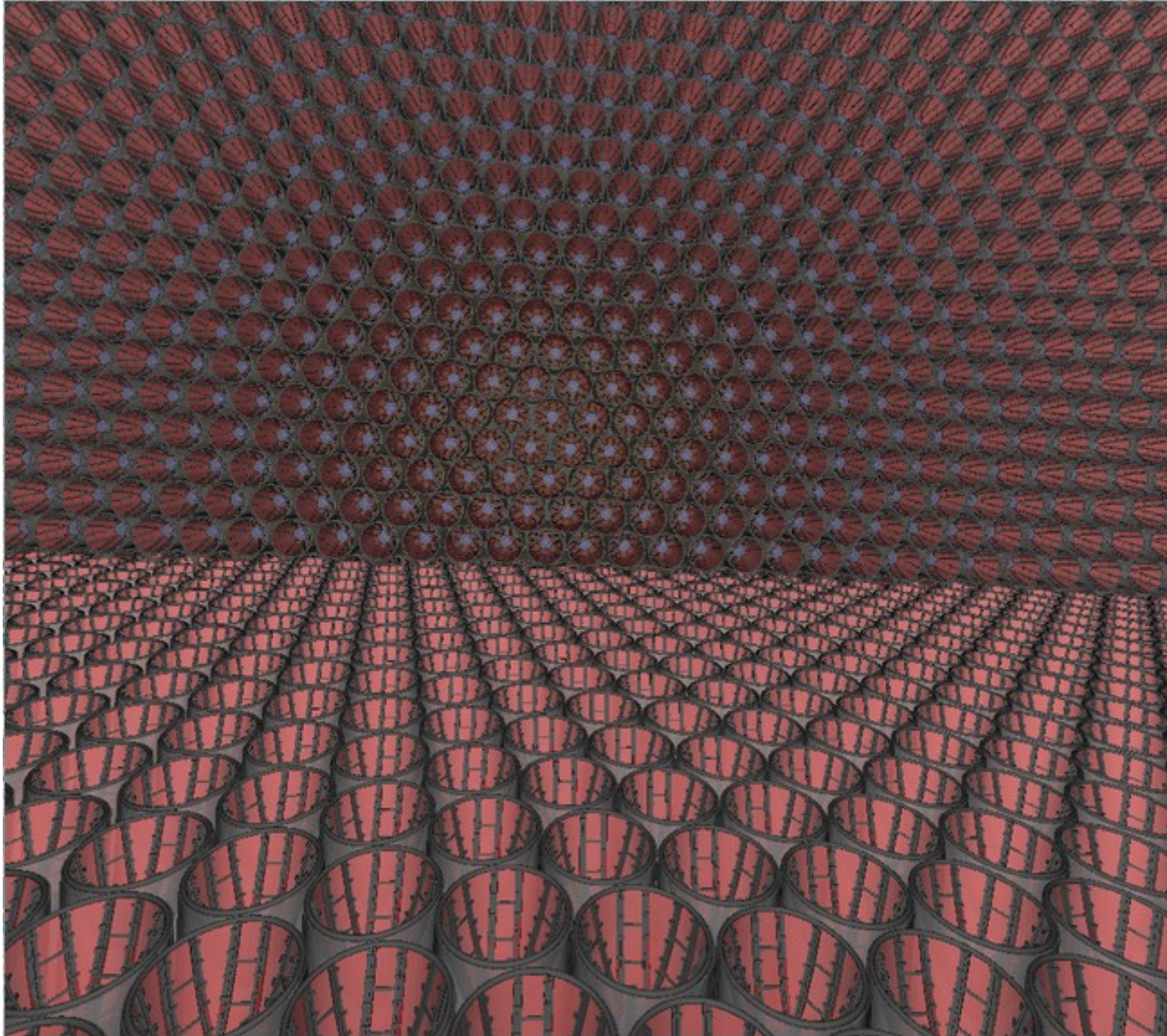


Dichroic
shortpass filters





THEIA Experiment (proposed)



- **Water based Liquid Scintillator**
- Read-out system possibly based on **LAPPD, PMTs and Dichroicon**
- Large-scale detector that can ***discriminate between Cherenkov and scintillation signals.***
- Reconstruct ***particle direction and species using Cherenkov light*** while having ***excellent energy resolution and low threshold of a scintillator detector***
 - *low- and high-energy solar neutrinos*
 - *Neutrino mass ordering*
 - *measurement of the neutrino CP-violating phase*
 - *observations of diffuse supernova neutrinos and neutrinos from a supernova burst*
 - *nucleon decay*

Light Yield of a scintillation detector

LY can be factorized as:

$$LY = N_{\gamma} \epsilon_{PSD} \epsilon_{OPT}$$

Where:

- ✓ N_{γ} is the *photon yield* of the scintillator => number of photons produced per unit of deposited energy by a certain radiation
- ✓ ϵ_{PSD} is the *conversion efficiency of the PSDs* => the efficiency of the PSD system in converting photons into signal (photo-electrons)
- ✓ ϵ_{opt} is the *optical efficiency* => the fraction of the originally produced photons that manages to cross the windows of the PSDs

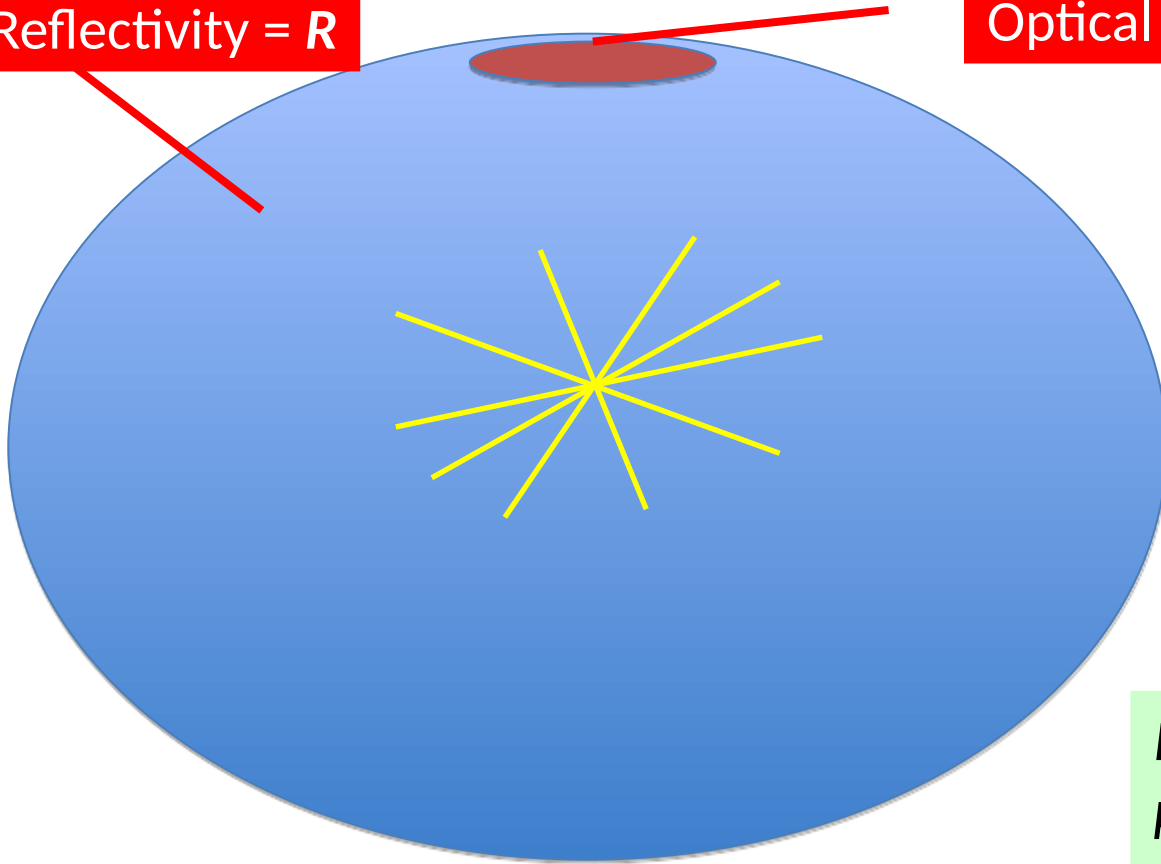
N_{γ} and ϵ_{PSD} in the majority of the cases are precisely known. On the other side ϵ_{opt} is typically unknown and needs to be estimated.

Recursivity of light propagation (think to a sphere...)

The propagation of photons inside a scintillation detector is an *intrinsically recursive process*.

Reflectivity = R

Optical window - photcatodic coverage = f



A photon produced in a **random point inside the sphere** with a **random direction** when reaches the boundary surface has an *average probability f to be detected*

And a probability $R(1-f)$ to be sent back into the chamber

Reflected photons has again a detection probability equal to f and a probability to be reflected equal to $R(1 - f)$ when hit the boundary surface for the second time

The same situation will repeat again *identical to itself after any reflection*.

...let's generalize a little bit (I)

- Consider a **general scintillation detector** and assume that the **process is recursive**
- It can be divided into a series of subsequent and indistinguishable steps and it is possible to define two quantities:
 - ✓ α is the average probability per step that a photon is detected
 - ✓ β is the average probability per step that a photon is regenerated, that is the probability that it is not lost (detected or absorbed) and that some physical process randomizes again its direction (reflection for instance)
 - ✓ α and β are constant for all the steps (recursivity of the process)
 - ✓ $\alpha \leq 1$ and $\beta < 1$
- **Detection and regeneration probabilities after n steps are easily calculated:**

	detection probability	regeneration probability
step 0	α	β
step 1	$\alpha\beta$	β^2
step 2	$\alpha\beta^2$	β^3
...
step n	$\alpha\beta^n$	β^n

...let's generalize a little bit (II)

$$E_{opt} = \sum \alpha \beta^n = \frac{\alpha}{1 - \beta}$$

For the *spherical scintillator* (and one can safely extend *to scintillators of regular shapes*) this means that:

$$E_{opt} = \frac{f}{1 - R(1 - f)}$$

$$\alpha = f$$

$$\beta = R(1 - f)$$

If the optical window has *transmissivity* T_w and *reflectivity* R_w :

$$E_{opt} = \frac{T_w f}{1 - R(1 - f) - R_w f}$$

$$\alpha = T_w f$$

$$\beta = R(1 - f) + R_w f$$

Including Rayleigh scattering and absorption

Define:
$$\frac{1}{\bar{\lambda}} = \frac{1}{\lambda_R} + \frac{1}{\lambda_A}$$

λ_R -> Rayleigh scattering length
 λ_A -> absorption length

and:

$$U_{RA}$$

probability that a photon reaches the end of the step, as defined in absence of scattering/absorption, without interactions

It is possible to define:

$$\alpha = U_{RA} \alpha_0$$

$$\beta = U_{RA} \beta_0 + (1 - U_{RA}) \frac{\bar{\lambda}}{\lambda_R}$$

Photon regenerated by reflections

Photon regenerated by scattering

with α_0 and β_0 detection and regeneration probabilities in absence of scattering and absorption

Including Rayleigh scattering and absorption (II)

After little algebra one finds:

$$E_{opt} = \frac{\alpha_0}{Q - \beta_0}$$

α_0 and β_0 detection and regeneration probability in absence of scattering and absorption

With:

$$Q = \frac{1 - (1 - U_{RA}) \frac{\bar{\lambda}}{\lambda_R}}{U_{RA}}$$

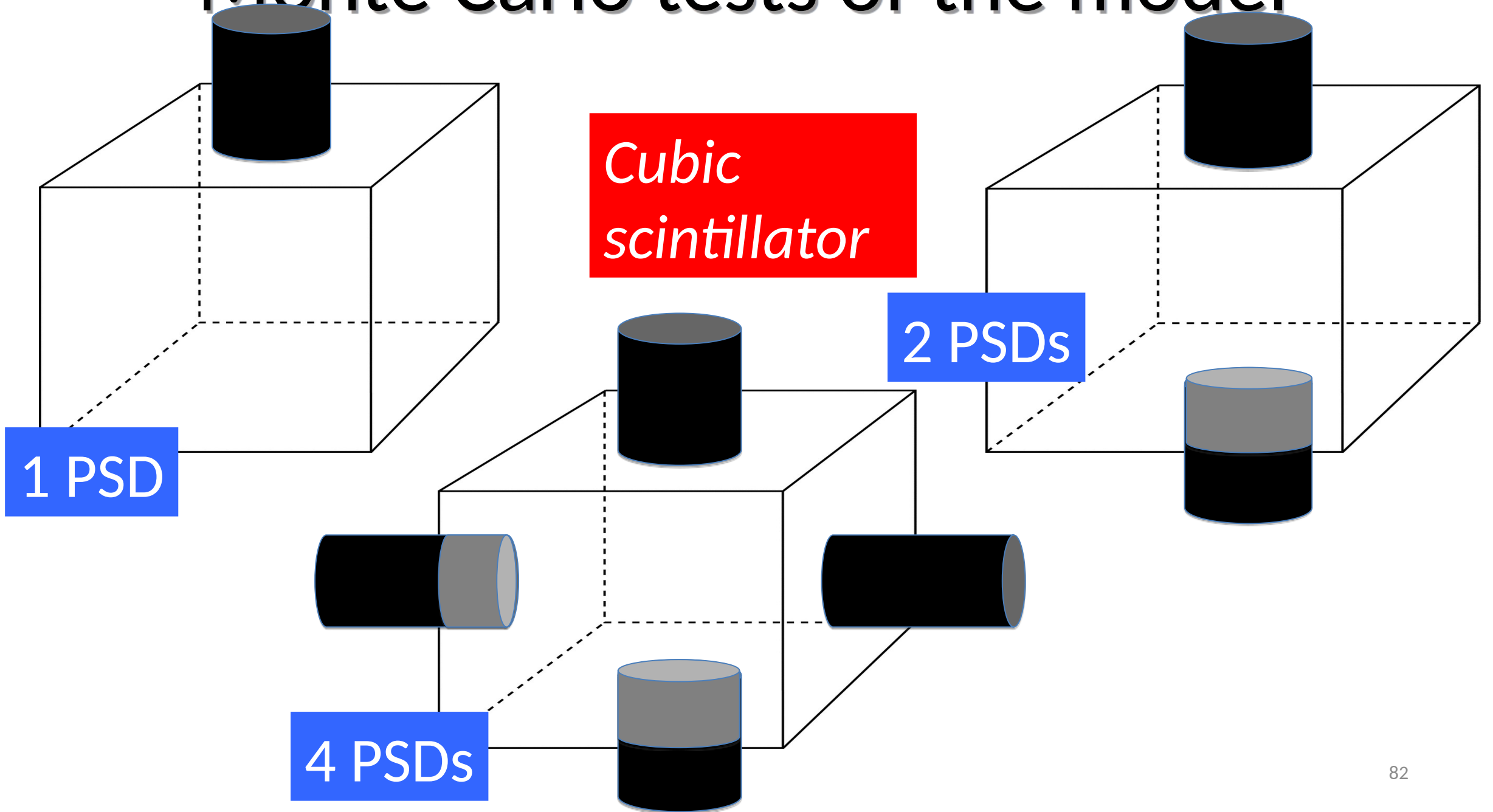
This factor takes into account **all the effects** of scattering and absorption

For our simple detector, under reasonable hypotheses, one obtains:

$$U_{RA} = \frac{\bar{\lambda}}{\bar{L}} (1 - e^{-L/\bar{\lambda}}) \quad \text{with:} \quad \bar{L} = 6 \frac{V}{S}$$

It is the characteristic linear dimension of the detector

Monte Carlo tests of the model



Monte Carlo tests of the model (II)

Specular reflectivity

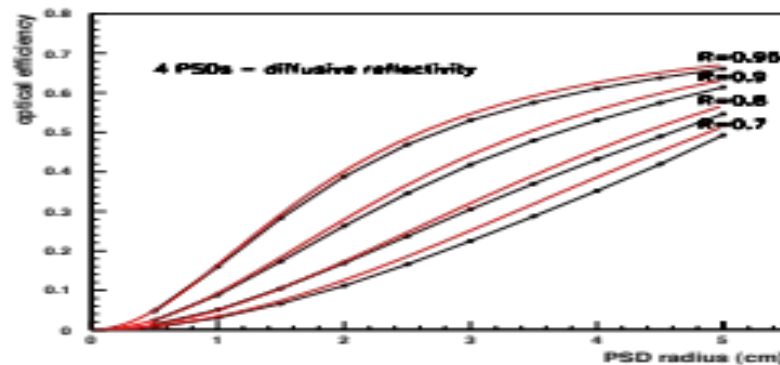
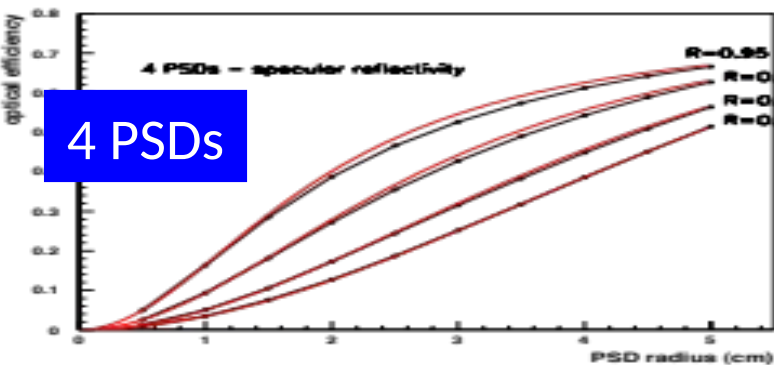
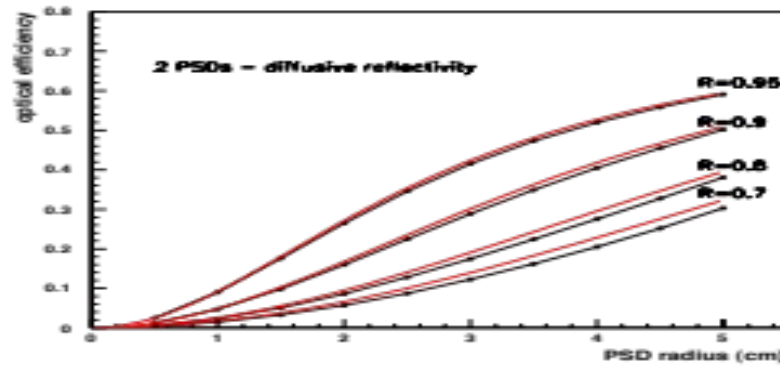
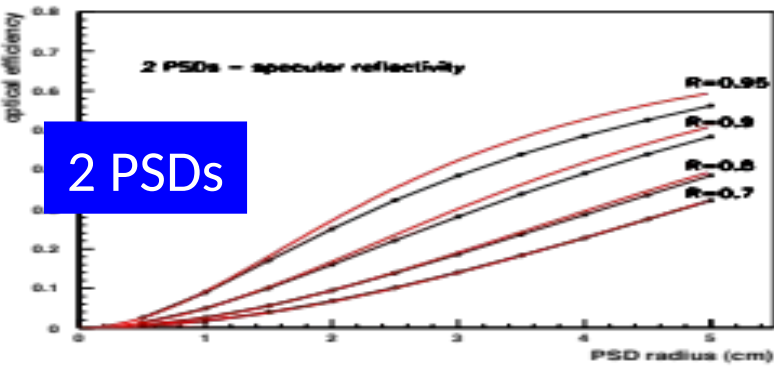
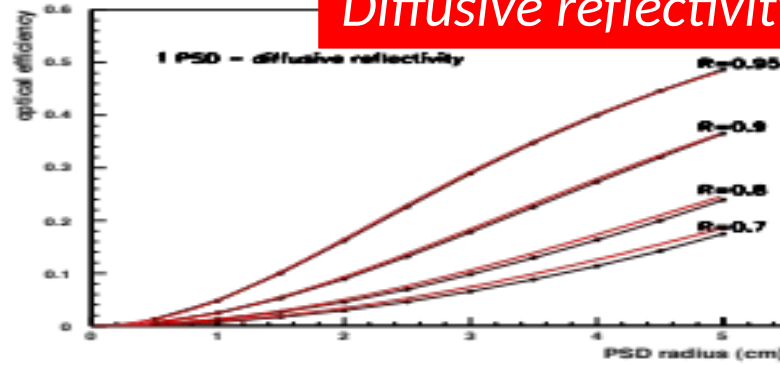
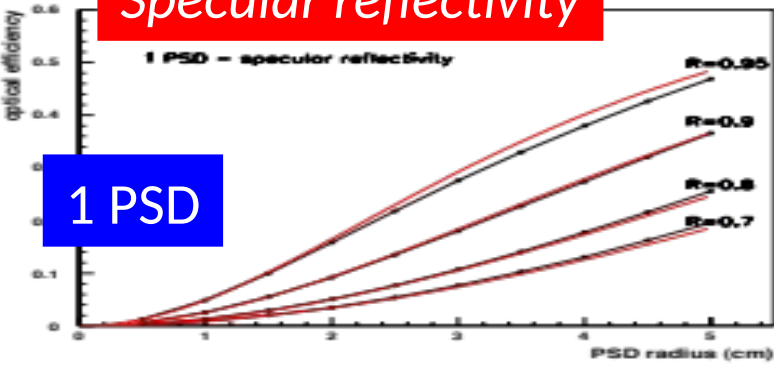
Diffusive reflectivity

1 PSD

RED LINES :

$$\epsilon_{opt} = \frac{T_w f}{1 - R(1 - f) - R_w f}$$

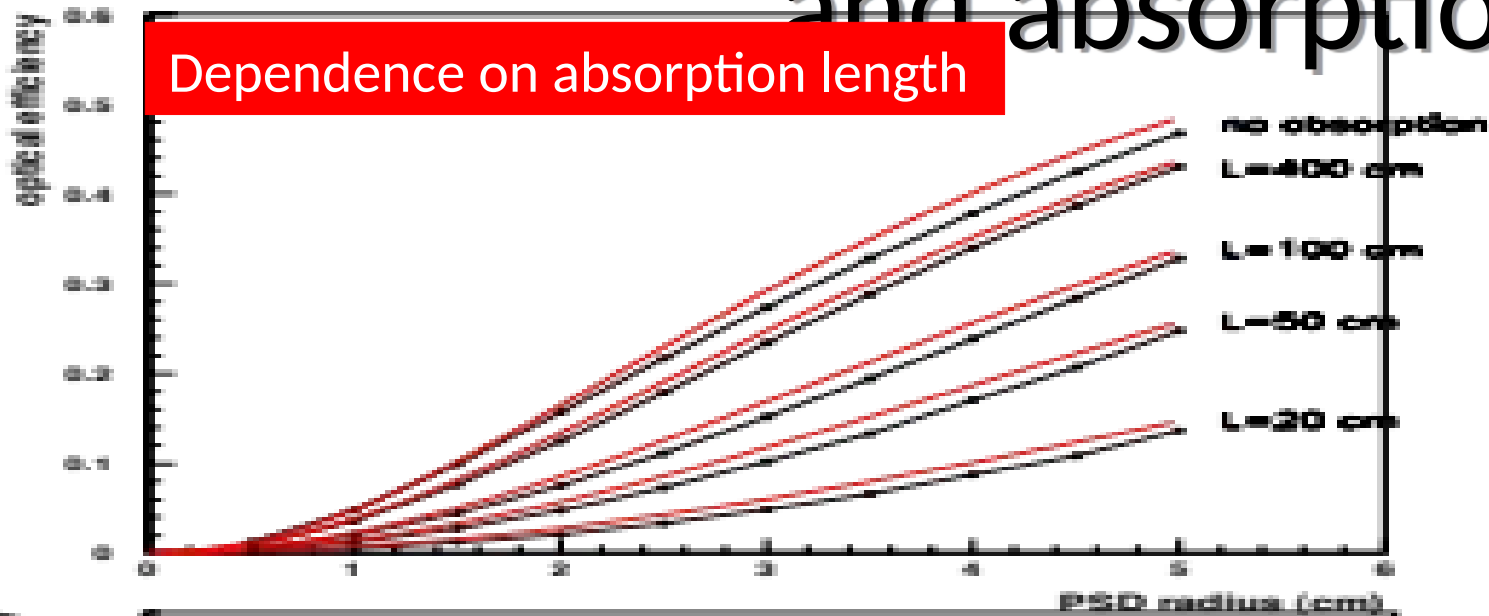
In the case of 2 (4) PSDs the formula is calculated with respect to one PSD. R is the average reflectivity of inactive surfaces and other PSDs' windows. The total efficiency is 2 (4) times the single PSD efficiency



4 PSDs

Monte Carlo tests of the model (scattering and absorption)

Dependence on absorption length

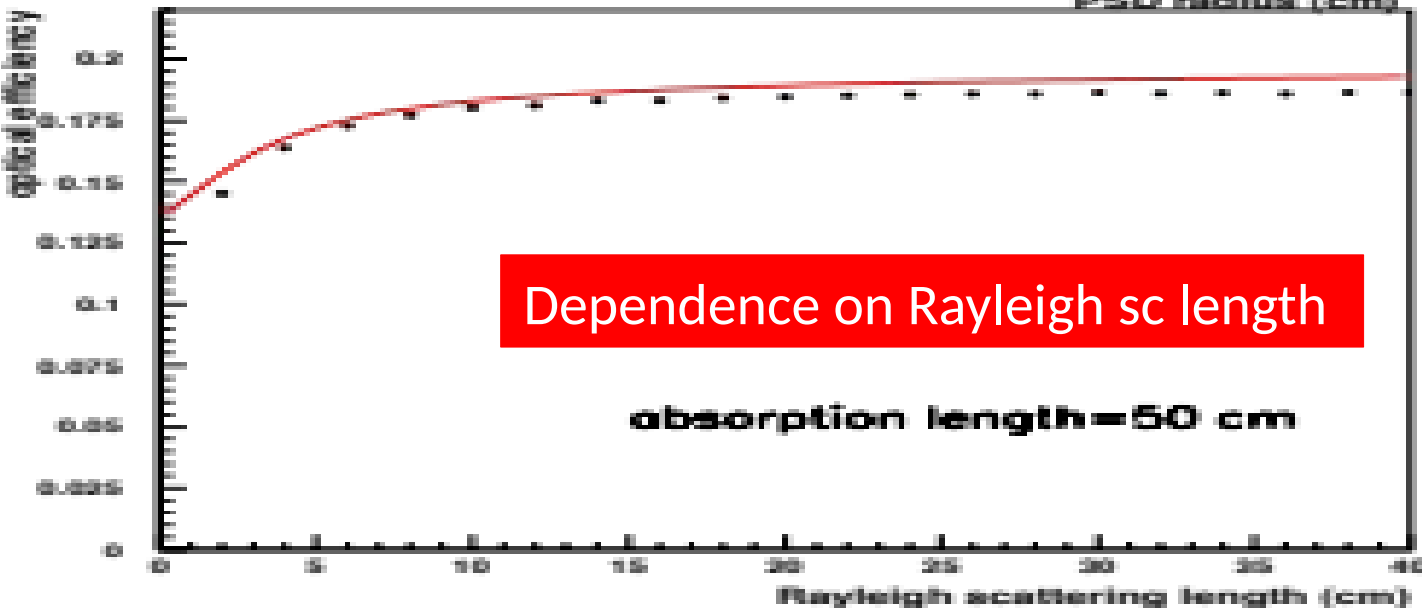


1 PSD
 Specular reflectivity
 $R = 0.95$
 Rayleigh scattering = 10 cm

1 PSD
 PSD radius = 4 cm
 Specular reflectivity
 $R = 0.95$
 Absorption length = 50 cm

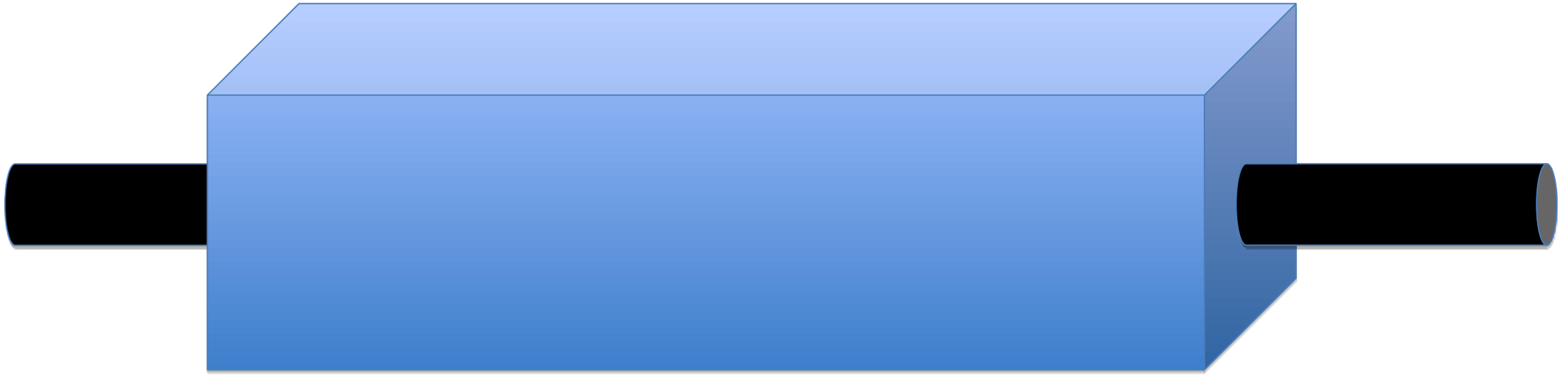
Dependence on Rayleigh sc length

absorption length = 50 cm



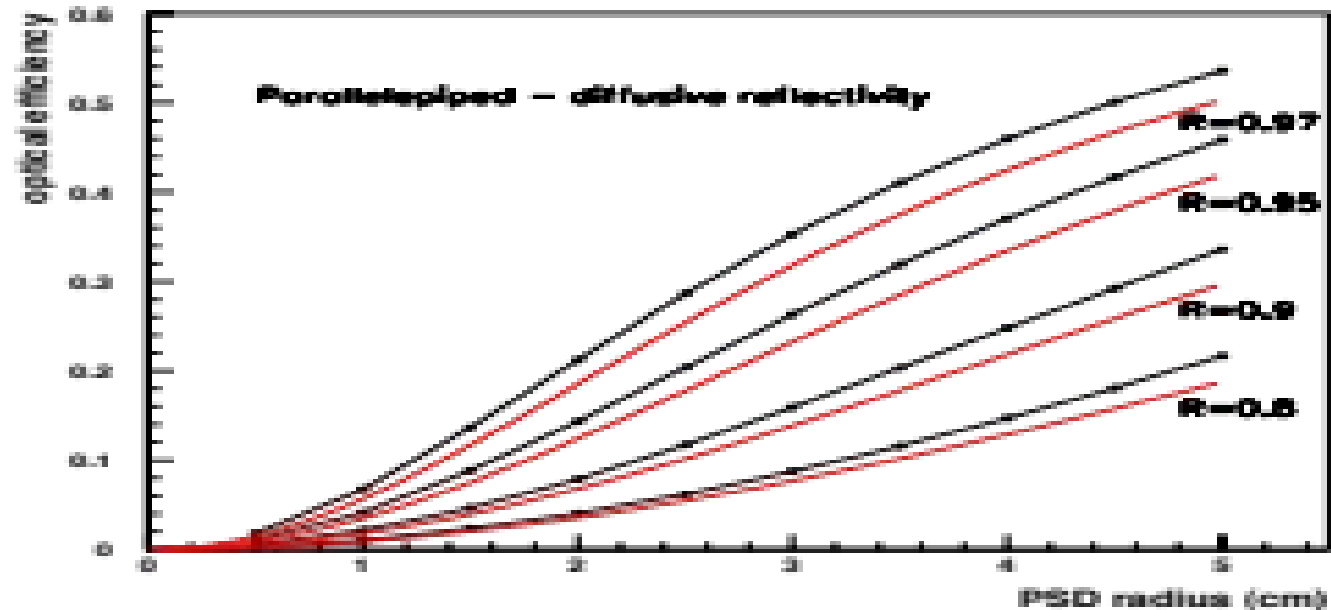
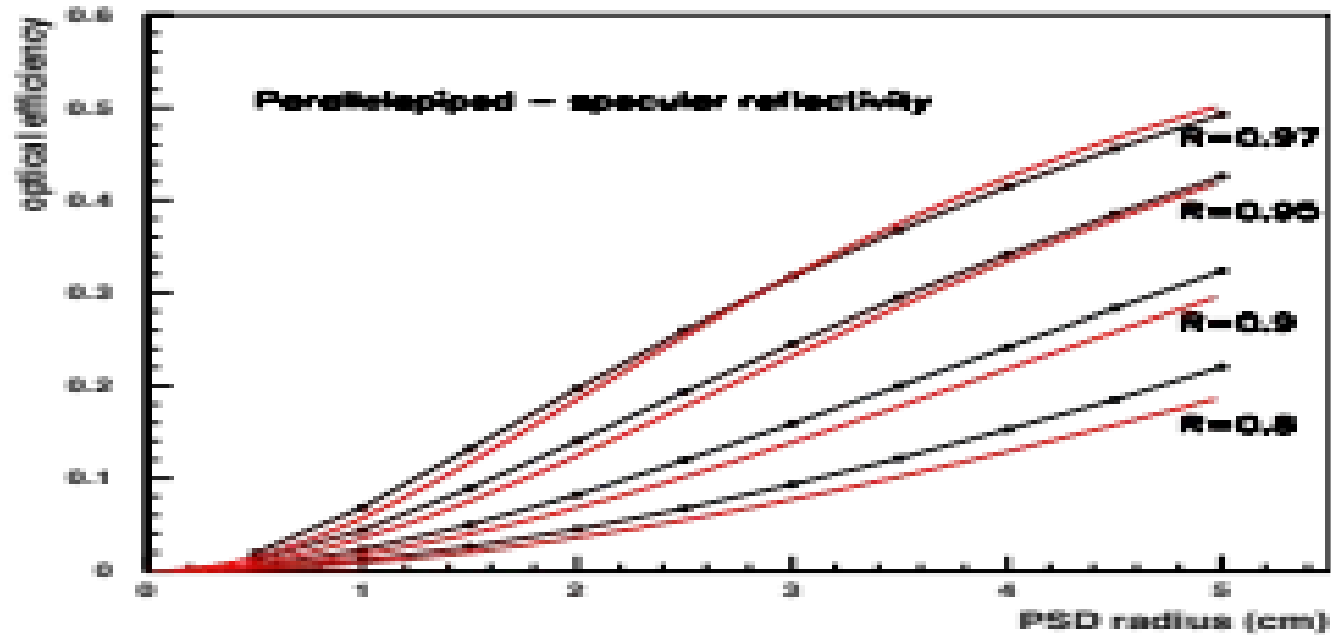
$$U_{RA} = \frac{\bar{\lambda}}{\bar{L}} (1 - e^{-U\bar{\lambda}})$$

Monte Carlo tests of the model: Parallelepiped



- ✓ Parallelepiped $10\text{ cm} \times 10\text{ cm} \times 30\text{ cm}$ ($l \times w \times h$).
- ✓ 2 PSDs on the opposite faces
- ✓ Windows' reflectivity is set at 0.3 and transmissivity at 0.5 (as for the cubic scintillator)

Parallelepiped (cont.)



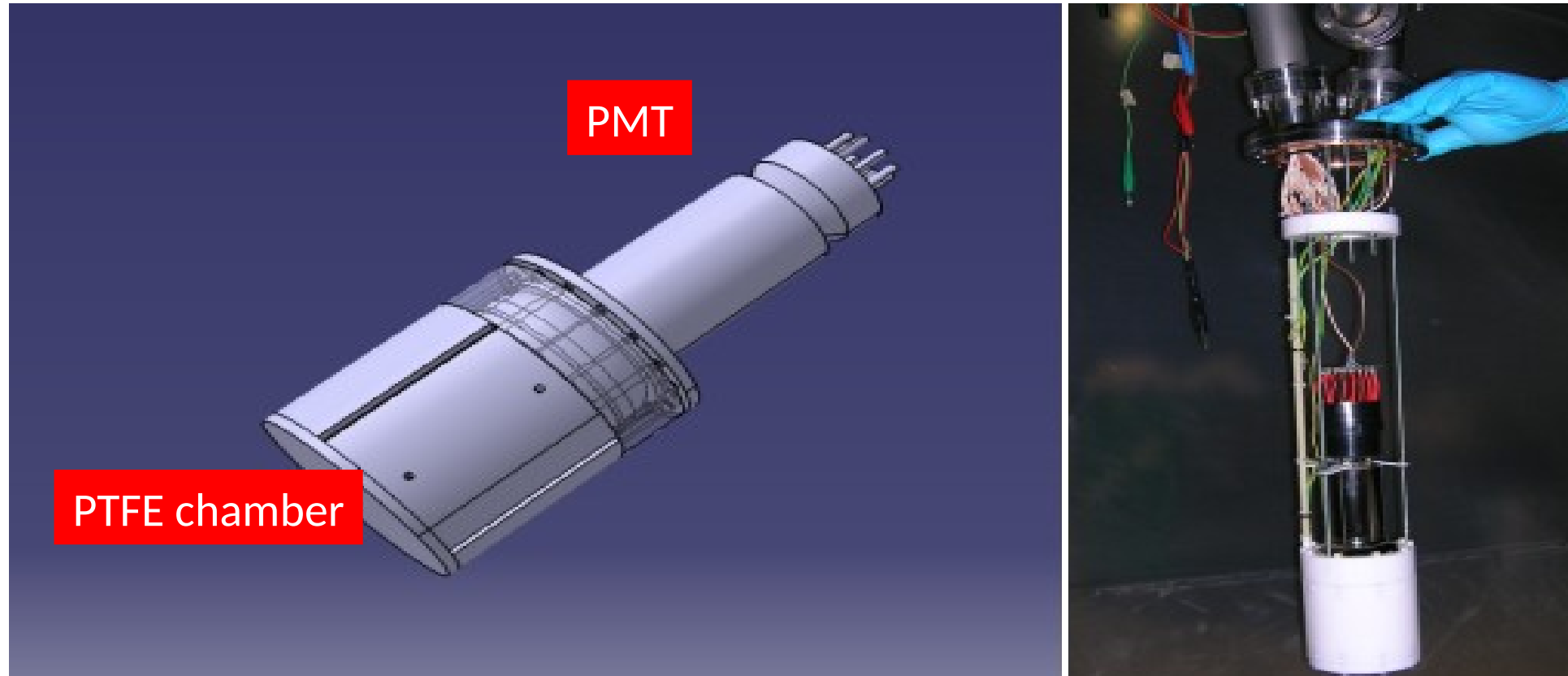
RED LINES :

$$\epsilon_{opt} = \frac{T_w f}{1 - R(1 - f) - R_w f}$$

Extremely asymmetric detector

- ✓ Surprisingly good agreement between MC simulation and model outcomes
- ✓ For specular reflectivity, above 0.9, discrepancies at the level of few percent are found
- ✓ In all other cases they are of the order of 10%.

LY estimation of a real detector



*LAr scintillation chamber - PTFE cell ($h = 9.0$ cm and $\varphi = 8.4$ cm) - observed by a single 3" photomultiplier (Hamamatsu R11065)
Internal surface of the cell completely covered with a reflective foil deposited with Tetra Phenyl Butadiene.*

WARP Collaboration, *Demonstration and comparison of photomultiplier tubes at liquid Argon temperature*, 2012 JINST 7 P01016 [arXiv:1108.5584].

LY estimation of a real detector (I)

Parameters used for LY estimation

photon yield	$N_\gamma = 40$ photons/keV [11]
photocathodic coverage	$f = 13\%$
transmissivity of PMT window	$T_w = 0.94$ [12]
reflectivity of PMT window	$R_w = 0$
conversion efficiency of PMT	$\epsilon_{PSD} = 28\%$
no absorption of VUV photons	$Q_{VUV} = 1$
no absorption of visible photons	$Q_{vis} = 1$
conversion efficiency of passive surface	$\epsilon_{WLS} = 1$ [13]
conversion efficiency of PMT window (no shifter)	$\epsilon_{wls} = 0.$
reflectivity of passive surface (reflector+TPB)	$R = 0.95$ [14]

LAr is assumed to be pure => no absorption ($Q = 1$)

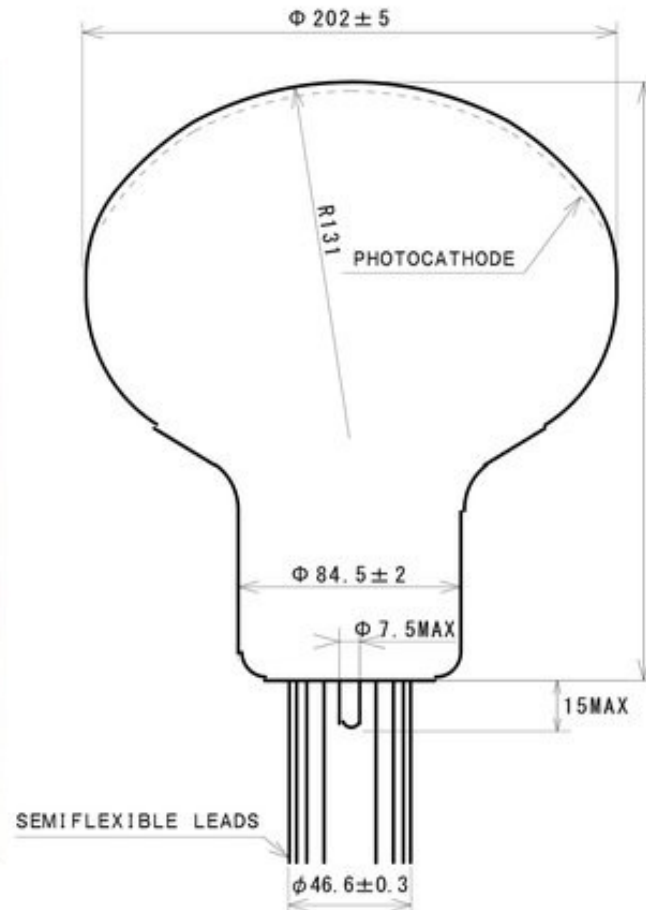
Photons converted on the walls

$$LY_{estimated} = N_\gamma \epsilon_{PSD} \epsilon_{WLS} (1 - f) \frac{T_w f}{1 - R(1 - f)} = 6.9 \frac{phel}{keV}$$

$$LY_{measured} = 7 \frac{phel}{keV} \pm 5\%$$

BACK-UP

Hamamatsu R5912



Spectral Response	300 ÷ 650 nm
Window Material	Borosilicate glass (sand blasted)
Photocathode	Bialkali with Pt under-layer
Max supply voltage (anode-cathode)	2000 V
Photocathode Q.E. at 420 nm	$\geq 16\%$
Typical Gain	1×10^7 at 1500 V
Nominal anode pulse rise time*	≤ 4 ns
Nominal P/V ratio*	2.5
Max. dark count rate*	5000 s^{-1}
Max. transit time variation	2.5 ns (center-border)

* Values for $G = 1 \times 10^7$

Hamamatsu R11065



HAMAMATSU

TENTATIVE DATA SHEET

Mar. 2009

PHOTOMULTIPLIER TUBE

R11065

For Low Temperature Operation down to -186 deg. C
Special Bialkali Photocathode (Bialkali LT), Low Radioactivity
76 mm (3 Inch) Diameter, 12-stage, Head-on Type, Synthetic Silica

General

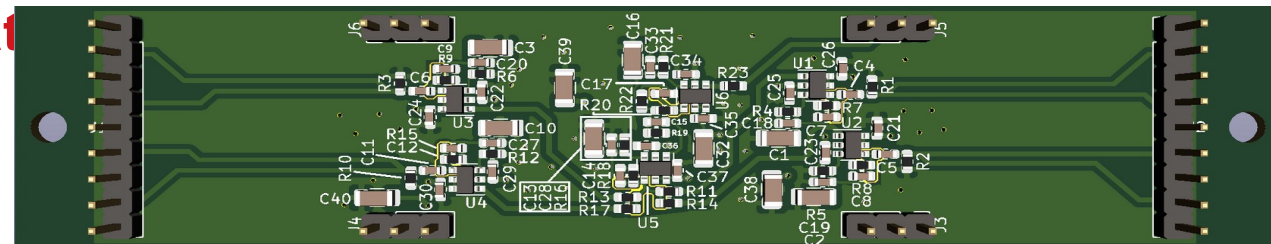
Parameter	Description / Value	Unit
Spectral response	160 to 650	nm
Wavelength of Maximum Response	420	nm
Window material	Synthetic silica	-
Photocathode	Material	Bialkali
	Minimum Effective Area	64
Dynode	Structure	Box & Linear-focused
	Number of Stages	12
Operating Ambient Temperature	-186 to +50	deg. C
Storage Temperature	-186 to +50	deg. C

Electronics – Cold active ganging

Read out electronic is divided into **two stages**: *Cold active ganging board* and *digitizing board*

- **Cold ganging (summing) board:**

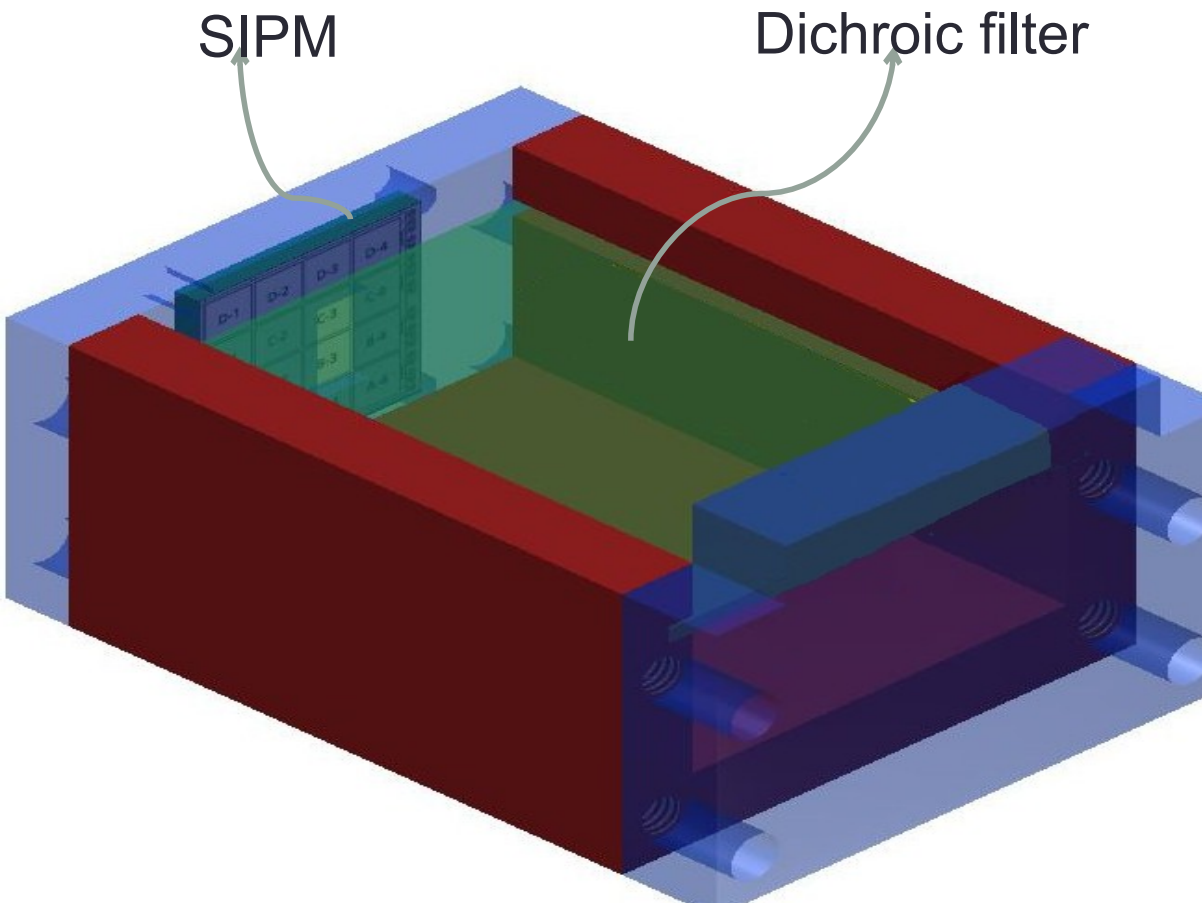
- SiPMs are small devices. They need to be ganged in order to contain the number of read-out channels. There is a limitation on the number of channels per ARAPUCA bar due to the space available to route the cables inside APA (see D. Warner talk). **There will be 4 readout channels per module** → *one channel per X-ARAPUCA supercell.*
- **48 SiPMs will be ganged together.** The ganging is active, that is using active components (Operational Amplifier)
- The active ganging board is installed on the X-ARAPUCA module and *operates at LAr temperature*
- *Two active ganging circuits developed by the Consortium.* With different degrees of maturity at this moment. Both **demonstrated LAr operation**



X-ARAPUCA concept

- There are **two main mechanisms** through which a photon can be detected by the X-ARAPUCA:
 - **Standard ARAPUCA mechanism.** The photon, after entering the X-ARAPUCA box, is converted by the WLS of the inner slab, but is not captured by total internal reflection. In this case the photon bounces a few times on the inner surfaces of the box until when it is or detected or absorbed;
 - **Total internal reflection.** The photon, converted by the filter and the slab, **gets trapped by total internal reflection**. It will be guided towards one end of the slab where it will be eventually detected. This represents an improvement with respect to a conventional ARAPUCA, which contributes to *reduce the effective number of reflections on the internal surfaces*. The sides of the slab where there are not active photo-sensors will be coated with a **reflective layer** which will allow to keep the photon trapped by total internal reflection.

Operating principle



- The simplest geometry is a **flattened box** with highly reflective internal surfaces (Teflon, VIKUITI, VM2000) with an open side.
- The open side hosts the **dichroic filter** that is the acceptance window of the device
- The filter is deposited with **TWO WAVELENGTH SHIFTERS (WLS)** – one on each side
- The shifter on the **external side**, S1, converts LAr scintillation light (128 nm) to a wavelength L1, with **$L1 < \text{cutoff}$**
- The shifter on the **internal side**, S2, converts S1 shifted photons to a wavelength L2, **with $L2 > \text{cutoff}$**
- **The internal surface** of the ARAPUCA is observed by **one or more SiPM**